

© 2019

Khashayar Mahani

ALL RIGHTS RESERVED

DISTRIBUTED NETWORK-AWARE PLANNING AND CONTROL SYSTEM WITH APPLICATION
IN ENERGY NETWORKS

By

KHASHAYAR MAHANI

A dissertation submitted to the

School of Graduate Studies

Rutgers, The State University of New Jersey

In partial fulfillment of the requirements

For the degree of

Doctor of Philosophy

Graduate Program in Industrial and Systems Engineering

Written under the direction of

Professor Mohsen A. Jafari

And approved by

New Brunswick, New Jersey

MAY 2019

ABSTRACT OF THE DISSERTATION

“Distributed Network-Aware Planning and Control System with Application in Energy Networks”

by KHASHAYAR MAHANI

Dissertation Director:

Mohsen A. Jafari

Significant increases in energy prices and price volatility, worsening global warming, adverse environmental footprints of fossil fueled energy and recent advances in energy system technologies have significantly elevated interest in clean distributed energy resources (DERs) and energy storage. Over the past decade, various forms of DERs, such as combined heat & power, fuel cells, hybrid power systems, microturbines, photovoltaic systems and reciprocating engines have been successfully integrated to the electric distribution systems. Moreover, environmental concerns have been urging for more and more integration of distributed renewable energy resources into the overall energy infrastructure. However, many challenges still remain; for instance, renewable generation (such as wind and solar) is not dispatchable and its production is not necessarily coincident

with system demand. As a result, cheap renewable may not efficiently be utilized at all times. In this context, battery energy storage systems can provide operation flexibility by storing excess renewable energy when there is low demand and dispatching it when its needed the most. With this in mind, the Federal Energy Regulatory Commission (FERC) recently enacted FERC Order 841, which attempts to remove barriers to the participation of electric storage resources in the capacity, energy, and ancillary service markets operated by Regional Transmission Organizations (RTO) and Independent System Operators (ISO).

In this work, a Distributed Network-Aware Planning and Control System is developed aiming at optimal sizing, capacity allocation and planning and control of energy storages using real-time information. A storage node in such network can be a single functional unit or an aggregation of multiple units (e.g. modular network of energy storages) owned by either a utility company or by a third party. Capacity of storage nodes in the network can be static and deterministic or change dynamically due to units' degradation and/or unavailability. For instance, a parking facility with EVs and Vehicle to Grid (V2G) charging stations can be a good example of an aggregate storage node. Arrival and departure of vehicles to this facility, permission for V2G by vehicle owners, and vehicles' scheduling and charging requirements all together define a complex stochastic process that govern the overall capacity of the facility's energy storage. We build a model that describes such a process and determines energy storage capacity of the aggregate node. The underlying model closely connects to business opportunities that such a facility can present to individual vehicle owners or to the facility operator.

The planning and control scheme, introduced in this dissertation has significant impacts on overall energy network performance and efficiency by balancing dynamic

demands with energy supply, and can be utilized to address a range of energy storage applications including power quality and network reliability. The undertaken research in this dissertation can provide guidance on DER and energy storage operation and maintenance (O&M) strategies which can be utilized as a means for supporting microgrid operators, regulators and utility capacity planners towards strategic planning decisions.

Acknowledgement

It is a treat to be able to express my gratitude to people and organizations that provided me with generous support throughout my graduate study. I would like to thank CAIT for their continuous support during my PhD years. When I look back to the past six years, I cannot stop thinking about individuals who had such significant impact on my life and education. I would like to take my opportunity here to let them know that how much I appreciate their presence in my life and that I am committed to keep up the hard work and to pass on the values and dreams they have given to me. I simply cannot afford letting them down.

I would like to thank my dearest advisor: Professor Mohsen Jafari. I could not have asked for better role model. He has been an awesome mentor in every aspect; I learned a great deal not only from our scientific discussions but also from his manner and his integrity. I admire his intelligence, his creativity and more importantly his being a free spirit and yet very much committed to human and ethics core values. It has been such a relief to know that Dr Jafari is always there for me and acting beyond call of duty to offer me both professional and moral support.

I am so grateful to have Dr Ajith Parlikad as my co-advisor. He is one of the smartest people I ever met. Working in his team during my stay in Cambridge university was a constant learning experience. I appreciate his amazing personality.

I have to thank the members of my PhD committee, Professor Boucher, Professor Jeong and Dr Raya Horesh who provided constructive advice in my research. Thank you for taking the time to review my thesis and for providing valuable comments.

I also want to thank my friends (so many to list but I am sure you know who you are!) for their friendship, support and all the fun memories we had together. You made me multiple my happiness by sharing it with you and let me up when I was down.

I am blessed with having the best and the most supportive relatives ever with whom I shared the best years of my life in Iran. I would like to dedicate this thesis to the memory of beloved grandmother, Mamani-Amme, who always believed in my ability. You are gone but your belief in me has made this journey possible.

I especially want to thank my beloved grandmother, Mamani-Babaji. I want to make sure she is happy with and proud of me all the time. I also want to thank my Aunts Parvin, Hamide and Shahla, my Uncles Mohammad, Behrouz and Saeid and their spouses and my cousins back in Iran. They kept lifting me up during all these years I was far from home by calling me regularly and showing their love when I most needed it. I have been lucky to have two of my cousins, Farnaz and Farbod, studying at Rutgers and living here very close to me. They are dear to me like a sister and brother and have made me feel stronger knowing that I could count on them anytime.

Finally, no words can convey my love to my dearest parents and brother. They are the most precious reason of my life and my best friends with their unconditional love and support. My parents taught us all the core values that we hold today. I would not have made it thus far without them. I have the smartest and wisest mother ever; an easy-going, yet very reliable father and a wonderful brother. I always knew that they believed in me and wanted the best for me. To my family, thank you, for having faith in me and for helping me to instill confidence. I love you so much!

Table of Contents

| | |
|--|-----------|
| Abstract..... | ii |
| Acknowledgement | v |
| List of Tables | x |
| List of Figures..... | xi |
| CHAPTER 1: INTRODUCTION AND RESEARCH BACKGROUND | 1 |
| 1.1. Objectives..... | 1 |
| 1.2. Brief Overview of Thesis Accomplishments | 2 |
| 1.3. Synopsis of Contributions | 4 |
| 1.3.1. Evaluation of the behind the meter benefits of energy storage systems with consideration of ancillary market opportunities (Chapter 2) | 4 |
| 1.3.2. Network-aware approach for energy storage planning and control in the network with high penetration of renewables (Chapter 3)..... | 4 |
| 1.3.3. Energy storage system with dynamic capacity – EV parking lot model (Chapter 4) | 5 |
| 1.3.4. Joint optimization of operation and maintenance policies for microgrid composing of energy storage system (Chapter 5)..... | 6 |
| 1.4. Motivation | 6 |
| CHAPTER 2: EVALUATION OF THE BEHIND THE METER BENEFITS OF ENERGY STORAGE SYSTEM WITH CONSIDERATION OF ANCILLARY MARKET OPPORTUNITIES..... | 10 |
| 2.1. Introduction | 11 |
| 2.2. Problem statement | 15 |
| 2.3. Modeling methodology | 22 |
| 2.4. Illustrative example | 29 |

| | |
|---|-----|
| 2.4.1. PV and electric storage (PV-ES)..... | 29 |
| 2.4.2. CHP, Electric storage and Thermal storage (CHP-ES-TS) | 36 |
| 2.5. Conclusion..... | 41 |
| CHAPTER 3: NETWORK-AWARE APPROACH FOR ENERGY STORAGE | |
| PLANNING AND CONTROL IN THE NETWORK WITH HIGH PENETRATION OF | |
| RENEWABLES..... | |
| 3.1. Introduction | 48 |
| 3.2. Optimal Planning..... | 52 |
| 3.3. Illustrative Example | 61 |
| 3.3.1. Capacity Planning | 64 |
| 3.3.2. Daily Operation Planning | 68 |
| 3.4. Network-Aware Real-Time Control..... | 72 |
| 3.5. Sensitivity Analysis on stochastic parameter changes | 84 |
| 3.6. Conclusion..... | 86 |
| 3.7. Appendices | 88 |
| 3.7.1. Appendix “A1” | 88 |
| 3.7.2. Appendix “A2” | 91 |
| CHAPTER 4: ENERGY STORAGE SYSTEM WITH DYNAMIC CAPACITY – EV | |
| PARKING LOT MODEL..... | |
| 4.1. Introduction | 94 |
| 4.2. Problem Statement and preliminaries | 97 |
| 4.3. Day-ahead stochastic planning..... | 101 |
| 4.4. Formulation of Optimal Facility Operational Control | 111 |
| 4.5. Illustrative case study | 119 |
| 4.6. Conclusion..... | 128 |

CHAPTER 5: JOINT OPTIMIZATION OF OPERATION AND MAINTENANCE
POLICIES FOR MICROGRID COMPOSING OF ENERGY STORAGE SYSTEM .. 130

- 5.1. Introduction 134
- 5.2. System description 137
- 5.3. Modeling Approach..... 139
 - 5.3.1. Upper layer (system operation model)..... 141
 - 5.3.2. Lower layer (asset maintenance model) 146
- 5.4. Illustrative case study 151
- 5.5. Conclusion..... 158
- References..... 159

List of Tables

| | |
|---|-----|
| Table 1- Customer segments information | 16 |
| Table 2- Critical loads as a percentage of electricity load of major end uses in building segments | 18 |
| Table 3- EDCs rate structure | 19 |
| Table 4- GDCs rate structure..... | 20 |
| Table 5- CHP prime mover characteristics..... | 21 |
| Table 6- CHP-ES-TS Economics; Hospital | 38 |
| Table 7- CHP-ES-TS Economics; Full-service restaurant | 39 |
| Table 8- CHP-ES-TS Economics; Strip-mall..... | 40 |
| Table 9-Capacity Planning Results | 65 |
| Table 10- Aggregate model vs. Hourly model (inputs from cluster 47)..... | 67 |
| Table 11 - Percentage error over all input clusters (Aggregate model vs. Hourly model) | 67 |
| Table 12 - Local zones' duration for different clusters (Clusters 44, 46 and 47) | 70 |
| Table 13-peak value, total reverse flow and total electricity cost for different ESS applications . | 72 |
| Table 14- Storage 4 control action representation..... | 81 |
| Table 15- Capacity planning for different electricity demand growth | 85 |
| Table 16 – parking lot characteristics | 121 |
| Table 17- Annual revenue (for all 4 cases)..... | 122 |
| Table 18 - April 18th total revenue in different cases | 125 |
| Table 19- Correlation value..... | 127 |
| Table 20 - maintenance parameters and costs..... | 152 |

List of Figures

| | |
|--|----|
| Figure 1- Energy flow in a facility level micro-grid..... | 15 |
| Figure 2- Hourly energy profiles for an average day | 17 |
| Figure 3- Hospital-EDC1; PV-ES; NPV/kW | 31 |
| Figure 4-Hospital-EDC2; PV-ES; NPV/kW | 31 |
| Figure 5-Hospital-EDC3; PV-ES; NPV/kW | 32 |
| Figure 6-Full service restaurant-EDC1; PV-ES; NPV/kW | 33 |
| Figure 7-Full service restaurant-EDC2; PV-ES; NPV/kW | 33 |
| Figure 8-Full service restaurant-EDC3; PV-ES; NPV/kW | 34 |
| Figure 9-Strip mall-EDC1; PV-ES; NPV/kW | 34 |
| Figure 10-Strip mall-EDC2; PV-ES; NPV/kW | 35 |
| Figure 11-Strip mall-EDC3; PV-ES; NPV/kW..... | 35 |
| Figure 12: An example circuit with multiple storage units, renewable resources and demand nodes..... | 53 |
| Figure 13-Temporal Zone Aggregation Example | 55 |
| Figure 14 - Distribution network..... | 61 |
| Figure 15- Input data in cluster 13..... | 64 |
| Figure 16-Aggregate model vs. Hourly model (SOC), Application: EBM..... | 66 |
| Figure 17- Average Input data in clusters 44, 46 and 47 | 69 |
| Figure 18- DER optimal dispatch with input data from cluster 44 | 70 |
| Figure 19- DER optimal dispatch with input data from cluster 46 | 71 |
| Figure 20-DER optimal dispatch with input data from cluster 47 | 71 |
| Figure 21-Stochastic Input pattern when charging from grid is the optimal action for ESS1 | 79 |
| Figure 22-Stochastic Input pattern when discharging to D1 is the optimal action for ESS1 | 80 |

| | |
|---|-----|
| Figure 23- Daily Cost Deviation (%) – a) $\tau= 0$ - b) $\tau= 4$ | 82 |
| Figure 24- Example day electricity price and outputs profile - (a) Purchased electricity from grid, (b) electricity price | 83 |
| Figure 25- Hourly demand profile boxplot (Heating season and cooling season)..... | 84 |
| Figure 26- Deviation from the daily optimal cost when elec. Demand increase by 5% - $\tau= 4$ | 86 |
| Figure 27- Optimal dispatch to 8 demand nodes (Cluster 44)..... | 91 |
| Figure 28- Optimal dispatch to 8 demand nodes (Cluster 46)..... | 91 |
| Figure 29- Optimal dispatch to 8 demand nodes (Cluster 47)..... | 92 |
| Figure 30- Schematic diagram of the proposed model | 98 |
| Figure 31- day-ahead planning - functional diagram..... | 102 |
| Figure 32- a) Boxplot- Number of EVs b) Boxplot - Aggregate capacity of batteries..... | 103 |
| Figure 33- a) Electricity price profile; b) Frequency regulation market clearing price | 104 |
| Figure 34 - a) Boxplot - FR capacity; b) Boxplot - elec. power required for charging; c) Boxplot - elec. power to discharge..... | 104 |
| Figure 35- a) Planned FR capacity; b) Planned net injected power | 105 |
| Figure 36- FR planning risk during different hours of the day | 106 |
| Figure 37- Example 5-node micro-grid | 108 |
| Figure 38 - voltage magnitude and phase at different nodes..... | 109 |
| Figure 39- Parking facility net demand (net injected power): a) without V2G; b) with V2G..... | 110 |
| Figure 40- Average net demand profile..... | 111 |
| Figure 41- Money flow and offered services in the proposed business platform..... | 111 |
| Figure 42: a) Dynamic storage aggregated capacity (kWh); b) % of occupied EV parking spaces | 120 |
| Figure 43: a) Average hourly LMP; b) Average hourly FR credit..... | 122 |

| | |
|--|-----|
| Figure 44- LMP and FR credit (18/4 - 19/4) | 124 |
| Figure 45- LMP and FR credit (2/2 - 3/2) | 125 |
| Figure 46- correlation analysis..... | 127 |
| Figure 47: An illustrative example of a MG configuration..... | 137 |
| Figure 48: Configuration of PV systems..... | 138 |
| Figure 49: Schematic diagram of the top-down approach | 140 |
| Figure 50-The state transition diagram of PV system maintenance mode | 147 |
| Figure 51: MG average annual operation cost with different performances of PV systems (in the existence of storage units)..... | 154 |
| Figure 52: MG average annual operation cost with different performances of PV systems (in the absence of storage units)..... | 155 |
| Figure 53: Comparing average annual total cost for different threshold states "b" of R1 and R2 in two examples..... | 157 |

CHAPTER 1: INTRODUCTION AND RESEARCH BACKGROUND

1.1. Objectives

This thesis intends to construct an integrated framework to model the behavior of complex power network and use it in the optimal short-/long-term planning, real-time operation and control of distributed energy resources (DERs). In this work, we are particularly interested in energy storage and the interaction of it with other network assets. The following lists the main features of such framework:

- **Distributed network-aware control module for long-term planning, real-time operation and control of complex and interconnected power distribution network;** A distributed control model is developed that utilize real-time communication and shared state knowledge of nodes to optimize operational efficiency.
- **Optimal short-/long-term planning module for power distribution networks (or micro-grids);** The operation of such network is formulated as a dynamic programming model. The objective is to minimize the operation cost (supply and delivery cost of power) of power distribution network, and to maximize assets performance (measured by value generated for power distribution network) over a short-/long-term planning time horizon.
- **Supervised learning approach to construct the real-time adaptive control module for network real-time operation;** A control model is formulated with the objective of minimizing the cost of operation in power networks.

- **Utilization of operational information for planning purposes at the asset level;** A continuous time Markovian model is developed to determine optimal maintenance planning for micro-grid assets with objective of minimizing ownership cost.
- **Stochastic representation of DER behavior;** The purpose here is to capture stochastic behavior of DER nodes (state and availability) and utilize these behavioral characteristics in network controls.

1.2. Brief Overview of Thesis Accomplishments

Chapter 2 covers discussion on development of an integrated framework to determine the key factors of the behind-the-meter benefits, generated by individual and combined DERs with storage for various customer facilities. The value of energy storages is assessed by weighing the costs against financial gains and other benefits considering ancillary services in energy market. In this context, critical issues such as configuration of DERs (sizing), demand load profiles and pricing elements of energy providers were studied to specify their impact on energy storage value and total cost of the system. The results from this chapter will be used to motivate energy storage applications, and our formulations in the other chapters.

Chapter 3 extends the current state of art in planning and control of a system with multiple storage nodes distributed over an arbitrary power distribution network. A set of simple but verifiable control strategies, which directly take into account network characteristics and states are developed. In the proposed Network-aware control model near optimal actions are taken in each individual storage unit based on the partial knowledge of the whole

network state. The supervised learning (classification) approach was adopted to construct the real-time adaptive control module for the network of energy storages.

Chapter 4 provides an insight into potentials of using electric vehicle (EV) parking garages (as energy storage with dynamic capacity) to participate in ancillary markets or other applications. We developed an integrated model, which optimally dispatches EVs in a large parking facility to maximize the parking facility benefits. Moreover, the impact of such planning on the power distribution network was quantified. In the planning phase, a queueing model was used to estimate the available aggregate capacity of batteries in the parking facility (energy storage system (ESS) with dynamic capacity) during different times of a day. The risks associated to the stochasticity of the available capacity are also formulated. The hourly charging/discharging for the available capacity is formulated as a mix-integer optimization problem.

In Chapter 5 we present an approach for optimizing operation and maintenance jointly for a microgrid (MG), which contains energy storage. A two-layered approach is developed. In the upper layer, we optimize the operation of MG by solving the optimal power dispatch within a MG network using mix-integer programming. In the bottom layer, by incorporating the upper layer information as input parameters, we use a continuous-time Markov chain model to calculate the optimal maintenance policy for the DERs. The proposed approach could be used in stipulation process between micro-grid owner and DER maintenance provider to optimize economies for both sides.

1.3. Synopsis of Contributions

1.3.1. Evaluation of the behind the meter benefits of energy storage systems with consideration of ancillary market opportunities (Chapter 2)

In this chapter we develop an integrated framework to determine the key factors of the behind-the-meter benefits, generated by DERs coupled with energy storages for different facilities. We analyzed the value of energy storage system by weighting the cost elements against financial gains and other benefits considering ancillary services in energy market. Critical principals such as configuration of DERs (sizing), demand load profiles and energy pricing were studied to specify their impact on energy storage value. We suggest an integrated design approach in which electrical and heating loads and the generation sources are modeled, to take full advantage of excessive electricity and heat generated in the microgrid and enhance the overall system efficiency, by formulating a mixed-integer linear programming (MILP) model. We focus on three applications: (i) Energy Bill Management (EBM), (ii) Frequency regulation (iii) resiliency enhancement.

1.3.2. Network-aware approach for energy storage planning and control in the network with high penetration of renewables (Chapter 3)

In this chapter we present a novel network-aware approach in planning and control of a system with multiple storage nodes distributed over an arbitrary power distribution network. In such power network we are interested in the following problems: (i) Where to locate static storage nodes and how much capacity to allocate to each node for optimal sizing and operation; (ii) How to day-ahead plan for the charge and discharge of these nodes, and (iii) How to control their operation in a near real time basis. Planning and real time control decisions need to be made in reference to the characteristics and state of

constituent elements (nodes and arcs) of the network and the overall control objective. The state description of an element includes, among other attributes, the element's availability and efficiency factors. We present two models: (i) A model for optimal location and capacity planning that also solves for day-ahead operational plan, and (ii) A model for optimal charge and discharge control of storage nodes in a near real time basis. We build a novel rule-based scheme for the near real time control of the storage network by mining the statistical relationship between input and optimal charge and discharge patterns. The supervised learning (classification) approach was adopted to construct the real-time adaptive control module for the network of energy storages.

1.3.3. Energy storage system with dynamic capacity – EV parking lot model (Chapter 4)

In this chapter we develop a novel approach for planning of energy storage with dynamic capacity. EV parking garage located in a distribution power network is considered as an energy storage node with dynamic capacity and stochastic charging demand. We provide an insight into potentials of using EV parking garage to participate in ancillary markets or other applications. We developed an integrated model, which optimally dispatches EVs in a large parking facility to maximize the parking facility benefits. Moreover, the impact of such planning on the power distribution network has been quantified. In the planning phase, a queueing model is adopted to estimate the available aggregate capacity of batteries in the parking facility during different times of the day. The risks associated with the stochasticity of the available capacity are also formulated. The hourly charging/discharging for the available capacity is formulated as a mix-integer problem. One key parameter in this problem is the permission from EV owners for vehicle-to-grid discharge. This parameter

is determined based on the incentive offered by the parking operator to the EV's owner.

1.3.4. Joint optimization of operation and maintenance policies for microgrid composing of energy storage system (Chapter 5)

In chapter 5 we present a novel approach for joint optimization of operation and maintenance of a microgrid (MG), composed of energy storage and considering the dependency between the operation and maintenance policies. The maintenance policies can evidently impact the availability of the DERs in a MG hence impacting its operational control policy. Moreover, an effective energy storage control policy reduces the downtime penalty if the stored energy can be used to satisfy demand during preventive maintenance or failure downtime. We introduce the term “operation dependency” for this problem. A two-layered approach was developed to address this dependency in MG operation and maintenance planning. In the upper layer, we optimize the operation of MG by solving the optimal power dispatch within the MG network using mix-integer programming. In the bottom layer, by incorporating the operation layer information as input parameters, we use a continuous-time Markov chain model to determine the optimal maintenance policy for the DERs.

1.4. Motivation

The reliability and aging of the US power grid, capacity constraints on transmission lines and the need for greener and more sustainable electricity have been driving the technological advances in this field. The penetration of renewable energy into the grid is increasing at a rapid pace. Carbon tax credits and emission control regulations, and the desire for higher degree of geographical proximity of generation to load are rapidly changing the face of the grid. The recent advances in electric battery technologies and the

reduced price of Electric Vehicles (EV) are significantly changing the adoption rate of EVs. These factors are shaping the supply and demand of electricity, and the changes are expected to happen at much higher pace between now and 2050.

Over the past decade, a push has begun for distributed energy resources (DERs), including Combined heat power (CHP), fuel cells, hybrid power systems (solar hybrid and wind hybrid systems), microturbines, photovoltaic systems, reciprocating engines, and more. The rush to DER is fueled by environmental concerns, aging power grid infrastructure and lowered technology cost of renewables. An unprecedented increase of renewable resources, particularly PV systems, has happened in power distribution grids. However, major challenges still remain, including PV power generation volatility due to weather uncertainty; in particular, power production peak of PV or wind farms do not necessarily coincide with peak demand cycles. Therefore, large amounts of valuable renewable generation are usually wasted. Allocation of energy storage systems over the power distribution network increases the hosting capacity of PV and other renewable generations. Energy storage systems can provide multiple benefits to the grid, including the ability to levelize electricity demand, provide ancillary services, and provide reserve capacity. Moreover, installing energy storage improves the resiliency of the power grid. Recently to remove barriers to the participation of electric storage resources in the capacity, energy, and ancillary service markets operated by Regional Transmission Organizations (RTO) and Independent System Operators (ISO), the Federal Energy Regulatory Commission (FERC) enacted FERC Order 841, which increases the adoption of energy storage systems.

With this background in mind, we are motivated to build the necessary tools to design, plan and control the complex network of energy storage systems. To the best of our knowledge,

there is a major gap in understanding how multiple storage units programmed for multiple applications should operate in a distribution network. The proposed approach is applicable to connected energy storage units in distribution networks with multiple applications. Capacity of each node could be static and deterministic or dynamic and stochastic. A good example of energy storage with dynamic capacity is a parking lot with multiple spaces for EV and V2G connections, where arrival and departure of vehicles are random and only a random portion of parked vehicles can serve vehicle to grid flow. Moreover, to the best of our knowledge the impact of energy storage operation on the performance degradation and maintenance strategy of other energy assets over the power distribution network or micro-grid has not been investigated. In this dissertation we intend to fill these gaps by introducing a “Distributed Network-aware Planning and Control model” which aims to minimize the ownership cost of complex interconnected power distribution (or microgrid) network. The optimal planning (both maintenance and operational) and real-time control actions are taken in each individual node based on the partial knowledge of the whole network state, characteristics and state of constituent elements (nodes and arcs), and market condition.

The following chapters are organized as follows: Chapter 2 focuses on the assessment of behind-the-meter value of energy storage system for different types of customer. Critical principals such as configuration of DERs (sizing), demand load profiles and pricing structure of energy providers are investigated to determine the key factors in energy storage evaluation. In Chapter 3, a novel network-aware approach is introduced for planning and control of a system with multiple storage nodes distributed over an arbitrary power distribution network, to determine where to locate storage nodes, how much capacity to allocate to each node, how to day-ahead plan for the charge and discharge of these nodes,

and how to control their operation in a near real time basis. Chapter 4 provides an insight into potentials of using electric vehicle (EV) parking garages (as energy storages with dynamic capacity) in energy market and the impact of such market participation on the power distribution network. Finally, Chapter 5 focuses on the impact of energy storage optimal operation on the long-/short- term maintenance planning of other DERs distributed over microgrid or power distribution network. The operational information produced by control module (introduced in chapter 3) is utilized to determine the optimal maintenance strategy for individual assets to minimize the total owner ship cost.

CHAPTER 2: EVALUATION OF THE BEHIND THE METER BENEFITS OF ENERGY STORAGE SYSTEM WITH CONSIDERATION OF ANCILLARY MARKET OPPORTUNITIES

Abstract

Significant increases in energy prices and price volatility, and recent advances in energy system technologies have raised interest in the potential economic opportunities for distributed energy resources (DERs) and energy storage. Moreover, to remove barriers to the participation of electric storage resources in the capacity, energy, and ancillary service markets operated by Regional Transmission Organizations (RTO) and Independent System Operators (ISO), the Federal Energy Regulatory Commission (FERC) enacted FERC Order 841. Furthermore, increases in DER and energy storage adoption enhance the resiliency of the power grid. In this chapter, we analyze behind the meter benefits and resiliency capability of the price-taking energy storage devices in order to understand the impact of the facility's electricity and thermal demand behavior, energy providers pricing structure, DER configuration, storage capacity, and facility criticality on the storage evaluation assessment. We will the analysis for PJM territory and using simulated data from EnergyPlus reference models of DOE. These are validated models that are typically used for such studies. We develop an integrated design that accounts for different facilities with variant thermal and electrical loads, different DER configurations and different energy tariff structures. The energy storage evaluation projects, conducted by our research team at Rutgers Laboratory for Energy Smart Systems (RULESS) for New Jersey state, motivates

the research undertaken in this work. The results from this chapter will be used to motivate energy storage applications, and our formulations in the subsequent chapters.

2.1. Introduction

Over the past decade, a move has begun on the use of the distributed energy resources (DERs), including Combined heat power (CHP), fuel cells, hybrid power systems (solar hybrid and wind hybrid systems), microturbines, photovoltaic systems, reciprocating engines, etc. DER increasingly plays an important role in power distribution systems [1]. Microgrid is a localized energy system which creates a platform for integrating different DERs into a balanced network to meet the local demand and provide reliable and affordable energy for communities such as commercial, industrial, and federal government consumers [2]. Moreover, at times of main macro-grid failure, a microgrid can operate independent of the larger grid and isolate its generation nodes and power loads from any disturbance without affecting the larger grid. Having the ability to change between islanded mode and grid-connected mode [3-5] provides resiliency solutions to the grid and communities. Microgrids can also cut costs and allow communities to be more energy independent and more environmentally friendly [5].

Energy generation comprises many different types of renewable and non-renewable energy sources technologies [6, 7]. Integrating DERs along with storage systems gives flexibility to the microgrid. Energy storage such as chemical storage (primarily battery, including electric vehicles) and thermal storage (heating or cooling) have the ability to absorb energy from the main grid or local generation and return it later. In this context, energy storage technologies play a key role as they enable the increased use of renewable electricity generation to match energy production to energy demand and independency

from the grid by charging the storage during off peak hours and using it in peak hours [8]. Since some of the distributed generation technologies generate excessive heat, the thermal energy storage represents a fundamental element in the management of thermal demand and results in improving the overall efficiency of the microgrid [9]. Energy storage allows collection of renewable energy during daytimes and using it during nighttimes [10]. Although energy storage devices make energy self-generation achievable by end users, the integration of the DERs along with the thermal and electrical storages create challenges for microgrid management [11]. DERs including Distributed Generations (DG) and storages can be managed and coordinated within a smart grid enabling a collection of energy resources to lower environmental impacts and improve security of supply. DER systems within a microgrid can employ renewable energy sources, such as solar power, wind power, solar biomass, and biogas to reduce the amount of carbon emission significantly. However, it should be noted that the supply of energy from renewable technologies is intermittent or stochastic in nature [12, 13] due to their reliance on weather conditions (i.e. sunlight, wind). The most important benefits of DERs include increased use of local energy resources toward the efficiency, reliability, and resiliency of energy network power in the microgrid, reduced carbon emissions and peak shaving [14]. These factors along with energy management strategies such as demand response, load shifting, and storage management will form a necessitating transition toward a smart grid, a framework for the generation mix of distributed energy resources (DERs) [15, 16]. Moreover, Storage and DR can be combined with DG technologies to achieve greater energy balance [17, 18]. Recently, a new and competitive business has been formed regarding the consumers' enthusiasm for generating and managing their own electricity. In this regard, utilities are

exploring opportunities to provide ancillary services and innovative legislation like incentives, tax credits which are all moving in a direction that makes energy services more beneficiary and attractive. Ancillary service markets include frequency up and down-regulation, net metering, reserve market and others each of which have a bidding structure and different rules, such as the time to react to a utility signal and the minimum asset size, depending on the ISO that the microgrids are operating within [19,20].

Aggregating different DERs and energy storage technologies will be associated with various problems and challenges in control and operation of the microgrid which directly impact the evaluation process. One of the challenges in the smart grids is the scheduling of these integrated DERs and storages to optimize the energy flows within the microgrids to minimize costs. Several studies [21-24] have investigated the optimization of the high-level design of microgrids with distributed generation and storage. In [25] a MILP model has been developed to determine the feasibility of investing in Thermal storage (TS) in interaction with other DERs. Recently, an optimization technique by the same group has been proposed adding cooling storage and electricity export to the model [26]. For isolated systems considering ancillary services a similar work has been done for the DERs' plan and operation[27].

While several studies have considered mathematical modeling of DERs, a very little work has been done to assess the value of DERs and storage systems optimally selected with respect to the consumer's territory as different energy providers have different pricing rate structures, facility demand load profile as well as the right sizing for the specific consumers. Each of these principals has been studied alone. In [28] the authors have shown the need for detailed knowledge of energy end use and their demand load profiles in

determining the capacity and operational strategy of DERs in order to achieve energy balance. From the literature reviewed, it was clear that an area of opportunity exists for a practical tool that can assist decision makers to evaluate the DER projects prior to the investment.

The main objective of this study is to determine the key factors of behind the meter benefits, generated by the individual and combined DERs and energy storage for various consumers, by weighing the costs against financial gains and other benefits. It is also our objective to investigate the effects of these selected DERs on generation scheduling and total cost of the system considering ancillary services in energy market. In this context, critical principals such as configuration of DERs (sizing), different demand load profiles and pricing elements of energy providers have been studied to determine their impacts on DERs' values and total cost of the system. We suggest an integrated design approach in which electrical and heating loads and the generation sources are modeled as mixed-integer linear programming (MILP). We will focus on the following applications: (i) Energy Bill Management (EBM), (ii) Frequency regulation (iii) resiliency enhancement.

The rest of this chapter is structured as follows: In section II we introduce the general set-up of micro-grid network and the major principles considered in this study. Section III describes the modeling approach to optimize the operation of microgrid. In section IV two comprehensive sets of case studies are presented with simulations carried out based on real data for specific period with the results and key findings. Finally, section V presents the concluding remarks of the study.

2.2. Problem statement

In this study, we consider a facility level micro-grid consisting of renewable resource (e.g. PV), CHP system, electric and thermal storages, which are installed behind the meter (BTM). The microgrid also connects to the grid (see Figure 1). The power and thermal energy produced by onsite generation assets – i.e. PV and CHP – will be used to meet electricity and thermal demand at the facility. Onsite generation output may exceed facility demand from time to time. Electric and thermal storage nodes absorb this excessive load. The energy charged from excessive energy can be used to reduce the cost of purchased energy from electricity distribution company (EDC) and gas distribution company (GDC). Moreover, DERs and electric storage can be used to increase the facility cash flow by increasing the net-metering (NM) revenue and participating in PJM frequency regulation market. The following figure depicts the energy flow in such facility level micro-grid.

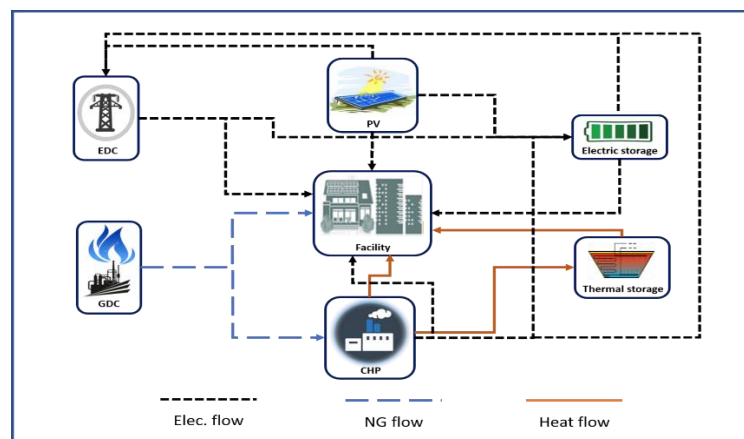


Figure 1- Energy flow in a facility level micro-grid

To quantify and confirm the benefits of BTM DERs and energy storage, an integrated operation model has been developed to illustrate the micro-grid operation. To determine

the key factors in micro-grid evaluation the proposed methodology is demonstrated and verified through use cases along with a sensitivity analysis. The following factors are considered:

- 1) **Facility type:** Three different facilities; namely “hospital”, “full-service restaurant” and “strip-mall” are considered in this study. These are commercial building benchmark models developed by US DOE. For compliance with geographical scope of this project (state of New Jersey), building’s load data is simulated using New Jersey weather data. An overview of these facilities along with their energy consumption characteristics is provided in the following table.

Table 1- Customer segments information

| Segment | Floor area | # floors | Electricity | | Natural Gas | |
|-------------------------|------------|----------|--------------------------|----------------|----------------------------|-------------------|
| | | | Annual consumption (kWh) | Peak load (kW) | Annual consumption (Therm) | Peak load (Therm) |
| Hospital | 241,351 | 5 | 6,500,906 | 1,262 | 97,684 | 38 |
| Strip mall | 22,500 | 1 | 290,780 | 89 | 8,150 | 9 |
| Full service restaurant | 5,500 | 1 | 314,700 | 68 | 9,914 | 6.5 |

These three facilities have different hourly energy profiles, which are illustrated in Figure 2. As shown in this figure, hospital and strip-mall have uncorrelated electricity and thermal demand, however full-service restaurant has correlated profiles. Hospital has the highest energy demand compared to other two facilities. Moreover, hospital and strip-mall have

electricity profile with prolonged peak, but full-service has energy profiles with lots of hills and valleys.

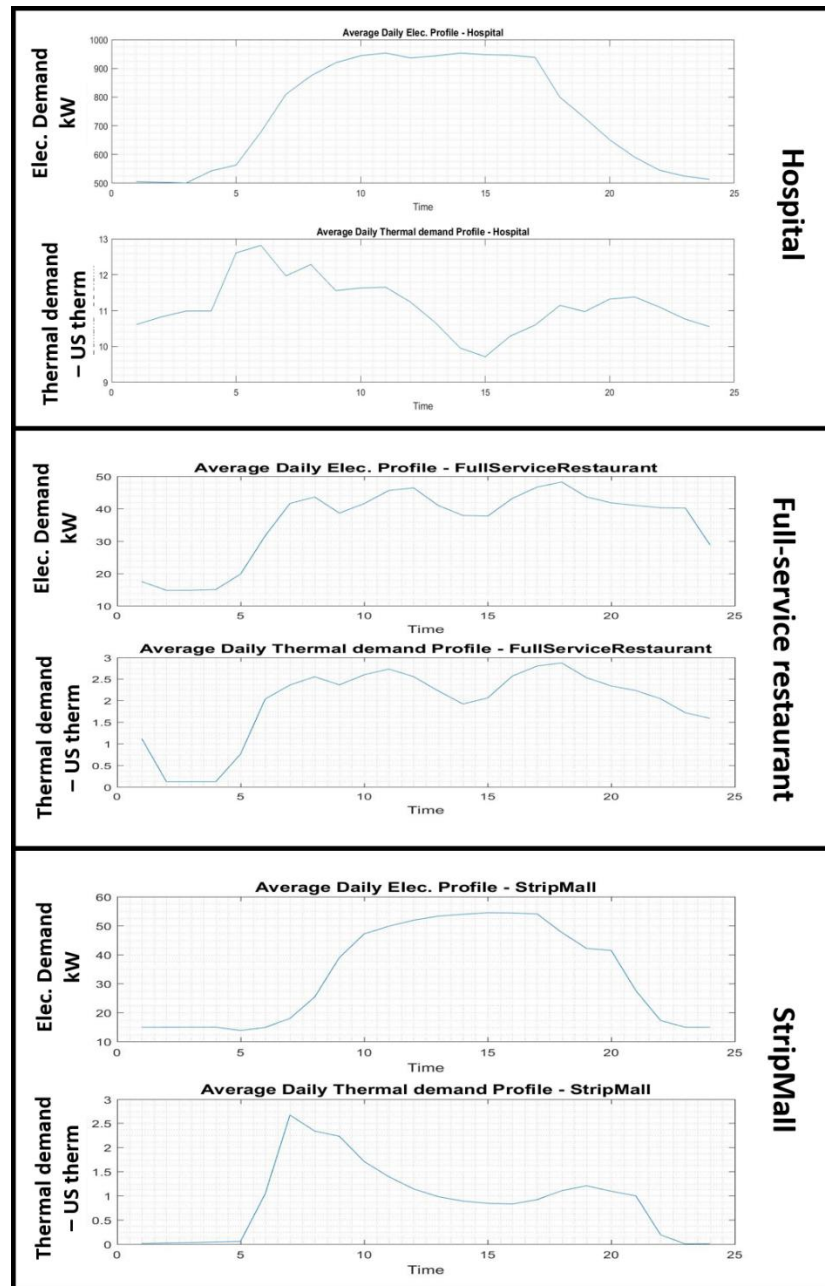


Figure 2- Hourly energy profiles for an average day

In each facility the critical load is defined as the portion of the load that should be severed at emergency incidents during grid outage. Critical load is calculated based on break-down

of end-use electricity load using EnergyPlus building simulation tool and assigning a percentage for critical portion of each end-use. In the following table, critical load for each building segment is provided. It should be noted that defined percentages are not exclusive.

Table 2- Critical loads as a percentage of electricity load of major end uses in building segments

| Strip mall | | Full service restaurant | | Hospital | |
|--------------------|------------------|-------------------------|------------------|--------------------|------------------|
| End use | % of actual load | End use | % of actual load | End use | % of actual load |
| Heating | 80% | Heating | 80% | Heating | 80% |
| Cooling | 80% | Cooling | 80% | Cooling | 80% |
| Interior Lights | 50% | Interior Lights | 50% | Interior Lights | 50% |
| Exterior Lights | 10% | Exterior Lights | 10% | Exterior Lights | 10% |
| Interior Equipment | 50% | Interior Equipment | 50% | Interior Equipment | 50% |
| Fans | 80% | Fans | 80% | Exterior Equipment | 80% |
| | | Pumps | 80% | Fans | 80% |
| | | Refrigeration | 100% | Pumps | 100% |
| | | | | Heat Rejection | 70% |
| | | | | Humidifier | 80% |
| | | | | Refrigeration | 80% |

2) **Energy tariff:** Different locations based on major Electricity and Gas providers' territories in NJ are defined in the set of scenarios. Different Electricity and Gas provider companies have different rating structure for electricity and gas, which affect the calculation in financial evaluation process. Three EDCs and two GDCs in NJ are

considered in this study. EDC billing components considered for analysis are delivery and supply charges. For supply charges, it is assumed that all customers have elected Rider BGS-CIEP indicating that they will be charged according to PJM hourly locational marginal prices (LMPs) for commodity. These three EDCs have completely different rating structures for delivery charges (both energy and demand charges). While EDC1 and EDC2 have seasonal tiered demand charge structure according to customer's peak shared level (PSL), EDC3's seasonal demand charge structure is not sensitive to customers' PSL. Moreover, EDC1 assigns time-of-use (TOU) demand charge for their customers with PSL > 150kW. Following table, summarizes the rating structure across the three EDCs.

Table 3- EDCs rate structure

| EDC1 | EDC2 | EDC3 |
|---|---|---|
| Customer differentiation factor: - PSL (150KW) | Customer differentiation factor: - PSL (750KW) | Customer differentiation factor: - N/A |
| Supply demand charge structure: - BGS CIEP | Supply demand charge structure: - BGS CIEP | Supply demand charge structure: - BGS CIEP |
| Supply energy charge structure: - BGS CIEP (real-time PJM LMP) | Supply energy charge structure: - BGS CIEP (real-time PJM LMP) | Supply energy charge structure: - BGS CIEP (real-time PJM LMP) |
| Delivery energy charge structure: - Seasonal - Flat | Delivery energy charge structure: - Seasonal - Tiered | Delivery energy charge structure: - Seasonal - Flat |
| Delivery demand charge structure: | Delivery demand charge structure: | Delivery demand charge structure: |

| | | |
|---------------------------------------|------------|------------|
| - Seasonal | - Seasonal | - Seasonal |
| - Tiered | - Tiered | - Flat |
| - TOU for PSL > 150KW | | |
| Aggregated KWH and KW charges ranking | | |
| - KWH: EDC3 > EDC2 > EDC1 | | |
| - KW: EDC1 > EDC2 > EDC3 | | |

GDC billing components considered in this analysis are delivery and supply charges. For supply charges, it is assumed that all customers have elected Rider “A” for Basic Gas Supply Service (BGSS). GDCs have completely different rating structures for delivery charges (energy charges, demand charges and balancing charges). Following table summarizes the rating structure across two GDCs.

Table 4- GDCs rate structure

| GDC1 | GDC2 |
|--|---|
| Customer differentiation factor: | Customer differentiation factor: |
| - Monthly consumption peak (3000Therm) | - DG installation - Annual consumption (5000Therm) |
| Supply charges structure: | Supply charges structure: |
| - Rider “A” BGSS | - Rider “A” BGSS |
| Delivery charges structure: | Delivery charges structure: |
| - Energy: Seasonal | - Energy: Seasonal |
| - Demand & balancing: Flat | - Demand & balancing: Flat |
| Aggregated per Therm, per demand Therm and per balancing Therm charges ranking | |

- Per Therm: $GDC1 > GDC2$
- Per demand therm: $GDC2 > GDC1$
- Per balancing therm: $GDC1 > GDC2$

- **** GDC2 incentivizes distributed generation (DG) owner by assigning lower charges**

3) **DER configuration:** Different combinations and sizes of CHP, PV, ES and TS are considered across the use cases. Moreover, since prime-movers have significant impact on CHP efficiency, two different technologies and prime movers are considered in this study:

- a. Fuel cell (SOFC) with heat recovery
- b. Reciprocating engine

Different CHP technologies/prime-movers have different operation and financial characteristics. Following table summarizes the parameters and characteristics of these technologies.

Table 5- CHP prime mover characteristics

| Prime mover | Average electric efficiency | Average heat to power ratio | Average total efficiency | Average installation and maintenance cost over lifecycle (\$/kW) |
|-------------|-----------------------------|-----------------------------|--------------------------|--|
| | | | | |

| | | | | |
|---------------------------------|------------------|------|-------|-------|
| FC | 47% ¹ | 0.87 | 87.9% | 9,500 |
| Reciprocating Engine (RECIP) | 38% | 1.3 | 87.4% | 5,500 |

2.3. Modeling methodology

The operation of facility micro-grid is formulated as a mixed-integer optimization problem to estimate the optimal value generated from DER and storages installation compared to the base-line. This value, along with the other cost elements such as project installation cost, will feed to a cost-benefit analysis model to determine the cost-effectiveness of the project. The model accounts for statistical nature of loads and various technology features and operational conditions of DERs. The model also accounts for different application scenarios. Detailed description of mathematical programming formulation including objectives and constraints for each application is provided next.

As we discussed before three applications are taken into account as objectives of optimization problem. Energy storage (thermal and electrical) and CHP will be utilized to manage net energy consumption (both electrical and thermal) in the facility level. Moreover, electric energy storage and CHP system may participate in ancillary market such as frequency regulation to generate revenue for the facility owner. These are all behind the meter applications, which are the focus of this study. Furthermore, during the power

¹http://www.nyiso.com/public/webdocs/media_room/publications_presentations/Other_Reports/Other_Reports/A_Review_of_Distributed_Energy_Resources_September_2014.pdf

outage event the facility level microgrid will be used to serve the critical demand in the facility, which results in resiliency enhancement. Therefore, two objective functions are pursued:

a) Economic objective function:

$$\min Obj_{economic} = \sum_t [C_t^E + C_t^{NG} + C_t^{CHP} - R_t^{NM} - R_t^{FR}] \quad (2.1)$$

where C_t^E is the electricity cost corresponding to the facility:

$$C_t^E = Pr_t^{elec} (e_t^{dem,g} + e_t^{ch,g}) \quad (2.2)$$

Pr_t^{elec} denotes the electricity price during time step “t”. $e_t^{dem,g}$ and $e_t^{ch,g}$ are the purchased power from electricity distribution company (EDC) to meet electricity demand at the facility and to store in the electric storage respectively.

C_t^{NG} is the cost related to purchasing natural gas from gas distribution company (GDC):

$$C_t^{NG} = Pr_t^{NG} (h_t^{dem,g}) \quad (2.3)$$

where Pr_t^{NG} and $h_t^{dem,g}$ denote the natural gas price and the heat energy purchased from GDC respectively.

C_t^{CHP} represents the operation cost related to CHP system:

$$C_t^{CHP} = \begin{cases} Pr_t^{NG} \left(\frac{e_t^{CHP}}{\eta_t^{CHP}} \right) + \alpha_{st} & \text{if } e_t^{CHP} > 0 \text{ and } e_{t-1}^{CHP} = 0 \\ \alpha_{sd} & \text{if } e_t^{CHP} = 0 \text{ and } e_{t-1}^{CHP} > 0 \\ Pr_t^{NG} \left(\frac{e_t^{CHP}}{\eta_t^{CHP}} \right) & O.W \end{cases} \quad (2.4)$$

e_t^{CHP} and η_t^{CHP} denote the electric power generated by CHP system and CHP electric efficiency. Note that the power generated by CHP will be used to serve the electric demand at the facility and the excessive generation could be stored in the electric storage device. α_{st} and α_{sd} represent CHP startup and shutdown cost respectively.

R_t^{NM} , R_t^{FR} and R_t^{SR} are the revenue generated for facility owner by doing net-metering, participating in frequency regulation market and spinning reserve market respectively.

Net metering is enabled through directly selling power from either PV or electric storage (ES) to the grid:

$$R_t^{NM} = Pr_t^{elec} (e_t^{PV,g} + e_t^{ES,g}) \quad (2.5)$$

where $e_t^{PV,g}$ and $e_t^{ES,g}$ show the electric power flow from PV and ES to the main grid.

In Frequency regulation (FR) application we assume that because of the fast response in ES, it generates revenue from participating in PJM fast regulation market (Reg D market) through capacity commitment and performance revenue. Moreover, CHP system makes benefit from participating in PJM traditional regulation market (Reg A market). Therefore:

$$\begin{aligned} R_t^{FR} = & FR_t^{ES} \times \rho_{ES} (RMCCP_t + \beta_t^{RegD} \times RMPCP_t) \\ & + FR_t^{CHP} \times \rho_{CHP} (RMCCP_t + \beta_t^{RegA} \times RMPCP_t) \end{aligned} \quad (2.6)$$

where, $RMCCP_t$ and $RMPCP_t$ denote Regulation market capacity clearing price (\$/kWh) and regulation market performance clearing price (\$/ΔkW) which are available in PJM website. β_t^{RegD} and β_t^{RegA} are PJM RegD and RegA mileage ratio (ΔkW/kW). Note that $\beta_t^{RegA} = 1$ in PJM market. ρ_{ES} and ρ_{CHP} are performance score corresponding to ES and CHP unit, which indicate units' performance in following the regulation signal. Since

battery storage response is quick, this performance score is close to 1 for ES however this score is around 0.6 for CHP unit. FR_t^{ES} and FR_t^{CHP} are the capacity allocated for regulation at time step “t” by ES and CHP.

b) Resiliency enhancement objective function:

The objective is to serve critical load (CL) during outage hours. Penalty structure in the form of \$/kWh of unserved CL is specified to minimize the unserved critical load to the extent possible. Net metering and ancillary services are disabled since the system is disconnected from the grid.

$$\min Obj_{Resiliency} = \sum_t [M_t^{pen}(CL_t^{unserved})] \quad (2.7)$$

where $CL_t^{unserved}$ is the unserved critical load during time step “t”:

$$CL_t^{unserved} = CL_t^{total} - e_t^{CHP,dem} - e_t^{PV,dem} - e_t^{ES,dem} \quad (2.8)$$

$e_t^{PV,dem}$ and $e_t^{ES,dem}$ respectively represent the power flow from PV and ES to serve electricity demand at the facility. Moreover, $e_t^{CHP,dem}$ denotes the electric power flow from CHP system to demand node.

The operational constraints regarding to different DER technologies are provided next:

c) Operational constraints:

Energy balance constraints at the facility: Both electrical and thermal demands have to be met during the normal operation. Therefor:

$$D_t^e - e_t^{dem,g} - e_t^{CHP,dem} - e_t^{ES,dem} - e_t^{PV,dem} = 0 \quad (2.9)$$

where $e_t^{ES,dem}$ and $e_t^{PV,dem}$ represent the power flow from electric storage and PV to the facility.

For the thermal demand we have:

$$D_t^h - h_t^{dem,g} - h_t^{CHP,dem} - h_t^{TS,dem} = 0 \quad (2.10)$$

where $h_t^{CHP,dem}$ and $h_t^{TS,dem}$ denote the heat flow from CHP system and thermal storage (TS) to serve the thermal demand at the facility.

Constraints of CHP operation: Electrical and heat power produced by CHP system will be used to serve electrical and thermal demand at the facility. The excessive generated energy could be stored at the ES and TS units. Therefore:

$$e_t^{CHP,dem} + e_t^{CHP,ES} = e_t^{CHP} \quad (2.11)$$

$$h_t^{CHP,dem} + h_t^{CHP,TS} = h_t^{CHP} \quad (2.12)$$

The maximum output power of CHP is limited to its nominal capacity and also the committed capacity to RegA market. In addition, if CHP output becomes less than a lower threshold, it should be turned off. The following inequality constraint represents this CHP operational limitation:

$$P_{min}^{CHP} + FR_t^{CHP} \leq e_t^{CHP} \leq P_{max}^{CHP} - FR_t^{CHP} \quad (2.13)$$

The heat power produced by CHP system depends on the prime-mover technology and also the electric power generated by CHP:

$$h_t^{CHP} = \frac{e_t^{CHP}}{\gamma_t^{CHP}} \quad (2.14)$$

where γ_t^{CHP} is the power to heat ratio which depends on the prime-movers technology. Both η_t^{CHP} and γ_t^{CHP} are prime-movers specification and are related to part load ratio (PLR), ratio of electrical generation to maximum CHP power rating:

$$\gamma_t^{CHP} = f_h \left(\frac{e_t^{CHP}}{P_{max}^{CHP}} \right) \quad (2.15)$$

$$\eta_t^{CHP} = f_e \left(\frac{e_t^{CHP}}{P_{max}^{CHP}} \right) \quad (2.16)$$

Two polynomial functions of degree-1 are assumed for $f_h(\cdot)$ and $f_e(\cdot)$.

Constraints of Electrical Storage device: The total amounts of inflow and outflow electricity for ES unit is limited based on its rated capacity:

$$e_t^{ES,dem} + e_t^{ES,g} + e_t^{CHP,ES} + e_t^{PV,ES} + e_t^{ch,g} \leq P_{max}^{ES} \quad (2.17)$$

where P_{max}^{ES} is the rated capacity of ES.

Energy level in ES unit (we define it as state of charge -SOC- in kWh) is moved from one time step to the next. Storage level updating at the end of time step based on the amount of charged and discharged energy.

$$SOC_t^{ES} = SOC_{t-1}^{ES} + \eta_t^{ES,ch} \times (e_t^{CHP,ES} + e_t^{PV,ES} + e_t^{ch,g}) - \frac{e_t^{ES,dem} + e_t^{ES,g}}{\eta_t^{ES,dis}} \quad (2.18)$$

where $\eta_t^{ES,ch}$ and $\eta_t^{ES,dis}$ are the charging and discharging efficiency of ES unit, which are degraded according to ES aging.

It is obvious that storage level cannot exceed its maximum capacity. Also, 20% of safety reserve capacity is considered for storage units. Moreover, the committed capacity in RegD market has to be considered in the ES operational constraints:

$$0.2 \times E_{max}^{ES} + FR_t^{ES} \leq SOC_t^{ES} \leq E_{max}^{ES} - FR_t^{ES} \quad (2.19)$$

where E_{max}^{ES} is the maximum energy capacity of ES (kWh).

Constraints of Thermal Storage (TS) device:

The total amounts of heat charged and discharged in TS unit are limited based on its characteristics:

$$h_t^{CHP,TS} \leq Q_{max}^{TS,ch} \quad (2.20)$$

$$h_t^{TS,dem} \leq Q_{max}^{TS,dis} \quad (2.21)$$

where $Q_{max}^{TS,ch}$ and $Q_{max}^{TS,dis}$ are the maximum thermal storage charging and discharging power.

Thermal energy level in TS unit is moved from one time step to the next. Storage level updating at the end of time step based on the amount of charged and discharged thermal energy.

$$SOC_t^{TS} = \eta_t^{TS,store} \times SOC_{t-1}^{TS} + \eta_t^{TS,ch} \times (h_t^{CHP,TS}) - \frac{h_t^{TS,dem}}{\eta_t^{TS,dis}} \quad (2.22)$$

where $\eta_t^{TS,store}$ is the efficiency ratio for storing heat for one time step in TS unit, which are degraded according to TS aging.

Again, the thermal energy stored in TS cannot exceed its maximum capacity:

$$0 \leq SOC_t^{TS} \leq E_{max}^{TS} \quad (2.23)$$

where E_{max}^{TS} is the maximum energy capacity of thermal storage.

Constraints of PV system:

Electricity generated in renewable unit is used to serve electric demand and charge the ES unit.

$$P_t^{PV} \geq e_t^{PV,dem} + e_t^{PV,ES} \quad (2.24)$$

where P_t^{PV} is the power generated by PV system at time step “t”. Note that the amount of electricity generated by PV is a function of solar radiation and nominal capacity of installed system.

2.4. Illustrative example

In this section, two combinations of DERs are illustrated as case studies. In each case study the impact of DER capacity and characteristics, energy tariff rate and facility energy profiles are studied. These two combinations are listed as below:

- I) PV and electric storage (PV-ES)
- II) CHP, electric storage and thermal storage (CHP-ES-TS)

2.4.1. PV and electric storage (PV-ES)

Different configurations of PV-ES systems are considered across three mentioned facilities. For PV system, it is assumed that installed capacity supplies 80% of annual electric consumption (AEC). For ES system, rated capacities of 50% and 100% of peak critical load (PCL) are considered. In addition, for each rated capacity, duration parameters ranging from 30 min to 5 hours are considered. Analysis of PV-ES system with respect to both resiliency and economics objectives are conducted for each facility, configuration and

EDCs. Detailed cash flow streams for all sizing configurations and EDCs are presented for each facility. Moreover, NPV per installed capacity of ES and resiliency evaluation across different sizing configuration are illustrated. It is worth noting that:

1. For ES resource, round trip efficiency (inverter and storage modules) is set to 90%.
2. Fixed costs associated to ES are: factory cost (~ 400\$/kWh), installation (~ 47% of factory cost), inverter (~300\$/kW), and O&M (~18\$/kW w/ 2% annual growth) costs.
3. Random outage events are generated using Monte Carlo (MC) simulations. 1000 MC simulations are performed.
4. Net metering is done through two resources: directly from PV to grid and discharging ES to grid. It is assumed that net metering will be credited back according to EDC energy tariffs.
5. In outage hours the objective of operation optimization is to serve critical portion of load. Unserved critical load is penalized on \$/kWh basis.
6. It is assumed that PV system is operational during power outage.
7. The investment tax credit (ITC) is included in NPV calculation.
8. NPV calculation is based on facility cash flow improvement compared to the base case, which there is only PV system (without ES) installed at the facility.

Case 1.1- Hospital; PV-ES

Cash flow stream for different configurations of PV-ES systems in a typical hospital facility has been analyzed. Following figures show the net present value of PV-ES project per installed capacity over the period of 4 years according to different EDCs' electricity tariff.

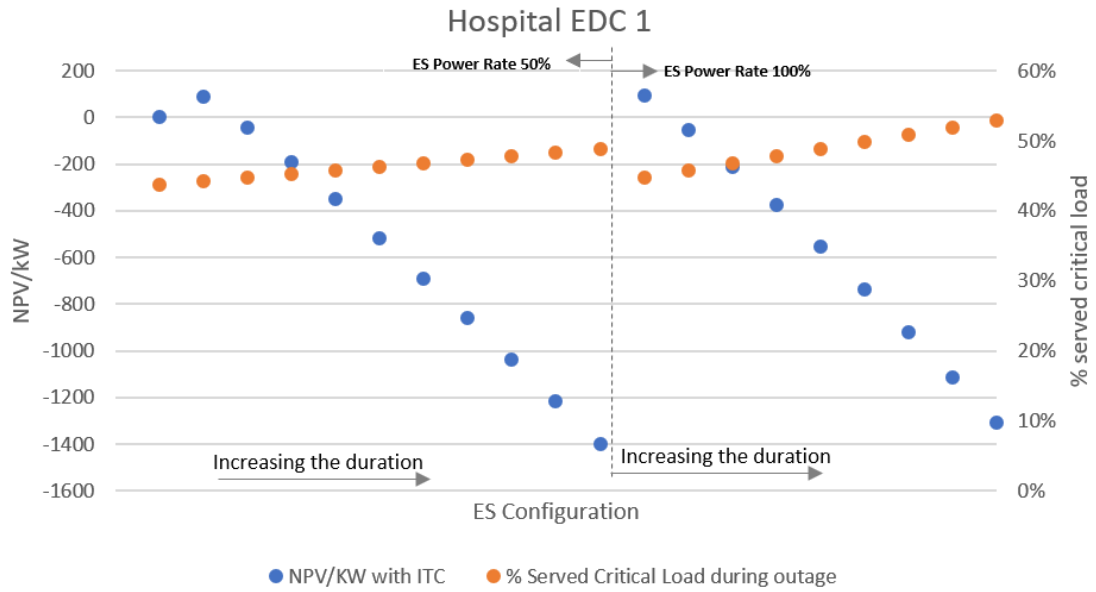


Figure 3- Hospital-EDC1; PV-ES; NPV/kW

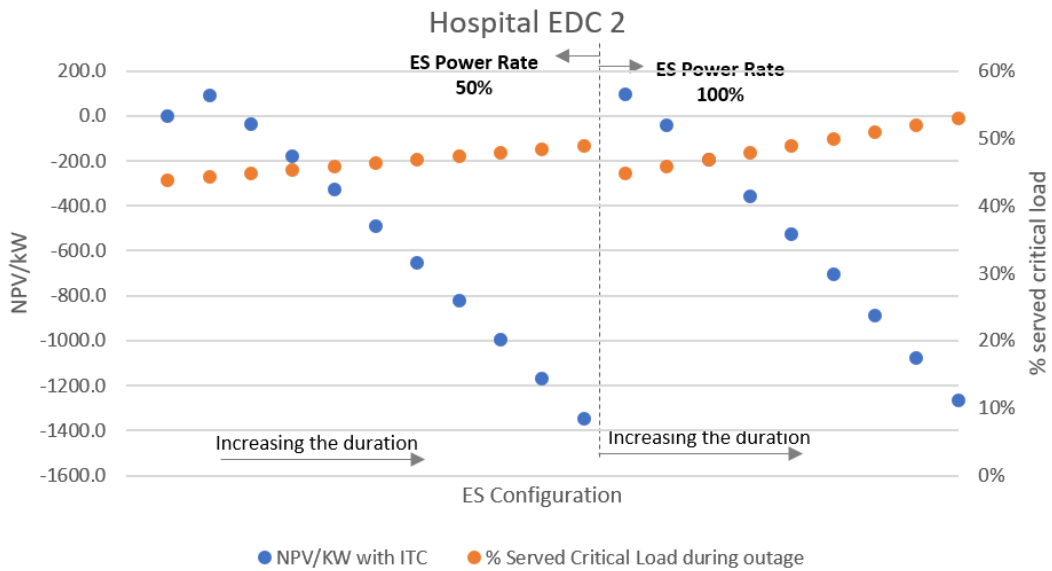


Figure 4-Hospital-EDC2; PV-ES; NPV/kW

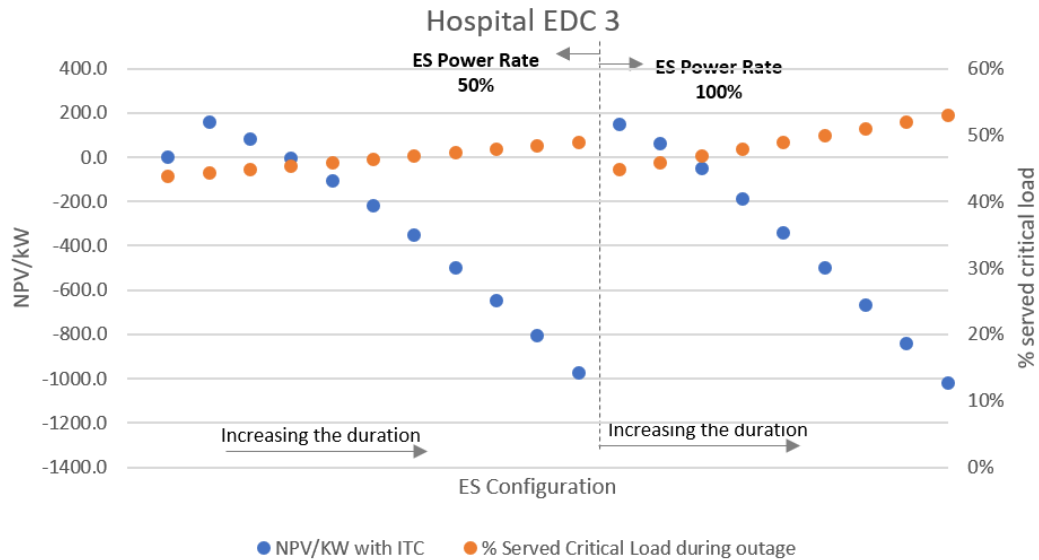


Figure 5-Hospital-EDC3; PV-ES; NPV/kW

As illustrated, increasing the duration of ES system improves the resiliency capability of installed system. Moreover, since EDC 3 has the higher energy charge (\$/ consumed kWh) and this facility has high level of energy consumption, PV-ES system is more beneficial for the customers located in EDC 3 territory. It is also worth to mention that, bigger system with higher duration results in higher cash flow values, however, the additional operational value out of larger systems does not justify the higher up-front cost for these systems. Therefore, the NPV/installed kW is lower for bigger systems.

Case 1.2- Full-service restaurant; PV-ES

Following figures show the net present value of PV-ES project at a typical full-service restaurant per installed capacity over the period of 4 years according to different EDCs' electricity tariff.

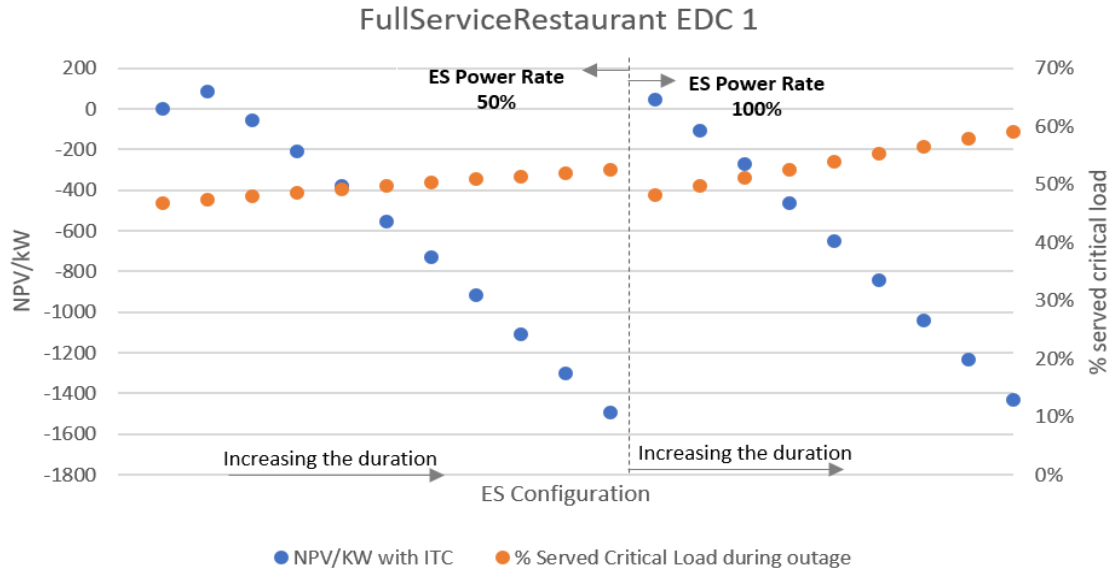


Figure 6-Full service restaurant-EDC1; PV-ES; NPV/kW

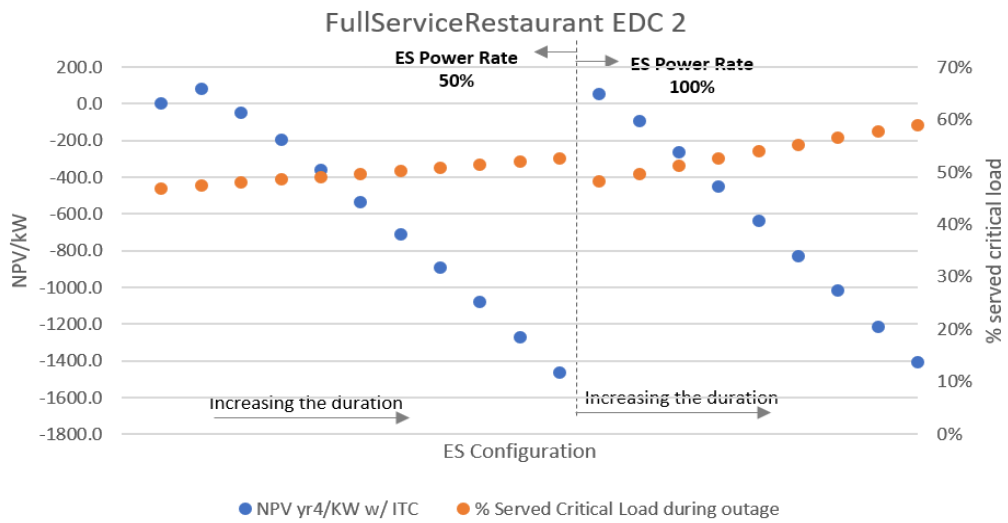


Figure 7-Full service restaurant-EDC2; PV-ES; NPV/kW

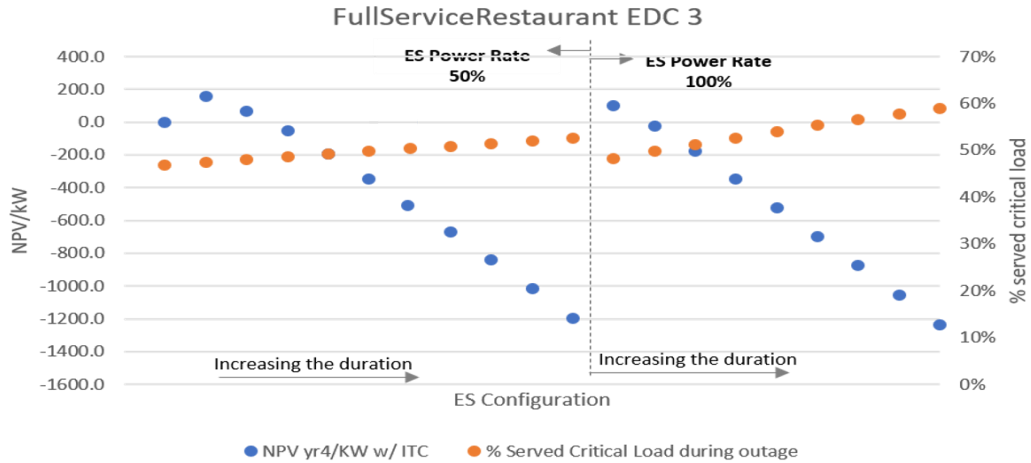


Figure 8-Full service restaurant-EDC3; PV-ES; NPV/kW

As shown in Figure 2, full-service restaurant demand profile has several peaks and valleys. Therefore, increasing the duration of ES system doesn't have significant impact on the facility revenue. In other words, increasing the duration of ES system results in less NPV/installed kW.

Case 1.3- Strip mall; PV-ES

NPV/kW values for a typical strip-mall facility are illustrated in the following figures.

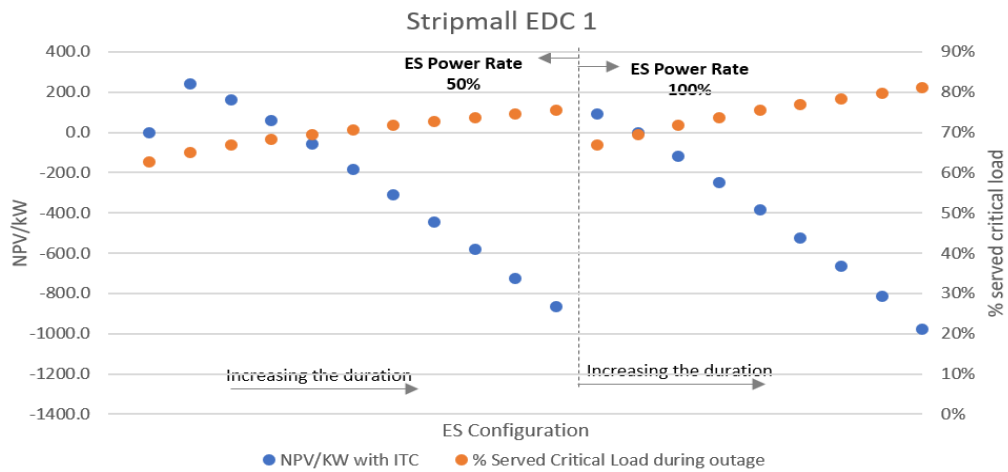


Figure 9-Strip mall-EDC1; PV-ES; NPV/kW

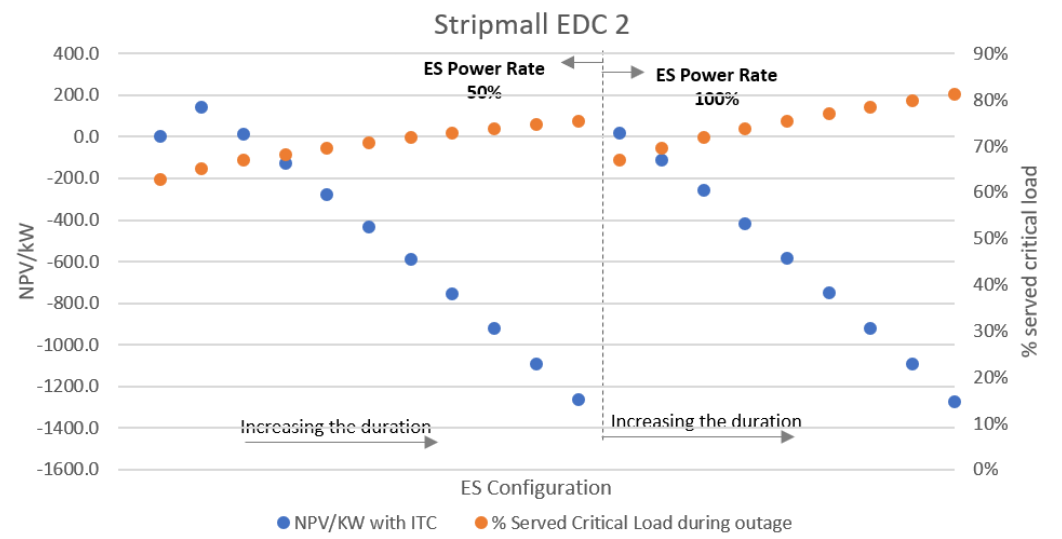


Figure 10-Strip mall-EDC2; PV-ES; NPV/kW

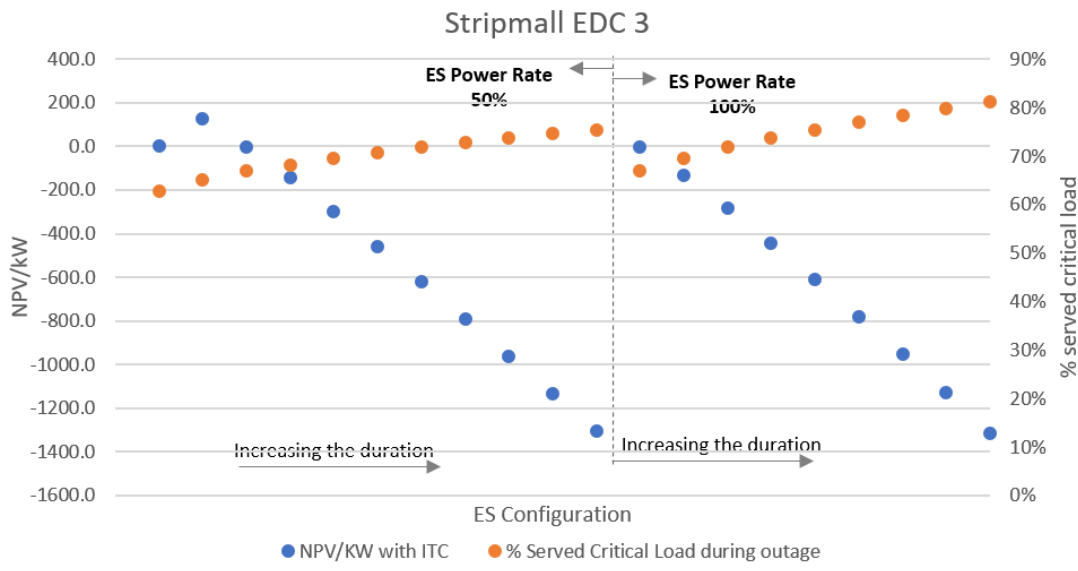


Figure 11-Strip mall-EDC3; PV-ES; NPV/kW

As illustrated, the installed system makes more revenue in the territory of EDC 1. The reason is that, stirp-mall has a high consumption after PV peak hours. Therefore, ES will generate more value if EDC 1 has the high demand charge (\$/kW demand).

According to the results presented for PV-ES case studies (NPV/kW), the following findings are worth mentioning:

- 1) Larger ES systems (both rated capacity and energy capacity) result in higher cash flows. However, the additional operational value out of larger systems does not justify the higher up-front cost for these systems.
- 2) Monetary benefits of larger ES systems depend on customers load shape characterized by peak time, peak duration, and number of peaks.
- 3) ES systems with higher discharging duration result in higher values in the facilities with prolonged peak.
- 4) ES systems with higher rated capacity are more beneficial in facilities with after-hours peak.
- 5) Larger ES configurations are more capable for the resiliency purpose during the outage events, however they cannot be cost effective during the normal operation. That's why critical facilities such as hospitals need incentive for ES installation in their facility to justify the high up-front cost for these configurations.

2.4.2. CHP, Electric storage and Thermal storage (CHP-ES-TS)

For each CHP technology, two different sizing approaches are considered:

- 1) Biggest rectangular method based on the facility electricity demand.
- 2) Biggest rectangular method based on the facility heat demand.

Basically, electricity (thermal) demand values are sorted in decreasing order and placed in a load-duration diagram. Then the dimensioning method (which is based on “biggest rectangle” method) was applied. The intersection of the biggest rectangle with the vertical

axis represent the useful electricity (thermal) output of CHP system. For Electric and thermal storage, rated capacity of 100% CHP electricity and use-full thermal output are considered, respectively. Moreover, one-hour duration is assumed for storage systems. Analysis of CHP-ES-TS system with respect to economics objective is conducted for each facility, CHP technology, configuration and energy provider. Two technologies; namely solid-oxide fuel cell (FC) and reciprocating engine (RECIP), and three combinations of EDC and GDC (according to energy utilities territory map in NJ) are considered. Net-metering is not enabled in this case study. Value of installed configurations and the corresponding pay-back period are illustrated for each use case. Note that all cost saving and additional regulation revenue are calculated by comparing the corresponding configuration and the base configuration (only CHP system), there for these numbers represent the value of ES-TS system.

Case 2.1- Hospital; CHP-ES-TS

Annual cost saving and revenue for different configurations of CHP-ES-TS with different prime-mover technologies and sizing methods in a typical hospital facility located in NJ have been analyzed. Following table demonstrates the economics of these cases.

Table 6- CHP-ES-TS Economics; Hospital

| Hospital | | | | | | | | | | |
|-----------------|-----|-----|--------------------|-----------------------|-------------------------------------|-------------------------|------------------------|-----------------------------|---|--|
| CHP prime-mover | EDC | GDC | CHP rated cap (kW) | Battery capacity (kW) | Thermal storage capacity (US-Therm) | Energy cost saving (\$) | Energy cost saving (%) | Regulation added value (\$) | Total added annual value by storage system (\$) | Simple Pay-back-period for storage system (year) |
| FC | 1 | 1 | 504.57 | 504.57 | 4.92 | 23,130.54 | 4.61 | 20,318.29 | 43,448.83 | 4.46 |
| FC | 1 | 1 | 771.94 | 771.94 | 7.53 | 31,837.26 | 7.94 | 36,579.34 | 68,416.60 | 4.26 |
| FC | 2 | 2 | 504.57 | 504.57 | 4.92 | 17,162.59 | 4.09 | 20,428.13 | 37,590.72 | 5.16 |
| FC | 2 | 2 | 771.94 | 771.94 | 7.53 | 24,895.33 | 7.61 | 36,532.47 | 61,427.80 | 4.74 |
| FC | 3 | 2 | 504.57 | 504.57 | 4.92 | 18,294.35 | 3.64 | 19,870.28 | 38,164.63 | 5.08 |
| FC | 3 | 2 | 771.94 | 771.94 | 7.53 | 32,197.57 | 9.08 | 35,131.57 | 67,329.14 | 4.33 |
| RECIP | 1 | 1 | 328.07 | 328.07 | 7.56 | 18,528.68 | 3.13 | 13,718.87 | 32,247.55 | 4.22 |
| RECIP | 1 | 1 | 504.57 | 504.57 | 11.63 | 23,535.87 | 4.51 | 19,322.10 | 42,857.97 | 4.76 |
| RECIP | 2 | 2 | 328.07 | 328.07 | 7.56 | 13,453.66 | 2.65 | 14,052.51 | 27,506.17 | 4.95 |
| RECIP | 2 | 2 | 504.57 | 504.57 | 11.63 | 17,661.20 | 4.02 | 19,754.03 | 37,415.23 | 5.45 |
| RECIP | 3 | 2 | 328.07 | 328.07 | 7.56 | 11,707.28 | 1.80 | 14,630.81 | 26,338.08 | 5.17 |
| RECIP | 3 | 2 | 504.57 | 504.57 | 11.63 | 17,649.17 | 3.39 | 20,071.09 | 37,720.25 | 5.41 |

As illustrated in Table 6:

- 1) Energy storage system coupled with FC generates more value compared to energy storage coupled with RECIP. The reason is more output power of FC due to its higher electricity efficiency. This results in lower pay-back-period of storage system coupled with FC.
- 2) The additional value out of larger storage systems justifies the higher up-front cost for these systems, therefore, their pay-back-period are lower compared to the smaller systems. The major contributor in bigger system revenue is the frequency regulation market participation.

Case 2.2- Full-service restaurant; CHP-ES-TS

Annual cost saving and revenue for different configurations of CHP-ES-TS with different prime-mover technologies and sizing methods in a typical restaurant facility located in NJ have been analyzed. Following table demonstrates the economics.

Table 7- CHP-ES-TS Economics; Full-service restaurant

| Full-service Restaurant | | | | | | | | | | |
|-------------------------|-----|-----|--------------------|-----------------------|-------------------------------------|-------------------------|------------------------|-----------------------------|---|--|
| CHP prime-mover | EDC | GDC | CHP rated cap (kW) | Battery capacity (kW) | Thermal storage capacity (US-Therm) | Energy cost saving (\$) | Energy cost saving (%) | Regulation added value (\$) | Total added annual value by storage system (\$) | Simple Pay-back-period for storage system (year) |
| FC | 1 | 1 | 34.22 | 34.22 | 0.33 | 3,081.33 | 8.86 | 1,228.00 | 4,309.33 | 5.22 |
| FC | 1 | 1 | 176.45 | 176.45 | 1.72 | 12,322.47 | 26.58 | 12,939.17 | 25,261.64 | 2.94 |
| FC | 2 | 2 | 34.22 | 34.22 | 0.33 | 2,005.77 | 8.02 | 1,221.23 | 3,227.00 | 6.97 |
| FC | 2 | 2 | 176.45 | 176.45 | 1.72 | 8,362.72 | 25.29 | 12,971.79 | 21,334.51 | 3.48 |
| FC | 3 | 2 | 34.22 | 34.22 | 0.33 | 2,266.92 | 8.42 | 1,265.91 | 3,532.82 | 6.36 |
| FC | 3 | 2 | 176.45 | 176.45 | 1.72 | 11,049.92 | 30.91 | 12,970.81 | 24,020.73 | 3.09 |
| RECIP | 1 | 1 | 34.22 | 34.22 | 0.79 | 3,014.77 | 8.49 | 1,191.19 | 4,205.97 | 5.51 |
| RECIP | 1 | 1 | 74.99 | 74.99 | 1.73 | 4,516.54 | 14.21 | 5,468.92 | 9,985.46 | 3.89 |
| RECIP | 2 | 2 | 34.22 | 34.22 | 0.79 | 1,986.34 | 7.76 | 1,189.03 | 3,175.37 | 7.29 |
| RECIP | 2 | 2 | 74.99 | 74.99 | 1.73 | 2,856.97 | 12.56 | 5,477.19 | 8,334.16 | 4.66 |
| RECIP | 3 | 2 | 34.22 | 34.22 | 0.79 | 2,154.37 | 7.84 | 1,266.97 | 3,421.33 | 6.77 |
| RECIP | 3 | 2 | 74.99 | 74.99 | 1.73 | 3,268.32 | 14.11 | 5,483.72 | 8,752.03 | 4.44 |

As illustrated in Table 7 since full-service restaurant has high thermal demand (see Figure 2), second sizing method, which is based on thermal demand suggests very big system. This bigger system increases the energy cost saving and frequency regulation revenue significantly therefore, it has much lower pay-back period. It is worth to mention that the contribution of frequency regulation revenue is more than energy cost saving.

Case 2.3- Strip mall; CHP-ES-TS

Annual cost saving and revenue for different configurations of CHP-ES-TS with different prime-mover technologies and sizing methods in a typical strip-mall located in NJ have been analyzed. Following table summarizes the economics.

Table 8- CHP-ES-TS Economics; Strip-mall

| Strip Mall | | | | | | | | | | |
|-----------------|-----|-----|--------------------|-----------------------|-------------------------------------|-------------------------|------------------------|-----------------------------|---|--|
| CHP prime-mover | EDC | GDC | CHP rated cap (kW) | Battery capacity (kW) | Thermal storage capacity (US-Therm) | Energy cost saving (\$) | Energy cost saving (%) | Regulation added value (\$) | Total added annual value by storage system (\$) | Simple Pay-back-period for storage system (year) |
| FC | 1 | 1 | 49.10 | 49.10 | 0.48 | 3,511.38 | 12.41 | 2,940.69 | 6,452.07 | 4.32 |
| FC | 1 | 1 | 253.90 | 253.90 | 2.48 | 24,195.50 | 43.05 | 17,857.33 | 42,052.84 | 2.44 |
| FC | 2 | 2 | 49.10 | 49.10 | 0.48 | 2,234.02 | 11.20 | 2,940.53 | 5,174.55 | 5.39 |
| FC | 2 | 2 | 253.90 | 253.90 | 2.48 | 16,636.91 | 40.22 | 17,906.31 | 34,543.22 | 2.97 |
| FC | 3 | 2 | 49.10 | 49.10 | 0.48 | 2,447.11 | 11.94 | 2,955.18 | 5,402.29 | 5.16 |
| FC | 3 | 2 | 253.90 | 253.90 | 2.48 | 24,897.99 | 50.17 | 17,905.99 | 42,803.98 | 2.40 |
| RECIP | 1 | 1 | 49.10 | 49.10 | 1.13 | 3,465.34 | 11.61 | 2,879.84 | 6,345.18 | 4.55 |
| RECIP | 1 | 1 | 107.91 | 107.91 | 2.49 | 6,733.81 | 22.36 | 7,588.39 | 14,322.20 | 3.60 |
| RECIP | 2 | 2 | 49.10 | 49.10 | 1.13 | 2,255.97 | 10.68 | 2,886.44 | 5,142.41 | 5.62 |
| RECIP | 2 | 2 | 107.91 | 107.91 | 2.49 | 4,705.41 | 21.48 | 7,611.83 | 12,317.24 | 4.18 |
| RECIP | 3 | 2 | 49.10 | 49.10 | 1.13 | 2,415.28 | 11.17 | 2,943.39 | 5,358.67 | 5.39 |
| RECIP | 3 | 2 | 107.91 | 107.91 | 2.49 | 6,817.17 | 28.39 | 7,624.76 | 14,441.93 | 3.57 |

As illustrated in Table 8, second sizing method, which is based on thermal demand suggests very big system, which increases the annual revenue significantly. As shown in Table 8, the contribution of energy cost saving is much higher (look at the energy cost saving percentage). The reason is that, since in electricity and thermal demand profiles are uncorrelated (see Figure 2) the excessive heat generation during day-time could be stored in the thermal storage and used early morning (peak-time for thermal demand). This phenomenon makes the bigger storage system more beneficial in energy cost saving.

According to the results presented for CHP-ES-TS case studies, the following findings are worth mentioning:

- 1) Larger storage projects generate higher revenue and their pay-back-periods are smaller compared to smaller projects.
- 2) In general, storage systems coupled with FC are more beneficial compared storages coupled with RECIP. The reason is higher output power of FC due to its higher electric efficiency.

- 3) Energy storage systems bring more energy cost saving opportunities in facilities with uncorrelated thermal and electricity demand profiles. The excessive electricity or thermal generation could be stored in storage devices and utilized when demand is high.
- 4) Revenue generated according to frequency regulation market participation is highly dependent on the capacity of electric storage system. Therefore, bigger systems are more beneficial in frequency regulation market.

2.5. Conclusion

This study proposed an integrated design approach to model both electrical and heating loads with generation sources. The idea is to take full advantage of excess heat in microgrid and enhance the overall system efficiency. Behind the meter benefits and resiliency capability of energy storage devices located in the PJM territory were analyzed in order to understand the impact of the facility's electricity and thermal demand behavior, energy providers pricing structure, DER configuration, storage capacity, and facility criticality. Energy bill management, frequency regulation, and resiliency enhancement were taken into account as the energy storage applications. We concluded that the economic benefits of energy storage are highly related to the technology and configuration of other DERs within the facility. For instance, PV-ES system is more beneficial in facilities with after hour electricity peak, but storage devices coupled with CHP system bring more energy cost saving opportunities to facilities with uncorrelated thermal and electricity demand profiles. Moreover the capacity of storage devices has significant impact on resiliency capability and economics of the project. For instance, larger solar powered ES systems result in higher resiliency enhancement, however, their higher up-front cost doesn't justify the economics of project. This emphasizes the vital importance of incentive programs for energy storage

systems to increase the resiliency of power grid during the major outage events. It is worth mentioning that pricing structure of energy carriers also affect the economics of DER-storage significantly.

CHAPTER 3: NETWORK-AWARE APPROACH FOR ENERGY STORAGE PLANNING AND CONTROL IN THE NETWORK WITH HIGH PENETRATION OF RENEWABLES

Abstract

In this chapter, we consider multiple energy storage nodes distributed over a power distribution network and are purposed for multiple applications. The research problems of interests are to optimally locate these nodes over the distribution network and to create day-ahead plans according to planned applications. The two problems are formulated as stochastic optimization problems, and hourly and time-aggregated approximate solutions are presented. The approximation identifies time periods where load and generation patterns demonstrate low variability and marks the whole period as a single time zone, thus significantly reducing the number of decision variables and the overall problem size. We show that aggregate and hourly planning solutions are close. The planning problem can handle any number of storage nodes with general topology and load connections, and deterministic or stochastic capacities. In this chapter, we focus on network of static energy storages with deterministic capacity. Finally, we build a novel rule-based control scheme for the near real time operation of the storage network by mining the statistical relationship between input and optimal charge and discharge patterns.

Nomenclatures

| | |
|---------------|---|
| t | Time index |
| s | Static storage node index |
| j | Demand node index |
| k | Renewable node index |
| i | Temporal Zone index |
| d | Day index |
| y | Year index |
| Sc | Scenario (cluster) index |
| b | Tree index in tree-bagging method |
| CL | Number of clusters |
| γ | Annual inflation rate (%/year) |
| α | Annual discount rate (%/year) |
| $En_{s,max}$ | Storage unit s energy capacity (kWh) |
| $P_{s,max}$ | Energy storage s rated capacity (kW) |
| Inv_s^{Cap} | Investment unit cost on storage capacity (\$/kWh) |

| | |
|-----------------------|---|
| Inv_s^{PR} | Investment unit cost on power rating (\$/kW) |
| $L_{Sc}(j, i)$ | Total electricity demand during zone i at demand node j for cluster Sc (kWh) |
| $R_{Sc}(k, i)$ | Total renewable generation during zone i at renewable node k for cluster Sc (kWh) |
| $L_{d,y}(\cdot)$ | Demand matrix for day “ d ” in year “ y ” |
| $R_{d,y}(\cdot)$ | Renewable generation matrix for day “ d ” in year “ y ” |
| $Pr_{d,y}(\cdot)$ | Electricity price matrix for day “ d ” in year “ y ” |
| $L_{Sc}(\cdot)$ | Representative demand matrix for cluster Sc |
| $R_{Sc}(\cdot)$ | Representative renewable generation matrix for cluster Sc |
| $Pr_{Sc}(\cdot)$ | Representative electricity price matrix for cluster Sc |
| $e_{s,i,Sc}^{ch,g}$ | Total energy charged from grid during zone i in storage unit s for cluster Sc (kWh) |
| $e_{s,k,i,Sc}^{ch,r}$ | Total energy charged from renewable node k during zone i in storage unit s for cluster Sc (kWh) |
| $e_{s,j,i,Sc}^d$ | Total energy discharged during zone i from storage s to demand node j for cluster Sc (kWh) |

| | |
|------------------------|---|
| $e_{j,i,Sc}^{dem,g}$ | Total energy from grid during zone i to demand node j for cluster Sc (kWh) |
| $e_{j,k,i,Sc}^{dem,r}$ | Total energy from renewable k during zone i to demand node j for cluster Sc (kWh) |
| $c_{i,j}$ | Configuration number between nodes i and j |
| $Eff_{ch,s}$ | Energy storage “s” charging efficiency |
| $Eff_{dis,s}$ | Energy storage “s” discharging efficiency |
| $Pr_{Sc}^w(i)$ | Average electricity whole sale price during the hours of zone i for cluster Sc (\$/kWh) |
| Pn_{sub} | Penalty for damage to substation due to reverse flow of power (\$/kWh) |
| Dem | Demand charge for peak demand (\$/kW) |
| $SOC_{s,i}$ | Storage s energy level at the end of zone i (kWh) |
| dr_i | Duration of temporal zone i |
| En^{max} | Maximum energy reservoir capacity |
| P^{max} | Maximum power rating |
| SF_s | Safety reserve capacity for storage unit s |

| | |
|---------------------|--|
| ESL | Storage - Demand Eligibility Matrix |
| ERS | Renewable - Storage Eligibility Matrix |
| ERL | Renewable - Demand Eligibility Matrix |
| ST_t | Network state vector at time t |
| π^s | Control policy for storage s |
| a_t^s | Control action of storage s at time t |
| $rw_t^s(ST, a_t^s)$ | Reward function for storage s when action a_t^s is taken in state ST |
| V^{π^s} | Value storage s under control policy π^s |
| Y | Classification response vector (Control action vector) |
| LR | Level of on-site renewable generation |
| LD | Level of demands |
| EP | Electricity price |
| X | Classification feature matrix |
| B | Number of bags |
| τ | Memory window in control module |
| d_n | n^{th} digit in control action code |

3.1. Introduction

Energy storage (ES) has the potential to offer a new means of added flexibility on the electricity distribution systems. This flexibility can be used in a number of ways, including adding value towards asset management, power quality and reliability. An important factor in evaluating the feasibility of ES technology is the application(s) for which the storage is used for [29]. ES can provide local level services such as, peak shaving and renewable integration ([30] and [31]), and network level services, such as voltage and frequency control [32]. It can also be utilized for loss minimization and deferral of network infrastructure upgrades. With the use of energy storage in a distribution networks for multiple applications, however, comes the challenge of determining how best to control these storage units under load and system state uncertainties. For example, with increasing number of Electrical Vehicles (EVs) the uncertainty in the electricity demand rises due to EV charging demand [33], [34] and [35]. But, on the other hand, Vehicle-to-Grid (V2G) technology, while mitigating some of this uncertainty, can add system dynamics complexities to the network [36], [37] and [38].

Han, et al. [39] and Wong, et al. [40] provide control algorithms to maximize EV owner's profit, which comes from selling power to grid and participating in the frequency regulation market. They formulate the problem as a discrete-time Markov decision process and solve it by introducing an online learning algorithm which iterates every hours based on available information. Koutsopoulos, et al. [41] study the optimal energy storage control problem by taking the point of view of a utility operator and focuses on arbitrage application of energy storage. The authors show that the model can be extended to account for a renewable source that feeds the storage device. The same problem was considered in [42], where the cost of

energy is minimized subject to both user's demands and prices using a Markov Decision Process. Dufo-Lopez, et al. [43] consider the energy storage in private facility to reduce the electricity bill. They conclude that electricity price variation has a great effect on the profitability of storage system. Renewable resource integration is an important application of energy storage, and charge-discharge control policy of energy storage to serve this application is presented by Wang, et al. [44]. Renewable energy sources are considered by Teleke, et al. [45] too, where an open-loop optimal control scheme was developed which incorporates the operating constraints of battery energy storage. They use the battery energy storage in a smoothing application where a wind farm is dispatched on an hourly basis based on the forecasted wind conditions.

Earlier works on component sizing or optimal operation employ different approaches, which are differentiated by decisional variables. Studies that take into account both sizing and scheduling problems are generally scarce. Ru, et al. in [46] determine the optimal size of a grid-connected PV-battery system which is used in an arbitrage application. Their objective is to minimize the net power purchase cost plus battery capacity loss, without considering any initial capital investment. Khalilpour, et al. [47] introduce a decision support tool for sizing and operation of PV-battery system in a single facility, with the objective of maximizing the net present value generated by bill reduction. Zhang et al. [48] introduce a rule based charge and discharge strategy which simultaneously optimizes the battery sizing and operation in a bill management application. The introduced rule-based approach works well for a single PV-battery system within the facility, however the interaction between multiple battery units in more complex distribution network has not been investigated. The similar problem was considered by Brekken et al. [49], where sizing

and control methodologies for a battery-based energy storage system is presented for wind farm applications. The sizing problem of distributed generator and energy storage system (single application – electricity cost reduction) for demand response applications in smart households has been studied in [50] and [51]. Andreotti et al. [52] consider a network of renewable generation units and formulate a single-objective optimization problem whose objective function is power loss minimization while satisfying constraints on active and reactive power at the interconnection bus. Nick et al. [53] studied the optimal allocation of storage systems in an active distribution network by defining a multi-objective optimization problem. The application of renewable generation integration is also considered in [54], [55], [56] and [57]. Van de ven et al. [58] present a battery control policy, which minimizes the total discounted costs, taking into account arbitrage application of energy storage. Jayawarna et al. [59] studied the energy storage power reliability application and present the concept of using central energy storage system as the main fault current source in micro-grid islanded mode.

To the best of our knowledge, there is a major gap in understanding how multiple storage units programmed for multiple applications should operate in a distribution network. This chapter intends to fill this gap by developing simple but verifiable control strategies, which directly take into account system characteristics and states. The proposed approach is applicable to connected energy storage units in distribution networks with multiple applications. More specifically, we consider a system with multiple storage nodes distributed over an arbitrary power distribution network, and given that there are infrastructure limitations on the use of energy storage over this power network. Capacity of each node is assumed to be static and deterministic. Stochastic energy storage nodes are

also possible, and will be examined in chapter 4. A good example of energy storage with dynamic capacity is a parking lot with multiple spaces for EV and V2G connections, where arrival and departure of vehicles are random and only a random portion of parked vehicles can serve vehicle to grid flow [32]. In this chapter, energy storage is considered as a node with two main parameters, namely; energy capacity (in kWh) and rated capacity (in kW). The behavior of storage nodes is deterministic. We also assume that the voltage of nodes across the distribution network will be maintained in the proper feasible region by network operator.

Figure 1 gives an example of a power distribution network with multiple loads or demand nodes, storage nodes, and renewable generation nodes as well as connectivity to a macro power grid. We are interested in the following problems: (i) Where to locate static storage nodes and how much capacity to allocate to each node for optimal sizing and operation; (ii) How to day-ahead plan for the charge and discharge of these nodes, and (iii) How to control their operation in a near real time basis. In this chapter, we use a *network-aware distributed planning and control approach* to solve these problems. Network-aware planning and control is an approach for near real time control of assets in an arbitrary interconnected network. Such a network has multiple nodes with different functionality and criticality. Planning and real time control decisions need to be made in reference to the characteristics and state of constituent elements (nodes and arcs) of the network and the overall control objective. The state description of an element includes, among other attributes, the element's availability and efficiency factors. We will present two models: (i) A model for optimal location and capacity planning that also solves for day-ahead operational plan, and (ii) A model for optimal charge and discharge control of storage

nodes in a near real time basis. This chapter is structured as follows. In Section 2, we describe the first model. Some illustrative case studies for planning phase are demonstrated in Section 3. Section 4 gives a data-driven network-aware control scheme with a number of case studies. To investigate the impact of behavior changes of stochastic input processes on the network planning and control we include sensitivity analysis in section 5. Conclusion and future work are explained in Section 6.

3.2. Optimal Planning

In this study, we consider a power distribution network, which could be utility-owned or a community level micro-grid, with high penetration of renewable resources, such that renewable output may exceed system load from time to time (see Figure 12). The reverse flow of power, resulting from the high level of renewable output and inability to absorb excessive power at loads, could damage the distribution network infrastructure. The storage nodes absorb this excessive power and mitigate the damages (Renewable reverse flow reduction). The energy charged from excessive renewable output can be used to reduce the cost of purchased energy from grid during peak hours, given that renewable peak and price peak do not coincide (Time of Use). The energy charged from renewable during off-peak hours can be utilized during on-peak hours to shave the peak demand as well (Peak Reduction).

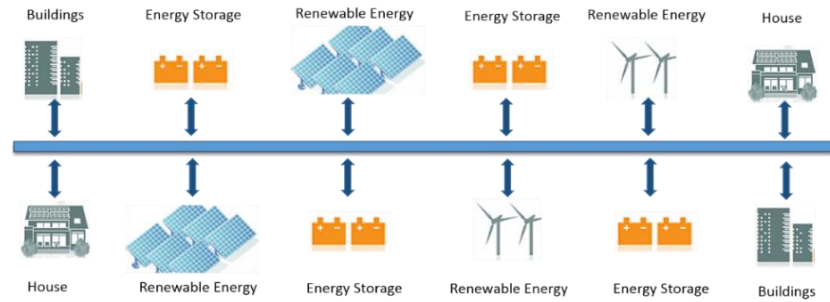


Figure 12: An example circuit with multiple storage units, renewable resources and demand nodes

Here we formulate a stochastic optimal planning problem that takes into account the long-term cost of investment on a network of storage nodes and their short-term operation costs calculated on the basis of day-ahead planning schemes. The formulation is general in such a way that time units can vary from sub-hourly to hourly to more aggregate temporal zones that are constructed on the basis of stochastic pattern changes of some or all of the input sources (e.g., electricity price and power demand). The aggregation is done in a way that the designated input processes have small variations within these temporal zones. Figure 13 illustrates a simple example of the temporal aggregation scheme over three stochastic input processes, namely, renewable generation, demand (in this specific example our network has two demand nodes) and electricity price. Coefficient of variation is used to measure the variation of the stochastic processes. In order to aggregate several hours into one temporal zone, we start from the first time slot (hour 1). The consecutive time slots (hours) are aggregated into a single temporal zone as long as the coefficient of variation (CV) for each input parameter (namely, demand, on-site power generation and electricity price) remains less than the selected threshold (0.3 in this example) for that temporal zone. If adding the next hour increases the inputs' CVs for the current temporal zone to more than 0.3 (in either of the input parameter), that hour is then considered for the next temporal

zone. It is intuitive that decreasing (or increasing) the threshold value for coefficient of variation increases (or decreases) the number of zones in the aggregate model.

Figure 13 (a), (b) and (c) show the example patterns of stochastic input processes. We note that within each temporal zone the input patterns are fixed at their average values (Figure 13.d, 2.e and 2.f). The advantage of the temporal aggregation over common hourly mixed integer programming is that, in the aggregate model, the planning period is decomposed into zones (usually in several hours), and the only variable which is moved from one zone to the next is the state of charge at the end of the zone. By the virtue of this decomposition, a problem with long planning periods and a complex network configuration does not suffer from excessive computational times.

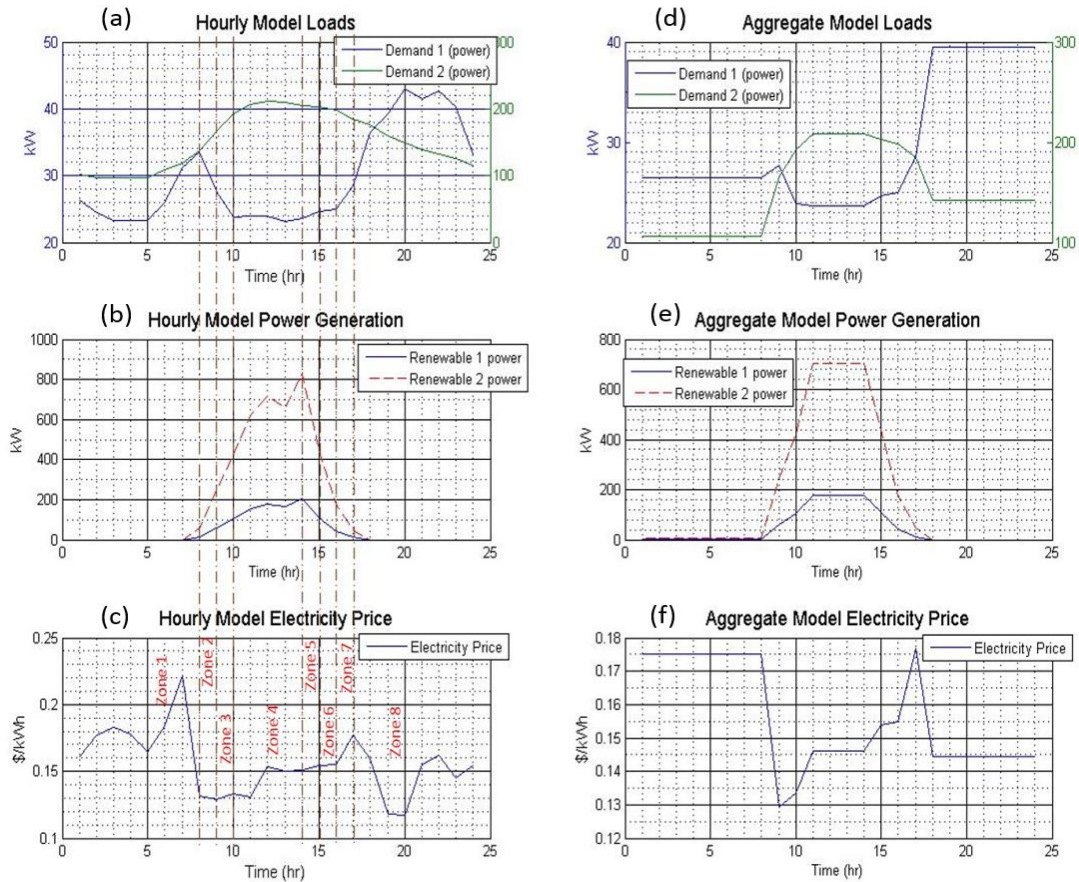


Figure 13-Temporal Zone Aggregation Example

Hereafter, we will use the term *temporal zone* to commonly refer to a time unit (sub-hourly or hourly). The objective function is the total operation and investment cost defined over these temporal zones, and energy storage capacity (both energy capacity and rated capacity), aggregate charge and discharge amounts within each zone (in kWh) are the decision variables. Multiple applications of energy storage are considered, namely, “Time of Use”, “Renewable Reverse Flow Reduction” and “Peak Shaving”. We borrow ideas from the classical multi-period inventory control problem [61], where each temporal zone represents a single period and the remaining energy in storage at the end of each period defines the storage state of charge at the beginning of the next period.

The total cost function is measured in net present value and includes the present value of investment costs and operation costs of the installed nodes during a lifetime period. That is,

$$\text{Minimize } (OBJ_{Inv} + OBJ_{op}) \quad (3.1)$$

For the investment part we have

$$OBJ_{Inv} = \sum_s (CAP_s \times Inv_s^{cap} + P_s \times Inv_s^{PR}) \quad (3.2)$$

where Inv_s^{cap} is investment cost related to the capacity of storage node s (measured in \$/kWh) and Inv_s^{PR} is cost related to power rating of the node (measured in \$/kW). For the short-term operation costs, we must cover the uncertainties over the planning horizon. We assume that input daily profiles of demand, renewable power generation and electricity price each follow a stochastic pattern, and together they can be clustered into groups of profiles over the planning horizon. We note that one can always form such clusters using historical data over the subject distribution network.

Total operation cost (OBJ_{op}) of network will be the sum of daily operation costs over the planning horizon. Daily operation cost is stochastic because of the uncertainty in daily profile of demand, renewable power generation and electricity price.

$$OBJ_{op} = \sum_y \left[\left(\frac{1+\gamma}{1+\alpha} \right)^{y-1} \times \sum_{d=1}^{365} \text{DailyOperationCost}(d, y) \right] \quad (3.3)$$

For the above problem, stochastic scenarios are generated over the stochastic inputs namely, demand, electricity price and renewable power generation, and on the basis of historical data from several years (we choose 3 for illustration). To reduce the computational complexity, we apply a high-dimensional data clustering method [62] to

group these profiles and reduce the number of scenarios [53]. Daily demand profile, electricity price and renewable power generation are considered as features in this clustering. Suppose that a total of “ CL ” clusters of input profiles exist. In each cluster we consider the representative average profile (over a cluster) for each demand node, renewable resources and electricity price. Now, depending on the size of each cluster the chance of its occurrence is calculated ($Prob_{Sc}$):

$$OBJ_{op} = \sum_y \left[\left(\frac{1+\gamma}{1+\alpha} \right)^{y-1} \times \sum_{Sc=1}^{CL} 365 \times Prob_{Sc} \times DailyOperationCost(Sc) \right] \quad (3.4)$$

where γ and α are annual inflation and discount rates (%/year), “Sc” is the index of scenarios according to the input data and $Prob_{Sc}$ is the probability of scenario “Sc”. $DailyOperationCost(Sc)$ is the daily operation cost given scenario “Sc”, which is the representative scenario for cluster “Sc”. Since multiple applications are considered, the daily operation cost includes multiple sections as described below:

- 1- Within each zone a portion of electricity at each demand node is served by the renewable nodes, which are connected to it. Also, a percentage of demand at that demand node is served by discharging energy from its connected energy storage nodes. The rest of the demand plus any amount to be stored in storage nodes are supplied by purchasing electricity from the grid.
- 2- The owner of the distribution system is usually charged for peak demand. High peak demand could also cause more depreciation of distribution devices. Charging storage nodes during off-peak hours and discharging during on-peak hours reduce the peak. Demand charge is usually defined in a monthly term. Here, we use the

same concept in daily planning. In order to consider the hourly peak demand in time aggregate approach we assume that the aggregate power flow is distributed uniformly within each zone.

- 3- It is assumed that the remaining power from renewable creates a reverse flow at the substation if it is not absorbed by storage. Cost of damage to substation due to the reverse power is estimated by multiplying the remaining renewable output by a penalty factor (Pn_{sub}).

The daily operation cost is then given by:

DailyOperationCost(Sc)

$$= (w_1 \times Obj\ 1(Sc) + w_2 \times Obj\ 2(Sc) + w_3 \times Obj\ 3(Sc)) \quad (3.5)$$

$$Obj\ 1(Sc) = \sum_i \left[Pr_{Sc}(i) \left(\sum_j e_{j,i,Sc}^{dem,g} + \sum_s e_{s,i,Sc}^{ch,g} \right) \right]$$

$$Obj\ 2(Sc) = Dem \times \max_i \left\{ \frac{1}{dr_i} \left(\sum_j e_{j,i,Sc}^{dem,g} + \sum_s e_{s,i,Sc}^{ch,g} \right) \right\}$$

$$Obj\ 3(Sc) = \sum_i \left[Pn_{sub} \left[\sum_k R_{Sc}(k, i) - \left(\sum_j e_{j,k,i,Sc}^{dem,r} + \sum_s e_{s,k,i,Sc}^{ch,r} \right) \right] \right]$$

where, $Pr_{Sc}(i)$ is the average electricity price during the hours of zone i for cluster Sc . w_1, w_2 and w_3 represent the importance of different storage applications in the planning phase. The constraints of the above problem are defined in two categories: ESS installation

constraints and operation constraints. “j”, “k” and “s” representing sets of demand nodes, renewable nodes and static storage respectively.

Installation Constraints: Constraints 3.6 and 3.7 show the maximum capacity (energy and power rating) of ESS that can be installed on possible node “s”.

$$0 \leq CAP_s \leq En^{max}, \quad \forall s \quad (3.6)$$

$$0 \leq P_s \leq P^{max}, \quad \forall s \quad (3.7)$$

Operation Constraints: Operation constraints are valid in every scenario (Sc). The total amount of inflow and outflow electricity for each static storage node is limited due to its power rating,

$$e_{s,i,Sc}^{ch,g} + \sum_k e_{s,k,i,Sc}^{ch,r} + \sum_j e_{s,j,i,Sc}^d \leq P_s \times dr_{i,Sc} \quad \forall s, i, Sc \quad (3.8)$$

As we mentioned before, storage level (state of charge) is moved from one temporal zone to the next. Storage level at the end of a zone is calculated based on the amount of energy charged and discharged during that zone. It is obvious that storage level cannot exceed its maximum capacity. Also, SF_s as a safety reserve capacity is considered for storage nodes. Since, according to (O.5), daily operation cost is calculated in objective function the initial state of charge in each individual day will be important. For daily optimization, we assume that all nodes have the same initial state of charge (e.g., 80% of maximum energy capacity (CAP_s)). Furthermore, the SOC of each storage at the end of a day is the same as its daily initial state.

$$SOC_{s,i,Sc} = SOC_{s,i-1,Sc} + Eff_{ch,s} \times \left(e_{s,i,Sc}^{ch,g} + \sum_k e_{s,k,i,Sc}^{ch,r} \right) - \frac{\sum_j e_{s,j,i,Sc}^d}{Eff_{dis,s}} \quad \forall s, i, Sc \quad (3.9)$$

$$SF_s \times CAP_s \leq SOC_{s,i} \leq CAP_s \quad \forall s, i \quad (3.10)$$

We assume that the electricity load at each demand node has to be satisfied, so:

$$L_{Sc}(j, i) = \sum_k e_{j,k,i,Sc}^{dem,r} + \sum_s e_{s,j,i,Sc}^d + e_{j,i,Sc}^{dem,g} \quad \forall j, i, Sc \quad (3.11)$$

Electricity generated by a renewable unit is used to serve demand nodes and charge the storage nodes which are connected to it. The remaining generation from renewable creates a reverse flow of power at the substation.

$$R_{Sc}(k, i) \geq \sum_j e_{j,k,i,Sc}^{dem,r} + \sum_s e_{s,k,i,Sc}^{ch,r} \quad \forall k, i, Sc \quad (3.12)$$

The power distribution network has “S” possible nodes for static ESS installation, “J” demand nodes and “K” renewable resources. Power can flow between two nodes if they are connected physically. The topology of the network is defined by configuration numbers (c_{i_1, i_2}). Configuration numbers have binary value; 1 means physical connection exists. $c_{i_1, i_2} = 1$ means that nodes i_1 and i_2 are connected. Following equations illustrate the network configuration constraints:

$$0 \leq e_{j,k,i,Sc}^{dem,r} \leq M \times c_{k,j} (i) \quad \forall j, k, i, Sc \quad (3.13)$$

$$0 \leq e_{s,j,i,Sc}^d \leq M \times c_{S,s,d} (i) \quad \forall j, s, i, Sc \quad (3.14)$$

$$0 \leq e_{s,k,i,Sc}^{ch,r} \leq M \times c_{k,S_s}(i) \quad \forall s, k, i, Sc \quad (3.15)$$

where, “M” is a very big number (e.g. 10 millions).

Solution methodology is illustrated using the following example.

3.3. Illustrative Example

A modified IEEE 13 node test feeder as a community level distribution system with high penetration of renewable resources is used as a case study (see Figure 14). We start with the clustering of stochastic input profiles and grouping of days in the planning horizon. Then we show optimal capacities for different network configurations with different applications. Finally, the day-ahead operation results will be demonstrated.

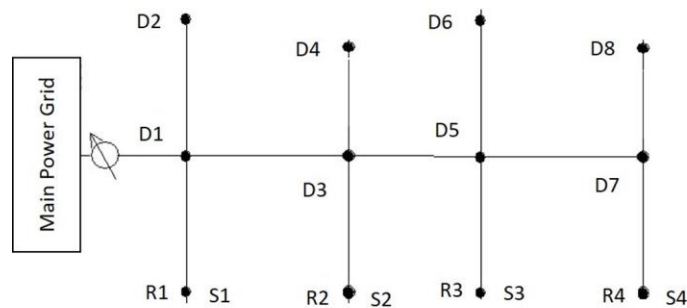


Figure 14 - Distribution network

As shown in Figure 14 eight demand nodes are considered in this network. Four residential sectors are considered in nodes D2, D5, D7 and D8. The other four demand nodes (D1, D3, D4 and D6) assumed to be commercial facilities. Four PV solar systems with generation rated capacity of, respectively, 1500 kW, 1600 kW, 800 kW and 600 kW are assumed as renewable resources at nodes R1 - R4. The hourly power generation of these nodes is related to hourly solar intensity (radiation). We assume the same solar radiation at the

locations of solar systems. Four nodes with renewable resources are considered as the potential nodes for energy storage installation.

Following eligibility matrices are assumed in this case study:

$$ESL = \begin{matrix} & D1 & D2 & D3 & D4 & D5 & D6 & D7 & D8 \\ S1 & \left[\begin{array}{cccccccc} 1 & 1 & 1 & 1 & 1 & 1 & 1 & 1 \end{array} \right. \\ S2 & \left[\begin{array}{cccccccc} 0 & 0 & 1 & 1 & 1 & 1 & 1 & 1 \end{array} \right. \\ S3 & \left[\begin{array}{cccccccc} 0 & 0 & 0 & 0 & 1 & 1 & 1 & 1 \end{array} \right. \\ S4 & \left[\begin{array}{cccccccc} 0 & 0 & 0 & 0 & 0 & 0 & 1 & 1 \end{array} \right. \end{matrix}$$

$$ERL = \begin{matrix} & D1 & D2 & D3 & D4 & D5 & D6 & D7 & D8 \\ R1 & \left[\begin{array}{cccccccc} 1 & 1 & 1 & 1 & 1 & 1 & 1 & 1 \end{array} \right. \\ R2 & \left[\begin{array}{cccccccc} 0 & 0 & 1 & 1 & 1 & 1 & 1 & 1 \end{array} \right. \\ R3 & \left[\begin{array}{cccccccc} 0 & 0 & 0 & 0 & 1 & 1 & 1 & 1 \end{array} \right. \\ R4 & \left[\begin{array}{cccccccc} 0 & 0 & 0 & 0 & 0 & 0 & 1 & 1 \end{array} \right. \end{matrix}$$

$$ERS = \begin{matrix} & S1 & S2 & S3 & S4 \\ R1 & \left[\begin{array}{cccc} 1 & 0 & 0 & 0 \end{array} \right. \\ R2 & \left[\begin{array}{cccc} 0 & 1 & 0 & 0 \end{array} \right. \\ R3 & \left[\begin{array}{cccc} 0 & 0 & 1 & 0 \end{array} \right. \\ R4 & \left[\begin{array}{cccc} 0 & 0 & 0 & 1 \end{array} \right. \end{matrix}$$

As an example based on the defined eligibility matrices, storage at node S2 can be charged from renewable R2. Furthermore, this storage node can serve electricity demand in nodes D3 to D8.

The following assumptions are considered in this case study:

- 1- Sodium-Sulfur energy storage with 15 years lifetime is candidate technology to install as energy storage system.
- 2- According to [63] 350 \$/kWh and 350 \$/kW are considered as investment unit cost related to ESS energy capacity and power rated capacity (Inv_s^{Cap} and Inv_s^{PR}).
- 3- Both charging and discharging efficiency are assumed at 90%.

- 4- 5% power loss is assumed for long distance transmission. Note that nodes shown in Figure 14 are grouped into four classes, class 1 includes D1, D2, R1 and Storage 1, class 2 contains D3, D4, R2 and Storage 2. D5, D6, R3 and storage 3 are in class 3 and class 4 includes the other nodes. Transferring power between two different classes is considered as long distance transmission.
- 5- $\gamma=2\%/year$ and $\alpha=10\%/year$ are assumed as annual inflation and discount rate [35].

Three years data for residential and commercial sectors, solar radiation and electricity price are grouped into several clusters. High Dimensional Data Clustering (HDDC) method is used to allocate input data into smaller number of groups [62]. This method is available in CRAN server and can be used in R. By applying HDDC algorithm, three years input data are grouped into forty-eight (48) clusters with each cluster associated with daily operation cost that varies in a small range. Figure 15 shows the input data with hourly mean value in one of these 48 clusters. More information about these clusters can be found in appendix “A1”. The cluster shown in Figure 15 (cluster 13) has population size of 41. All of these 41 individual input data are within a heating season, specifically from December to February. Since the total sample size is 1095 (3×365), the probability of having inputs similar to data in cluster 13 is $41/1095 = 0.0374$.

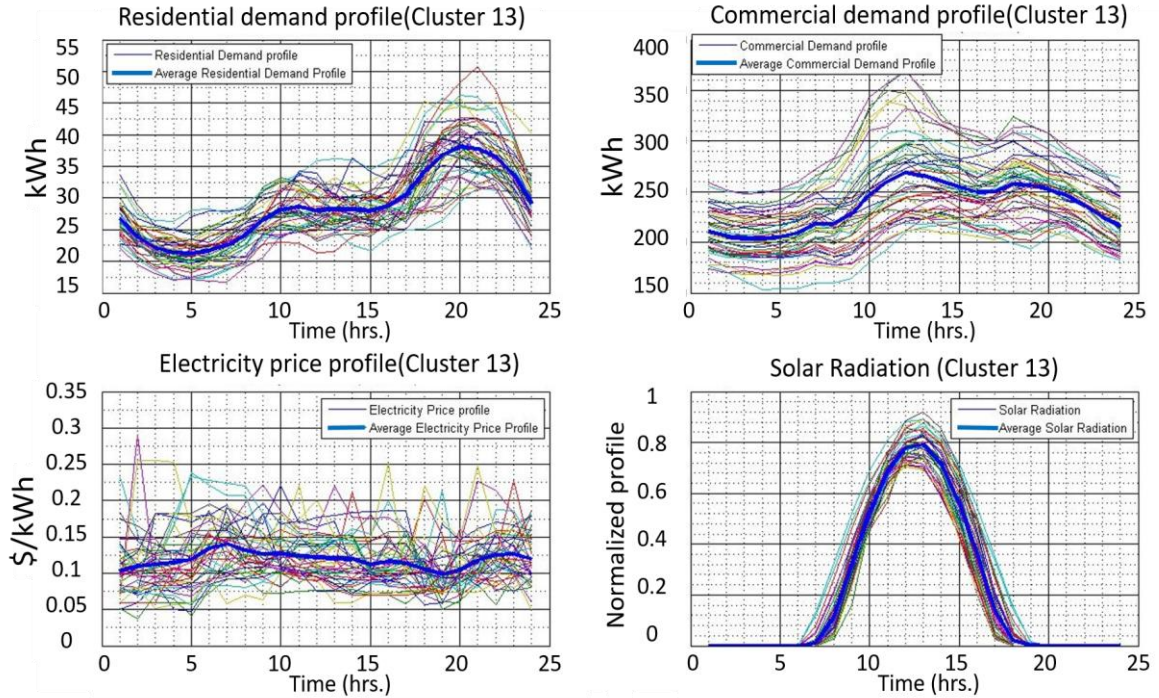


Figure 15- Input data in cluster 13

Next, we present our results for the optimal capacity planning with different weights for different storage applications. This will be followed by the optimal operation planning for some sample clusters.

3.3.1. Capacity Planning

The capacity planning optimization problem is solved using both hourly and aggregate temporal zones. The same optimal capacity plans were obtained from both cases; the reason being that the variation of stochastic input processes within each temporal zone is small, as per approximation scheme. Multiple applications of storage with weights w_1 , w_2 and w_3 are considered in both cases. Note that each storage application has its own cost elements, and using these weights we are able to obtain a weighted objective function that includes multiple applications. Table 9. **Error! Reference source not found.** shows four different

combinations of storage applications with different weights. In the first three cases a single application is considered in planning and in the last case (Case 4) multiple applications are investigated. This table also shows the optimal capacity for these cases.

Table 9-Capacity Planning Results

| Case | (W ₁ , W ₂ , W ₃) | Storage 1 | | Storage 2 | | Storage 3 | | Storage 4 | |
|------|---|-------------------|-----------------------|-------------------|-----------------------|-------------------|-----------------------|-------------------|-----------------------|
| | | Capacity (kWh) | Power Rate (kW) | Capacity (kWh) | Power Rate (kW) | Capacity (kWh) | Power Rate (kW) | Capacity (kWh) | Power Rate (kW) |
| 1 | (0, 1, 0) | 17000 | 1500 | 700 | 90 | 290 | 40 | 690 | 90 |
| 2 | (0, 0, 1) | 0 | 0 | 0 | 0 | 80 | 20 | 1500 | 300 |
| 3 | (1, 0, 0) | 6200 | 2000 | 6600 | 2200 | 1000 | 300 | 600 | 120 |
| 4 | (1, 1, 1) | 10000 | 1500 | 2000 | 500 | 900 | 160 | 1800 | 300 |

Clearly, capacity plans depend on the intended storage applications. For instance, for renewable reverse flow reduction application installing storage system in nodes S3 and S4 is sufficient. The reason is that renewable R1 and R2, which respectively can charge storage S1 and S2, are serving more electricity demands, therefore there exist less excessive reverse power flow in these two nodes. In the following section the day-ahead planning results will be demonstrated for some sample clusters. The hourly model is used for the day-ahead planning problem. The results from the aggregate model are then compared to the results from the hourly model.

3.3.1.1. Aggregate model Validation

In the aggregate model electricity flows from the main grid and DER resources are distributed uniformly within each temporal zone. Hence, the aggregate state of charge at storage nodes and the overall objective function are expected to closely approximate the hourly results. Moreover, one would expect that the computational complexity of the aggregate model to be significantly lower than the exact hourly model especially for large networks and higher temporal resolution. Next, we compare the results of aggregate model to the exact hourly model. Note that both aggregate and hourly models produce the same optimal sizing. We illustrate results from one of the representative clusters that we will later use for daily planning, as shown in Table 10. Figure 16 compares the state of charge of ESSs in hourly and aggregate models when the optimal configuration of case 3 (EBM application) is installed in the distribution network and inputs come from cluster 47.

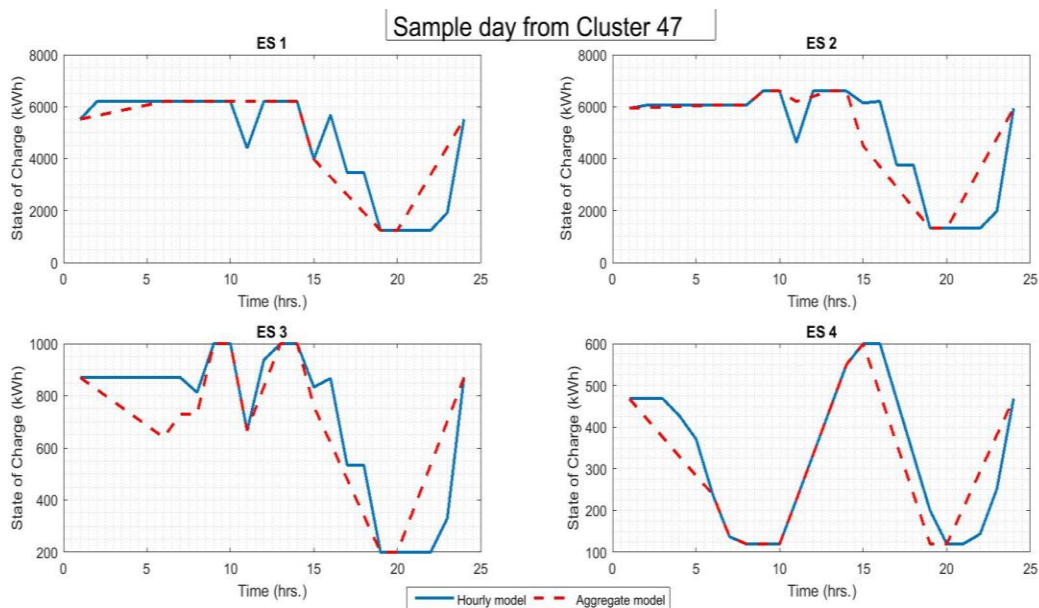


Figure 16-Aggregate model vs. Hourly model (SOC), Application: EBM

As demonstrated in the above figure the state of charges at the end of each temporal zone in aggregate model are close to the hourly model. Table 10 compares the two models in different cases. As illustrated in Table 10 the values of objectives in aggregate and hourly model are close.

Table 10- Aggregate model vs. Hourly model (inputs from cluster 47)

| Case | Application | Electricity Cost (\$) | | Peak value (kW) | | Total Reverse Flow (kWh) | |
|------|------------------------|-----------------------|-----------|-----------------|-----------|--------------------------|-----------|
| | | Hourly | Aggregate | Hourly | Aggregate | Hourly | Aggregate |
| 1 | Peak shaving | | | 7,331 | 7,849 | | |
| 2 | Reverse flow reduction | | | | | 0 | 0 |
| 3 | EBM | 46,246 | 47,498 | | | | |
| 4 | Bundle | 46,940 | 48,044 | 7,696 | 7,912 | 0 | 0 |

Recent table compares the objective values for different cases for one specific cluster. Analyzing the results from aggregate model shows the little error for all input clusters. Following Table 11 illustrates the mean value and standard deviation of error over all input clusters for each objective in different applications.

Table 11 - Percentage error over all input clusters (Aggregate model vs. Hourly model)

| % error for each objective for different applications (average over all clusters) | | | | |
|---|-------------|-----------------------|-----------------|--------------------------|
| Case | Application | Electricity Cost (\$) | Peak value (kW) | Total Reverse Flow (kWh) |
| | | | | |

| | | Mean value | Standard deviation | Mean value | Standard deviation | Mean value | Standard deviation |
|---|------------------------|------------|--------------------|------------|--------------------|------------|--------------------|
| 1 | Peak shaving | | | % 6 | % 1.5 | | |
| 2 | Reverse flow reduction | | | | | % 0.2 | % 0.05 |
| 3 | EBM | % 3.5 | % 0.8 | | | | |
| 4 | Bundle | % 3 | % 0.6 | % 5.5 | % 1.2 | % 0.2 | % 0.05 |

Table 11 verifies that proposed aggregate model is a good approximation for exact hourly model in day-ahead planning. Using aggregate model lowers the computational complexity of optimization problem significantly. For instance, in our example case (Figure 14 - Distribution network, which is defined by configuration matrices ESL, ERS and ERL; there are 56 possible directions for power flow in the distribution network. Also as mentioned earlier 48 input clusters exist based on historical input data. Using hourly model results in $56 \times 48 \times 24 = 64512$ operational decision variables in the capacity planning problem, however, using the aggregate model reduces the decision variables to $56 \times 672 = 37632$ (almost % 45 reduction). Reduction in the number of decision variables has a significant value especially in the complex and large networks.

3.3.2. Daily Operation Planning

In this section, daily operation planning for different capacity configuration are discussed for some sample input clusters. For each capacity arrangement the impact of different

application weighting values on daily operation planning are studied. For daily operation planning analysis, we focus on three different clusters of input data (clusters 44, 46 and 47) - Figure 17 shows the mean value of input data for these clusters. Cluster 44 has low level residential demand, but a high-level commercial demand. It also represents days with medium-level of solar intensity. Cluster 46 has low levels of residential and commercial demand with a high-level of solar intensity. Cluster 47 represents days with a high mean value and variance in hourly electricity price. Both residential and commercial nodes have a high-level of demand in this cluster.

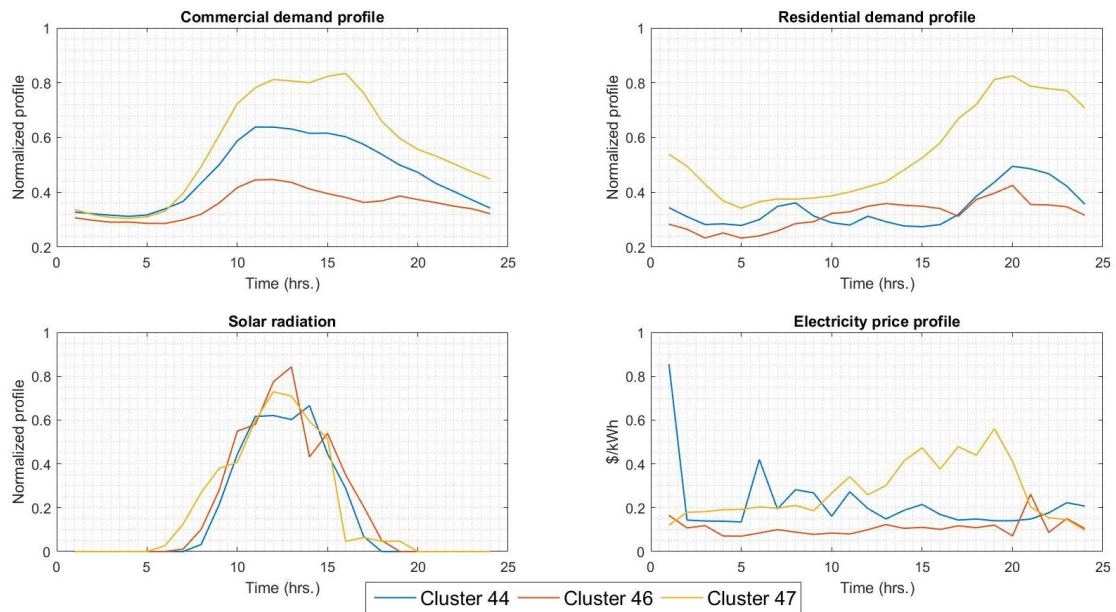


Figure 17- Average Input data in clusters 44, 46 and 47

In each cluster, a 24-hours planning horizon is divided into temporal zones and used to find the optimal amount of charge and discharge for a given cluster representative profiles. Table 12 shows the number of zones and their duration (in hours) for each input cluster.

Table 12 - Local zones' duration for different clusters (Clusters 44, 46 and 47)

| Cluster Number | Number of temporal zones | Duration of temporal zones |
|----------------|--------------------------|-----------------------------------|
| 44 | 13 | [1,4,1,1,1,1,1,2,2,1,1,1,7] |
| 46 | 16 | [3,4,1,1,2,2,1,1,1,1,1,1,1,1,1,2] |
| 47 | 12 | [6,1,1,1,1,1,2,1,1,4,1,4] |

In this example, we assume that ESS units are installed for TOU application to reduce the cost of purchasing electricity from the main grid. So according to the capacity planning results, shown in Table 9, ESSs with capacities given by case 3 are installed in the subject distribution network. Based on capacity planning results, this configuration is optimal when reducing the cost of purchasing electricity from grid is the only goal for ESS installation. Figure 18, Figure 19 and Figure 20 show the optimal power dispatch of DER assets (renewable resources and energy storages) to demand nodes 1 and 8 when the input data, respectively, come from clusters 44, 46 and 47. Note that aggregate model is used to find the optimal dispatch and aggregated amount of power is depicted uniformly within each temporal zone in these figures.

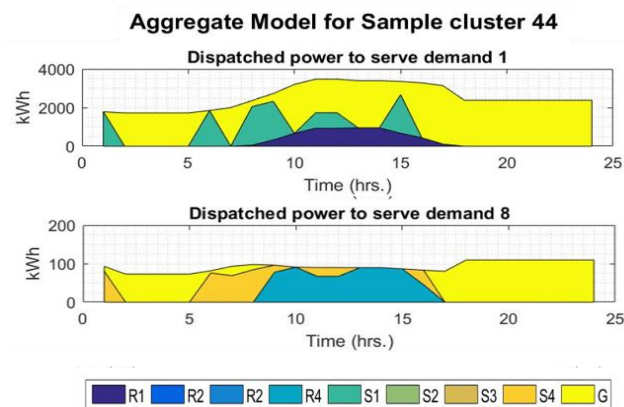


Figure 18- DER optimal dispatch with input data from cluster 44

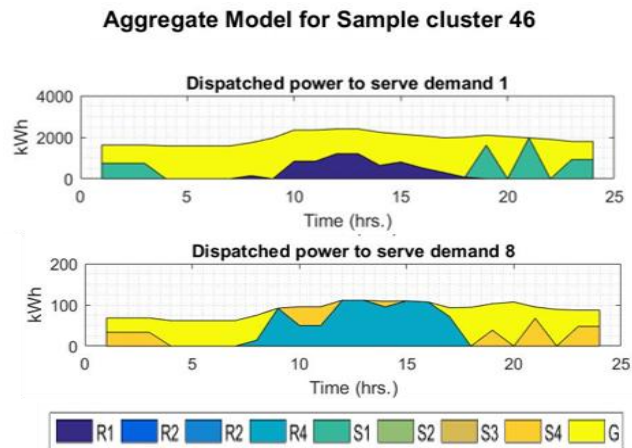


Figure 19- DER optimal dispatch with input data from cluster 46

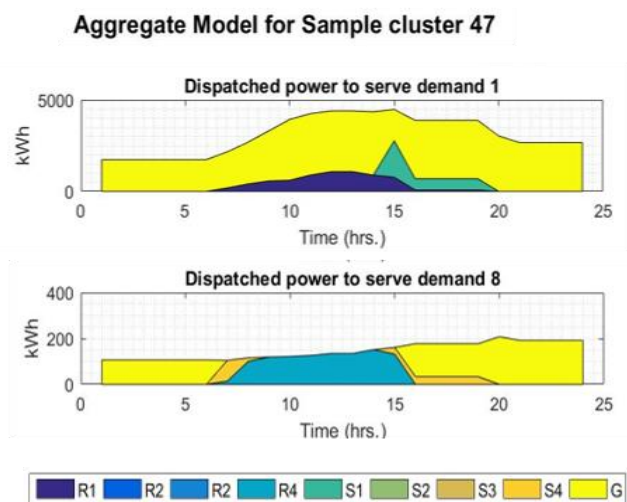


Figure 20- DER optimal dispatch with input data from cluster 47

As illustrated in the above figures the optimal dispatch of DER resources is sensitive to input profile. For instance, in all the three clusters a major portion of demands are satisfied from renewable resources during the noon time when sunlight is available, and stored energy in ESSs is utilized in peak price periods. As shown in Figure 17 peak price times are different in the three representative clusters. In cluster 44 peak price is at 1:00 AM and as illustrated in Figure 18 during that period stored power in ESS is discharged to supply electricity demand and reduce the network electricity cost. The above figures also show

that the configuration of network affects the dispatch of DERs. For example, demand 8 is connected to all storage and renewable resources, but because of the higher power loss in long transmission, R4 and S4 are used to serve this demand node. As another example, D1 could be served only by R1 and S1, so these two resources are used to provide electricity to D1. The optimal dispatch of DERs to other six demand nodes are presented in appendix “A2”. Finally Table 13 illustrates the interaction between storage application and optimal operation for input cluster 47.

Table 13-peak value, total reverse flow and total electricity cost for different ESS applications

| Case | Weights ([w ₁ ,w ₂ ,w ₃]) | Application | Peak value (kW) | Total Reverse Flow (kWh) | Electricity Cost (\$) |
|------|--|------------------------------|--------------------|-----------------------------|--------------------------|
| 1 | [0,1,0] | Peak shaving | 7,849 | 955 | 48,499 |
| 2 | [0,0,1] | Reverse flow reduction | 9,313 | 0 | 50,376 |
| 3 | [1,0,0] | EBM (Energy Bill Management) | 8,559 | 374 | 47,498 |
| 4 | [1,1,1] | Bundle | 7,912 | 0 | 48,044 |

3.4. Network-Aware Real-Time Control

The above Day-ahead planning was performed based on the forecast of stochastic input processes. But what happens if the real-time inputs are not close to the forecast values? For real time control, one could always update the forecast values of input patterns and repeatedly carry online optimization by solving the optimization problem at some predefined time steps [64] and [65] (on-line optimization). Running on-line optimization for complex networks with large number of components and inputs is not practical,

however. Here, we propose a rule-based control approach that determines the optimal real-time actions for each storage node by monitoring the state of components and inputs across the network. We adopt a reinforcement learning approach and build a control policy, which maps the actions and network state, by a supervised learning classification model.

In the proposed Network-aware control model the near optimal actions are taken in each individual storage unit based on the partial knowledge of the whole network state. The state space SS of the distribution network is defined by: (i) electricity consumption trend at demand nodes, (ii) renewable power generation trend at renewable nodes, (iii) state of charge at each storage unit, and (iv) electricity price trend. That is,

$$ST_t = [LD_{d,t-\tau}, \dots, LD_{d,t}, LR_{k,t-\tau}, \dots, LR_{k,t}, EP_{t-\tau}, \dots, EP_t, SOC_{i,t}]^T \in SS \quad (3.16)$$

$$\forall d \in \text{Demand nodes}, \forall k \in \text{Renewable nodes}, \forall i \in \text{Storage units}$$

where $LD_{d,t}$ represents the level of electricity demand at node d at time step t , $LR_{k,t}$ represents the level of power generation at renewable k at time step t , EP_t represents the electricity price at time step t and $SOC_{i,t}$ represents the level of energy at storage node i at the beginning of time t . In order to investigate time series impact of these variables we define a new variable “ τ ” for a time window.

At each time step t , control agent s (for storage s) receives state ST_t of the network and selects an action $a_t^s \in A^s(ST_t) \subseteq A^s$, where $A^s(ST_t)$ is the set of actions available for storage s in state ST_t and A^s is the set of all possible actions for storage s . A^s is defined by the amount and direction of power at any given state. Since A^s has a finite possible actions the amount of power has to be discretized. Power directions are: charging from grid, charging from different connected renewable nodes and discharging to different demand nodes. We

note that depending on the network topology, storage nodes will have different action spaces. For illustration, storage unit S4 in our example case study is connected to two demand nodes (D7 and D8), renewable node R4 and also main electricity grid (4 directions). If the amount of power in each direction discretized into three levels, then 4^3 will be the maximum number of actions in action set A^4 . We should note that some of these actions won't be feasible because of rated capacity limit on storage unit, hence will be removed from the action set.

Since our focus in this section is electricity bill management as a primary application of storage units, for each individual storage s , the reward function $rw_t^s(ST_t, a_t^s)$ during time interval t , is the saving in network electricity cost as a result of storage s . Since action (a_t^s) at time t affects the state of network at the next time step (ST_{t+1}), a_t^s should be taken in a way to maximize rewards during that and all future time intervals. For storage s we seek a control policy π^{*s} , such that $a_t^{*s} = \pi^{*s}(ST_t)$, which minimizes the overall network electricity cost. Value of the storage s under the control policy π^s when network starts in state ST at time t is defined as:

$$V^{\pi^s}(ST) = rw_t^s(ST, a_t^s) + E \left\{ \sum_{i=1}^{\infty} \varepsilon^i \times rw_{t+i}^s(ST_{t+i}, a_{t+i}^s) \right\} \quad (3.17)$$

where,

$$rw_t^s(ST, a_t^s) = Pr(t) \times \left(\sum_j e_{s,j,t}^d - e_{s,t}^{ch,g} \right) \quad (3.18)$$

$e_{s,t}^{ch,g}$ is the amount of power flow from grid to the storage s during time interval t and $\sum_j e_{s,j,t}^d$ represents the total amount of power flow discharged from storage s to serve

connected demand nodes. These quantities are determined according to action a_t^s . Note that future states and rewards are not only dependent on the action taken by storage unit s , but also are dependent on the actions of the other agents. This brings uncertainty to the future rewards, hence, expected value of the value function is used. A threshold value $0 < \varepsilon < 1$ is introduced to ensure convergence. The optimal policy π^{*s} then maximizes the value of storage s , so that,

$$\pi^{*s} = \underset{\pi^s}{\text{Arg max}}(V^{\pi^s}(ST)) \quad (3.19)$$

The above optimal control problem is solved using the following three steps:

- (i) Compute the optimal hourly charging and discharging actions for each storage node in the network using the above hourly optimization model. Several points are in order: (a) Hourly model is used since control actions are to be made at the top of each hour; (b) The optimization model is run for 365 days per year times the number of years for which historical data exist. In practice the sample size (N_S) can be very large. For illustration, we will use a sample size $N_S = 3 \times 365 \times 24$ hourly data each described by a state vector ST_t and a set of corresponding actions a_t^s for storage unit s . For the illustrative distribution network, there are four storage units, so in each sample data there exist four sets of actions ($a_t^s; \forall s \in \{1,2,3,4\}$).
- (ii) Construct simple rules that characterize the optimal actions as a function of network state and its stochastic input patterns. The output of this step is π^{*s} for all storage units ($\forall s \in \{1,2,3,4\}$) in illustrative case. The construction is carried out using a classification algorithm, which will be discussed next in details.
- (iii) Monitor and match the real-time values of inputs and the network state to the most similar stored patterns computed in step (i). Use rule set from Step (ii) to take the

optimal actions. After a predefined time window (usually a day), the state space and action spaces will be updated and rules will be reconstructed (repeat steps (i) and (ii)). This will ensure that the control model is robust to the changes in the input patterns.

Algorithm 1 - Offline classifier construction algorithm:

Estimate the optimal control policy π^{*s}

For ($\forall s$) repeat: /storage index/

1.1- Construct the response vector: $Y = [\alpha_1^s, \alpha_2^s, \dots, \alpha_{N_s}^s]^T$

1.2- Construct the feature matrix: $X = [ST_1, ST_2, \dots, ST_{N_s}]^T$

For ($\forall b$) repeat: /tree index in tree bagging method (denoted by “B”)/

1.3- Calculate classifier $\pi_b^s(ST)$ based on bootstrapped training data set
(X_b, Y_b)

End

1.4- Calculate $\pi^{*s}(ST) = \frac{1}{B} \sum_{b=1}^B \pi_b^s(ST)$ (3.20)

End

As described in “Algorithm 1” a classification technique is used to characterize the optimal actions as a function of state of the network components and stochastic inputs. The hourly optimization model is utilized to generate the required data for classification. The hourly decision variables of the day-ahead optimization problem, namely, charge and discharge quantities for each storage node, are the designated response variables in the classification

(optimal control actions). A unique class label is then assigned to each action for the classification purposes. We note that the number of classes changes according to the configuration and topology of distribution network. The response of the classification for each storage system is a vector with labels associated with optimal actions for that storage unit. Tree bagging technique [66] is used to build a classification model to predict the optimal action in each individual storage node as a function of stochastic input values and the SOC of ESSs in the entire network. Tree bagging creates and ensembles decision trees for predicting response variable (optimal action at each time step) as a function of predictors (network state). Given a training set of predictors with corresponding responses, tree bagging repeatedly selects a random sample with replacement of the training set and fits trees to these samples (Algorithm 1 - step 1.3). Number of trees “B” is not a critical parameter with bagging; using a very large number of “B” will not lead to overfitting [66]. We used a sufficiently big number (e.g., 500) to achieve a good performance with low out-of-bag error. After training, predictions for unseen samples may be created by taking the average of predictions from all the individual trees (equation (5) in step 1.4). Since the classification model is built based on the optimization model, which has been solved for all available data in historical data set, this classifier is expected to be a good estimation of optimal control policy. However, this control policy is updated continuously according to the new occurred network state as described below in “Algorithm 2”.

Algorithm 2 - Online monitoring and classification:

Assign the optimal action α_i^s

For ($\forall \mathbf{d}$) repeat: /day index/

For ($\forall t$) repeat: /time interval index/

2.1- Monitor the state of the network; \mathbf{ST}_t

For ($\forall s$) repeat: /storage index/

2.2- Assign action $\mathbf{a}_t^s = \boldsymbol{\pi}^{*s}(\mathbf{ST}_t)$ to storage unit s

End

End

2.3- Solve the exact optimization problem for day “ d ” and update the state space SS and action space \mathbf{A}^s ; $\forall s$ (**storage index**)

2.4- Repeat the steps in “**Algorithm 1**” with updated response vector and feature matrix and update the optimal policy $\boldsymbol{\pi}^{*s}(\mathbf{ST}) \forall s$ (**storage index**)

End

Next, the proposed control algorithm is applied to our example distribution network. The configuration defined in “Case 3” with electricity cost reduction application is considered for the illustration. To devise a classifier, we explore the relationship between stochastic patterns of input variables and optimal actions. This is followed by a discretization process according to the network configuration and topology. We also discuss the accuracy of the control model using sensitivity analysis.

Our hypothesis is that there exists a strong correlation between the stochastic input patterns and optimal charge and discharge actions. Here we investigate this hypothesis by analyzing input patterns in a time window defined by $(t-\tau;t)$. In Figure 21 and Figure 22 (with $\tau=4$)

we show the average patterns for these inputs with two different actions at storage node 1. We assume that the solar radiation at renewable nodes are close (due to the same geographical zone), therefore, there is no need to consider separate levels of renewable electricity generation for different PV systems in the classification phase. Hence, instead of analyzing the level of generation at the renewable nodes we look at the solar intensity patterns.

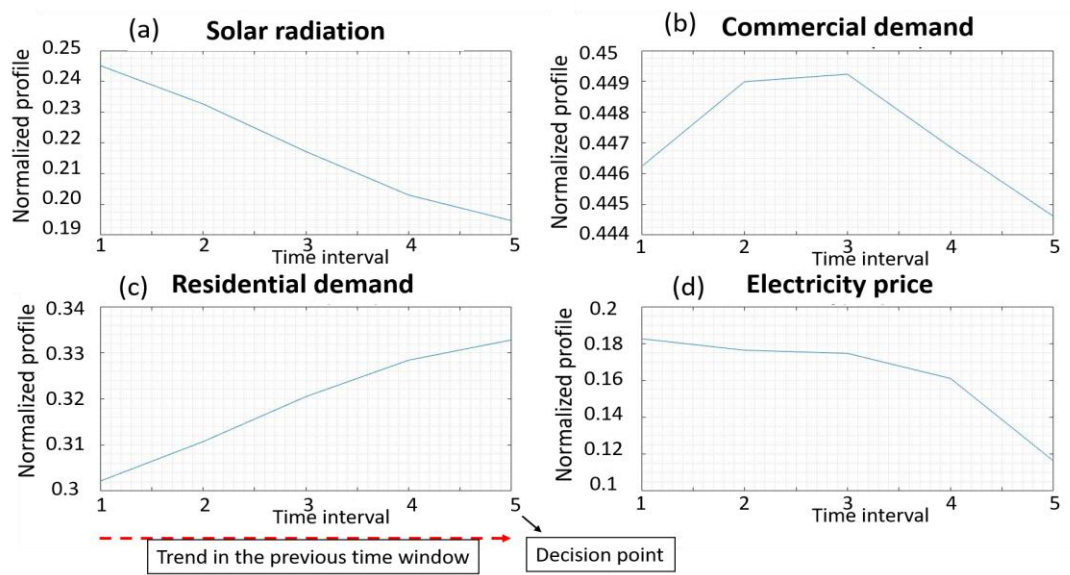


Figure 21-Stochastic Input pattern when charging from grid is the optimal action for ESS1

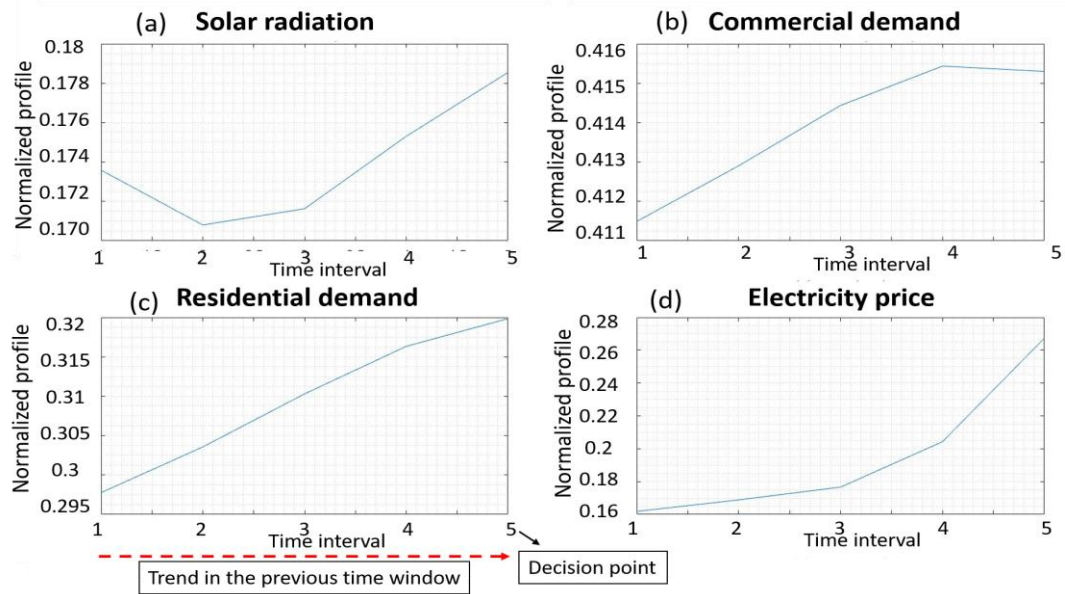


Figure 22-Stochastic Input pattern when discharging to D1 is the optimal action for ESS1

Figure 21 and Figure 22 confirm the correlation between charge/discharge controls of electricity storage and input patterns. According to Figure 21-a and Figure 21-d, charging from grid actions of S1 should follow decreasing trends in electricity price and solar radiation. This is expected since electricity storage application is intended to reduce the electricity bill. Figure 22-a to Figure 22-d illustrate that discharging to commercial demand D1 follow the increasing trends in demand profiles and electricity price.

According to the illustrative network configuration, the possible directions for power flow in storage “S4” are: discharge to demand nodes D7 and D8, charge from renewable R4 and charge from grid. In each of these directions the amount of electricity flow is discretized into three levels based on power rating: at 0%, between 0% and 50% and greater than 50%. As a result, there are $3^4 (=81)$ total possible actions for storage “S4” during a given time step. A four-digit number in turnary (the base-3 numeral) system $(d_1 d_2 d_3 d_4)_3$ is used to represent each action for this storage. Each digit represents the amount of electricity flow

in specific direction. The following table shows the meaning of each digit for control actions in storage 4.

Table 14- Storage 4 control action representation

| Value of each digit (d_n ; $n=1,2,3$ and 4) | d_1 (level of charging from grid) | d_2 (level of charging from R4) | d_3 (level of discharging to D7) | d_4 (level of discharging to D8) |
|--|-------------------------------------|-----------------------------------|------------------------------------|------------------------------------|
| 0 | 0% of rated power ² | 0% of rated power | 0% of rated power | 0% of rated power |
| 1 | 50% of rated power | 50% of rated power | 50% of rated power | 50% of rated power |
| 2 | 100% of rated power | 100% of rated power | 100% of rated power | 100% of rated power |

For example, action number 3, which is represented as $(0010)_3$ in ternary system, represents discharging to D7 with 50% power rating. Control actions for other storage units are defined similarly. It is obvious that some of these actions (for instance, multiple charging and discharging during same time step) are not feasible because of the limitation on the power rating (see Eq. (7)).

Finally, we note that, in addition to state of charge of ESSs at time “ t ”, the level of renewable generation, electricity demands and electricity price from time “ $t-\tau$ ” to “ t ” will be considered as classification features. Furthermore, we expect that higher values of τ will improve the misclassification and control errors. Next, we present the above methodology for our case study network with two different values of τ .

² in the focused case in control problem (case 3) rated power is 120 kW for storage 4

First, we assume $\tau=0$, which means that no memory is considered for the control algorithm. Therefore, only the current state of charge of ESS nodes, electricity generation in renewable nodes, electricity demand and electricity price are taken into account. Two-third (2/3) of the sample data (the same three years historical data) is used to train the classification model. The daily cost is calculated for each individual day and the deviation from optimal daily cost is also calculated. Figure 23-a shows the histogram chart of daily cost deviation when $\tau=0$. The mean value of the cost deviation from optimal case (with exact information) is 6%, which means that by using approximation rule-based control (with zero-hour memory); on the average, the daily operation cost will be 6% more than the optimal cost.

Repeating the above for $\tau=4$ demonstrates that deviation from the optimal cost reduces significantly with the size of time memory window (Figure 23-b).

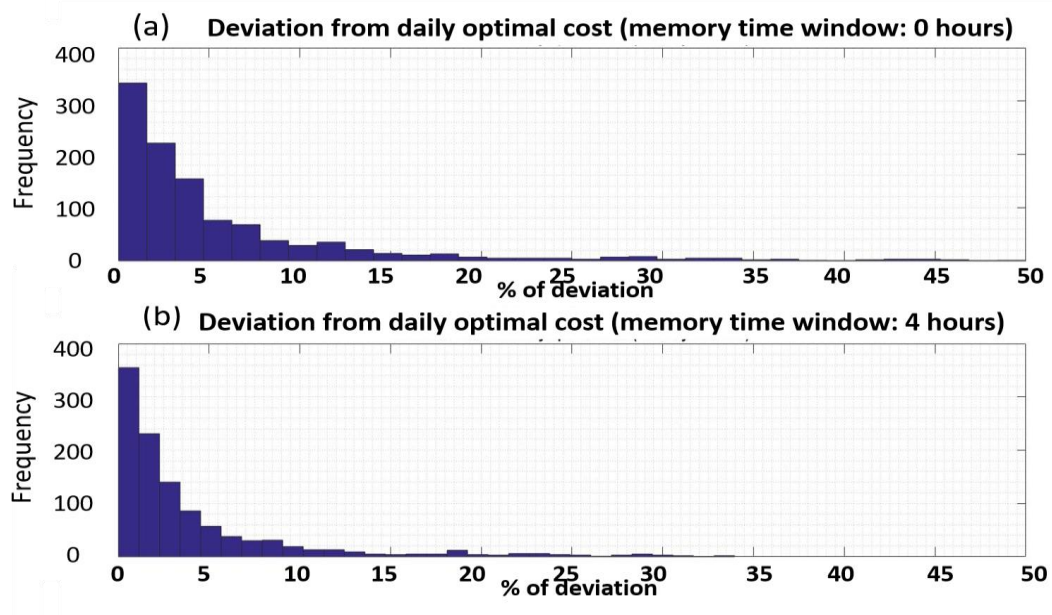


Figure 23- Daily Cost Deviation (%) – a) $\tau=0$ - b) $\tau=4$

The mean value of the cost deviation from optimal case (with exact information) is 4% when memory window of 4 hours considered for control algorithm. As expected, by increasing the memory window the error of model decreases. In the following Figure 24-a the amount of electricity required to be purchased from the main grid as a result of executing control actions (for both $\tau=0$ and $\tau=4$) during an example day are illustrated. Figure 24-b shows the electricity price this example day.

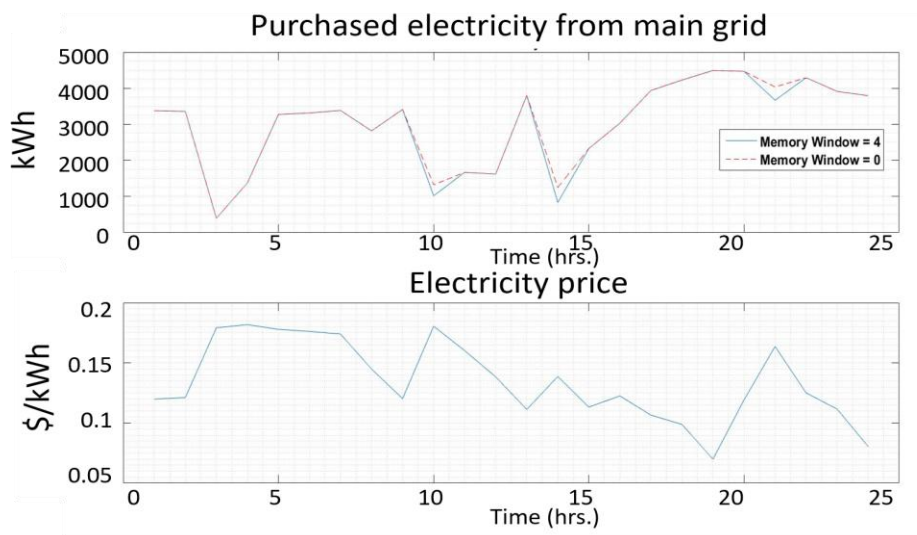


Figure 24- Example day electricity price and outputs profile - (a) Purchased electricity from grid, (b) electricity price

Figure 24-a shows that by increasing the memory window the rule-based control assigns charge and discharge actions to storage nodes in a way to reduce the purchasing electricity from grid during the peak hours. Note that, none of controllers ($\tau =0$ and $\tau =4$) has information about future and they assign control actions according to their prediction ability. But it seems that higher sizes of the memory window improve the future prediction capability of patterns, which results in less daily cost and better performance of the control model.

3.5. Sensitivity Analysis on stochastic parameter changes

Thus, far, the planning and real-time controlling models have been made based on the available historical data. In this section, we conduct a sensitivity analysis and investigate the impact of load changes on planning decisions and control actions. We will experiment with data of Figure 25 which gives the hourly profile boxplot for two demand nodes in our distribution network during cooling season and heating seasons.

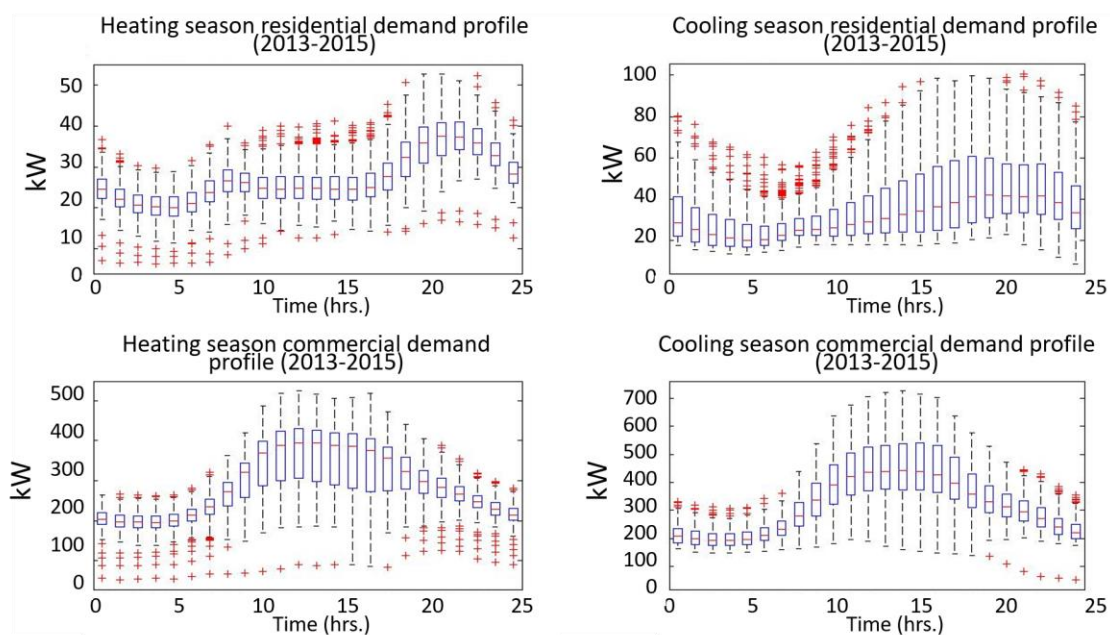


Figure 25- Hourly demand profile boxplot (Heating season and cooling season)

We fit a multi-variate log-normal distribution to each demand data and compute mean value and covariance matrix. We consider 5%, 10%, 15% and 20% growth in demand for each node and investigate the impact of these increases on capacity planning and control for distribution network. We focus on energy bill management application.

The following table confirms that increasing in electricity demand results in higher value of investment in energy storage, therefore capacity planning model suggests higher capacity of energy storages.

Table 15- Capacity planning for different electricity demand growth

| Growth in elec. demand | Storage 1 | | Storage 2 | | Storage 3 | | Storage 4 | |
|------------------------|----------------|-----------------|----------------|-----------------|----------------|-----------------|----------------|-----------------|
| | Capacity (kWh) | Power Rate (kW) |
| Baseline (0%) | 6200 | 2000 | 6600 | 2200 | 1000 | 300 | 600 | 120 |
| 5% | 6500 | 2200 | 6800 | 2300 | 1000 | 300 | 600 | 120 |
| 10% | 6900 | 2300 | 7200 | 2400 | 1100 | 350 | 600 | 130 |
| 15% | 7200 | 2500 | 7500 | 2500 | 1150 | 350 | 650 | 130 |
| 20% | 7500 | 2600 | 7800 | 2600 | 1200 | 400 | 650 | 130 |

Now let's move to the proposed network aware control model. Capacity of storage units are same as baseline (no growth in electricity demand). The initial control policy is determined based on base-line demand scenario (Step "A" in Algorithm 1). Now consider that the level of demand is increasing with 5% growth. This results in new state vectors which do not exist in the initial state space. As described in steps B-3 and B-4 in algorithm 1, the control policy will be updated continuously according to the new occurred states to adjust control actions with new states and maintain the performance of control module.

Following Figure 26 demonstrates the deviation from optimal cost as a result of applying proposed network aware control algorithm on the new state space with %5 growth in electricity demand. The mean value of the cost deviation from optimal case is %4.5.

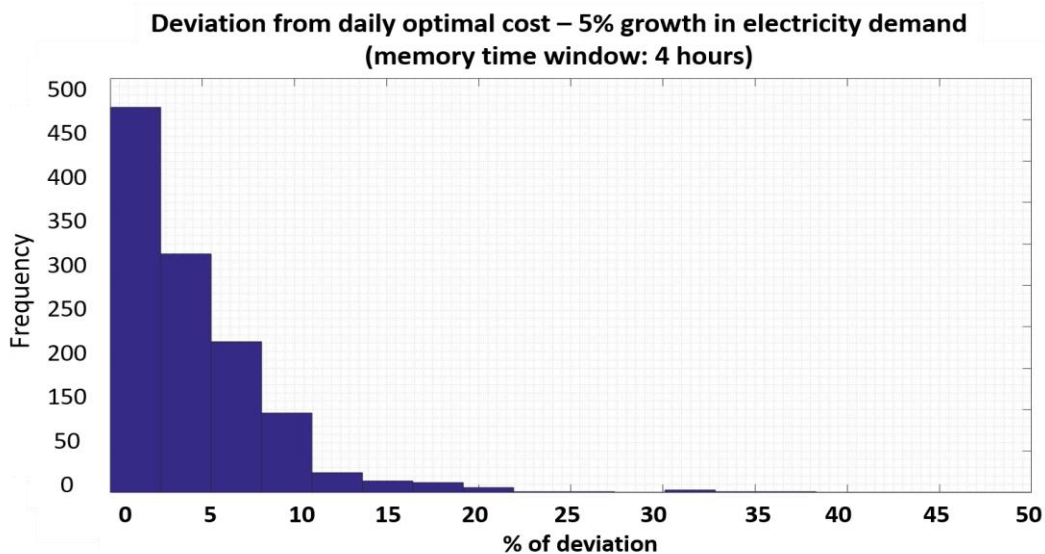


Figure 26- Deviation from the daily optimal cost when elec. Demand increase by 5% - $\tau=4$

3.6. Conclusion

This chapter proposed “Network-aware planning and control approach” for multiple energy storage nodes distributed over power distribution network. We were interested in optimally locate these storage units over distribution network and to create day-ahead plans according to planned application. An approximation model has been proposed for planning purpose, which lowers the computational complexity of optimization problem by 45 % in our illustrative example (in terms of number of decision variables). Two types of storage system with static and dynamic capacity are considered in the planning model.

Furthermore, a novel rule-based control scheme for the near real time operation of the storage network has been built. Tree-bagging classification technique is utilized to

determine the near optimal control policy, which maximizes the value of storage nodes. In the proposed Network-aware control model the near optimal actions at a time “ t ” are taken in each individual storage unit based on the partial knowledge of the whole network state from time “ $t-\tau$ ” to “ t ”. Comparing the daily costs of approximate control model with the exact optimal case when $\tau = 0$ shows 6% difference in average. Increasing the memory (τ) of the model from 0 hours to 4 hours reduces this deviation to 4%. In the proposed model the control policy is being updated frequently to adjust the control rules with any changes in network components’ behavior and increase the robustness of control module.

3.7. Appendices

3.7.1. Appendix "A1"

Following table shows the population size and corresponding probability value for each cluster.

| Cluster number | Population size | Cluster probability |
|----------------|-----------------|---------------------|
| 1 | 11 | 0.01005 |
| 2 | 43 | 0.03927 |
| 3 | 10 | 0.00913 |
| 4 | 14 | 0.01279 |
| 5 | 14 | 0.01279 |
| 6 | 9 | 0.00822 |
| 7 | 11 | 0.01005 |
| 8 | 42 | 0.03836 |
| 9 | 34 | 0.03105 |
| 10 | 12 | 0.01096 |
| 11 | 33 | 0.03014 |
| 12 | 19 | 0.01735 |
| 13 | 41 | 0.03744 |

| | | |
|----|----|---------|
| 14 | 12 | 0.01096 |
| 15 | 11 | 0.01005 |
| 16 | 21 | 0.01918 |
| 17 | 40 | 0.03653 |
| 18 | 12 | 0.01096 |
| 19 | 49 | 0.04475 |
| 20 | 11 | 0.01005 |
| 21 | 45 | 0.04110 |
| 22 | 49 | 0.04475 |
| 23 | 12 | 0.01096 |
| 24 | 13 | 0.01187 |
| 25 | 13 | 0.01187 |
| 26 | 41 | 0.03744 |
| 27 | 52 | 0.04749 |
| 28 | 45 | 0.04110 |
| 29 | 14 | 0.01279 |
| 30 | 11 | 0.01005 |
| 31 | 12 | 0.01096 |

| | | |
|----|----|---------|
| 32 | 9 | 0.00822 |
| 33 | 15 | 0.01370 |
| 34 | 28 | 0.02557 |
| 35 | 44 | 0.04018 |
| 36 | 22 | 0.02009 |
| 37 | 12 | 0.01096 |
| 38 | 9 | 0.00822 |
| 39 | 11 | 0.01005 |
| 40 | 22 | 0.02009 |
| 41 | 11 | 0.01005 |
| 42 | 41 | 0.03744 |
| 43 | 16 | 0.01461 |
| 44 | 40 | 0.03653 |
| 45 | 18 | 0.01644 |
| 46 | 16 | 0.01461 |
| 47 | 13 | 0.01187 |
| 48 | 12 | 0.01096 |

3.7.2. Appendix “A2”

Optimal dispatch to different demand nodes in different example clusters:

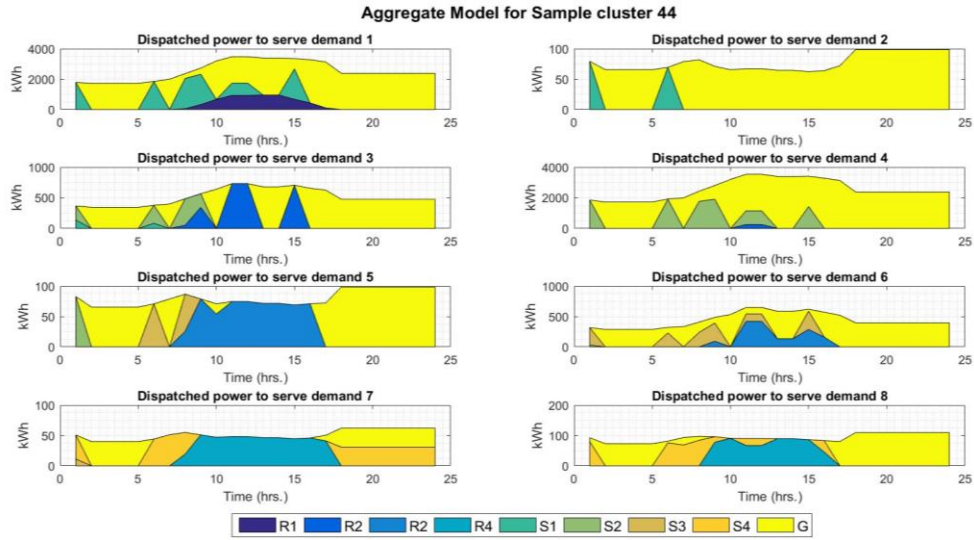


Figure 27- Optimal dispatch to 8 demand nodes (Cluster 44)

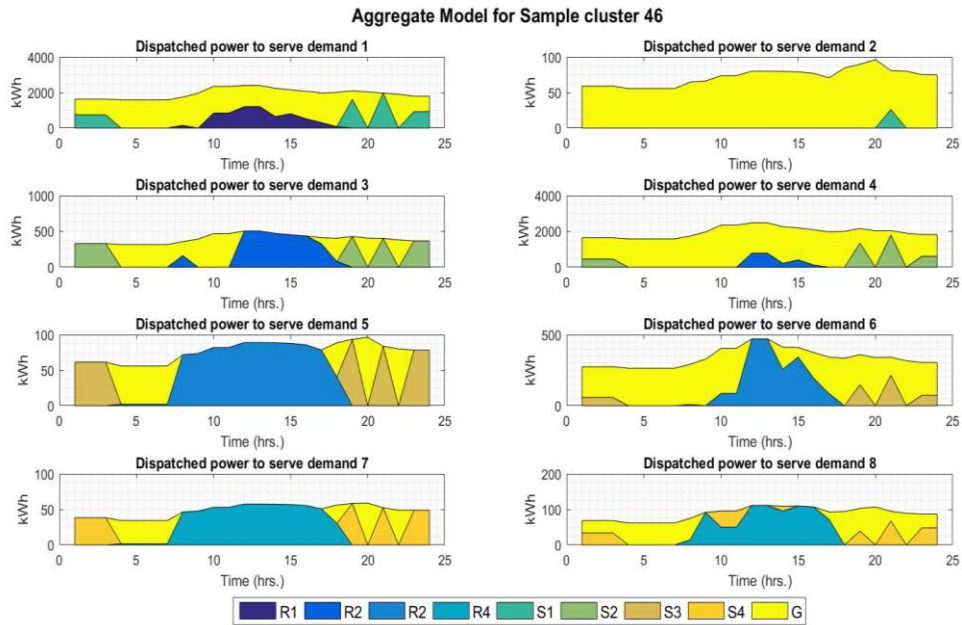


Figure 28- Optimal dispatch to 8 demand nodes (Cluster 46)

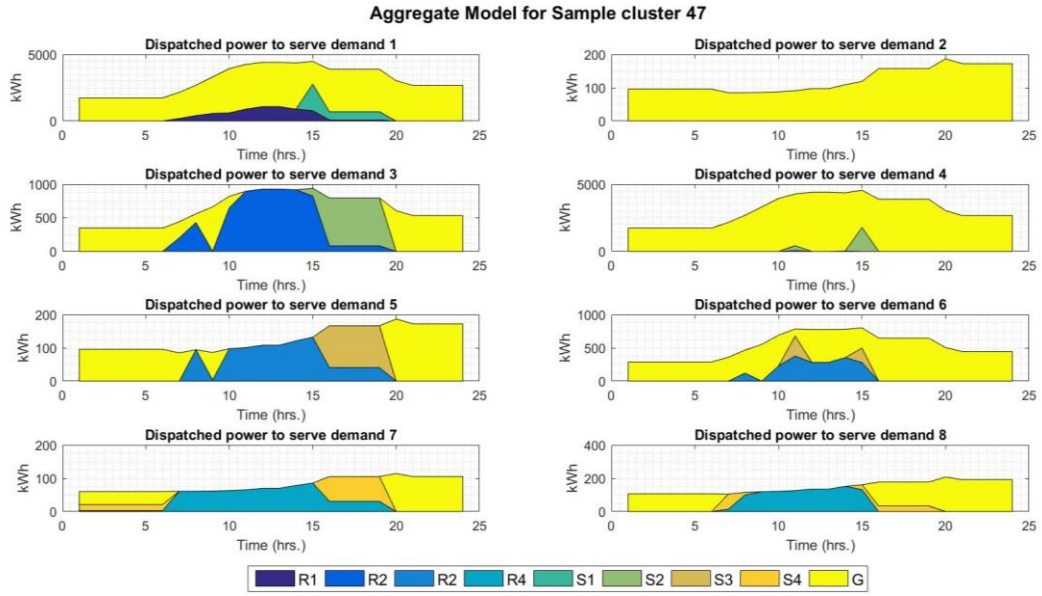


Figure 29- Optimal dispatch to 8 demand nodes (Cluster 47)

CHAPTER 4: ENERGY STORAGE SYSTEM WITH DYNAMIC CAPACITY – EV PARKING LOT MODEL

Abstract

The recent advances in electric battery technologies and the reduced price of Electric Vehicles (EV) are significantly changing the adoption rate of EVs. With the increasing number of EVs on the roadways the demand for power increases. New emerging Vehicle-to-Grid (V2G) technology brings the opportunity for large facilities, such as EV parking garages, to participate in wholesale energy and ancillary markets such as frequency regulation to dampen the effect of increase in EV load by allowing energy flow from these vehicles to the grid at times of stress and peak loads. In this study, we propose an integrated framework which optimally dispatches EVs in a large parking facility to maximize the parking facility benefits. It also offers economic benefits to EV owners through reduced parking fees or discounted charging fees which compensate the additional degradation of the vehicle battery. Moreover, this framework is capable to quantify the impact of such planning on the power distribution network. In this study, we show that optimal charging and discharging of EVs in a large garage with 120 charging stations reduces the peak demand of the facility by almost 40%. In the planning phase, queueing model is adopted to estimate the available aggregate capacity of batteries in the parking facility (energy storage system (ESS) with dynamic capacity) during different times of the day. The risks associated to the stochasticity of the available capacity are also formulated. The hourly charging/discharging for the available capacity is formulated as a mix-integer problem.

4.1. Introduction

The recent advances in battery related technologies and the reduced price of Electric Vehicles (EV) are significantly changing the landscape of roadway transportation [67] and [68], and more than ever before, the nexus between transportation and energy becomes evident. With the increasing number of EVs on the roadways and the flexibility to charge at home, or at public and private facilities, the demand for power increases and load uncertainty widens [69] [70] [71]. The recent advances in Vehicle to Grid (V2G) technology and the lowering cost of bi-directional charging units bring new investment opportunities, especially in the emerging energy storage market. To remove barriers to the participation of electric storage resources in the capacity, energy, and ancillary service markets operated by Regional Transmission Organizations (RTO) and Independent System Operators (ISO), the Federal Energy Regulatory Commission (FERC) enacted FERC Order 841 [72]. Large facilities, such as EV parking garages, can participate in wholesale energy and ancillary markets such as frequency regulation to dampen the effect of increase in EV load by allowing energy flow from these vehicles to the grid at times of stress and peak loads [72], [73] and [74]. It can also offer economical benefits to electric vehicle owners through reduced parking fees or some income sharing schemes. Such a facility can also be part of a larger but modular network of energy storages, or an Energy Storage System (ESS), at power distribution network. An ESS can provide multiple distribution applications such as facilitating renewable integration, load leveling, peak shaving, along with participation in wholesale energy and ancillary markets [75]. All these benefits come with strings attached, though, for instance, it is generally perceived that batteries residual life has a strong correlation with the number of charge-discharge cycles and the depth of

discharge. Furthermore, the random nature of vehicle arrivals and departures, and the initial and final required State of Charge (SoC) for individual vehicles complicate the behavior of the ESS that a parking garage is member of. These random patterns along with other unplanned failures and planned maintenance events will make the overall capacity of the ESS stochastic and dynamic as perceived by the distribution network that is serving.

This chapter provides an insight into potentials of using such facilities to participate in ancillary markets or other applications. We propose a model, which determines the upper bound for the value of a parking garage as an energy storage with dynamic capacity. Mixed-integer programming is utilized to find the maximum value of this modular storage system. One key parameter in this problem is the permission from EV owners for V2G connections. This parameter is determined based on the incentive offered by the parking operator to the EV's owner. We formulate a queueing model to estimate the vehicles arrival time for the next day. This is crucial for day-ahead wholesale market participation since it gives an insight regarding the available capacity. The queueing model comes very handy in predicting the number of vehicles in the facility at any time bucket during a day. We also compute the quantity risks of the day-ahead commitments.

EV integration studies in the literature mainly focused on analyzing the impacts of EV adoption on electricity demand and the required upgrades in generation, transmission and distribution systems to meet the demand [76] and [77]. The increased peak load demand due to plugged-in EVs may also overload service transformers resulting in transformer overheating and subsequent deterioration [78] and [79]. EV charging is also likely to cause power quality problems, including, under-voltage conditions, voltage and current harmonics, and etc. [80], [81] and [82]. To mitigate the negative impacts of EV charging

[83] and [84] proposed customer incentives by utilities to charge their EVs during off-peak hours. The idea is that assigning Time-Of-Use (TOU) electricity pricing will help utility to control the charging actions indirectly [85] and [86] proposed utility owned smart controls aiming to maximize utility and costumers' benefits. [87] considers the problem of maximizing the profits for the EV owners by selling excessive energy to the grid. [88] and [89] provided control algorithms to maximize EV owner's profit earned from selling power to grid and participating in a frequency regulation market. The coordination of large-scale EV charging in a parking garage emerges as a more promising candidate for demand response (DR) and ancillary services. The aggregated charging load of EVs in parking garage with flexible and interruptible characteristics brings opportunity in DR market. Yao, et.al. in [90] analyzed the EV charging coordination based on both price-based and incentive-based DR programs. Moreover, aggregated capacity of batteries in EV parking garage can also be used in ancillary market. The impact of a unit unavailability on the overall system capacity depends on configuration and series/parallel connections among individual batteries or storage units [91], [92] and [93].

Although there have been many studies investigating the EV charging coordination, advanced managed charging and V2G control; However, to the best of our knowledge, there is a major gap in understanding how the EV parking facility as a large energy storage with dynamic and uncertain capacity should operate in a distribution network. Moreover, the cost and benefit of such parking facility for parking owner, EV owners and power distribution network require being investigated.

The rest of the chapter is structured as follows. Section 2 states the problem and explains the queue model which has been deployed to simulate the behavior of EV parking garage

as a dynamic storage system. The day-ahead stochastic planning problem is formulated in section 3. This section continues with risk formulation associated to operational stochasticity of the facility. In section 4, mixed-integer programming formulation for the operational control is demonstrated. Section 4 concludes with EV garage Cost and benefit analysis. In section 5 a set of example case studies are illustrated to evaluate the proposed integrated framework.

4.2. Problem Statement and preliminaries

The problem we are trying to solve here has multiple facets: The facility owner wants to maximize his/her revenue by optimally controlling bi-directional power flow in the facility. For this to happen, the facility owner must have vehicle owner's permission, which is partially dependent on what this owner receives in return, either as discount for the use of the facility or as an expedited payback. The vehicle owner needs to weigh this return against battery degradation. On the other hand, for the owner to participate in wholesale energy and ancillary market such as frequency regulation, the facility (as an energy storage) must conduct day-ahead plans, which is contingent on vehicle queues. With the underlying stochastic queueing process, the day-ahead plan will be subject to uncertainties and risks. To tackle this multifaceted problem, as depicted in Figure 30, queueing model has been developed that explains vehicle arrivals and departures. With the number of vehicles in the facility computed from the queueing model, a day-ahead planning model is then formulated that simulates the facility participation into frequency and energy markets (see Figure 30; day-ahead stochastic planning block). The day-ahead model assumes optimal operational control for each of many scenarios that are generated according to the stochastic inputs. We also formulate risks associated with a plan and compute damages to distribution

network as a result of operational stochasticity of the facility (Figure 30; Distribution network impact model block). The developed optimal operational control model, governs bi-direction power flow in the facility. This model works closely with a facility and vehicle owner's revenue model. Following figure illustrates the holistic view of proposed approach.

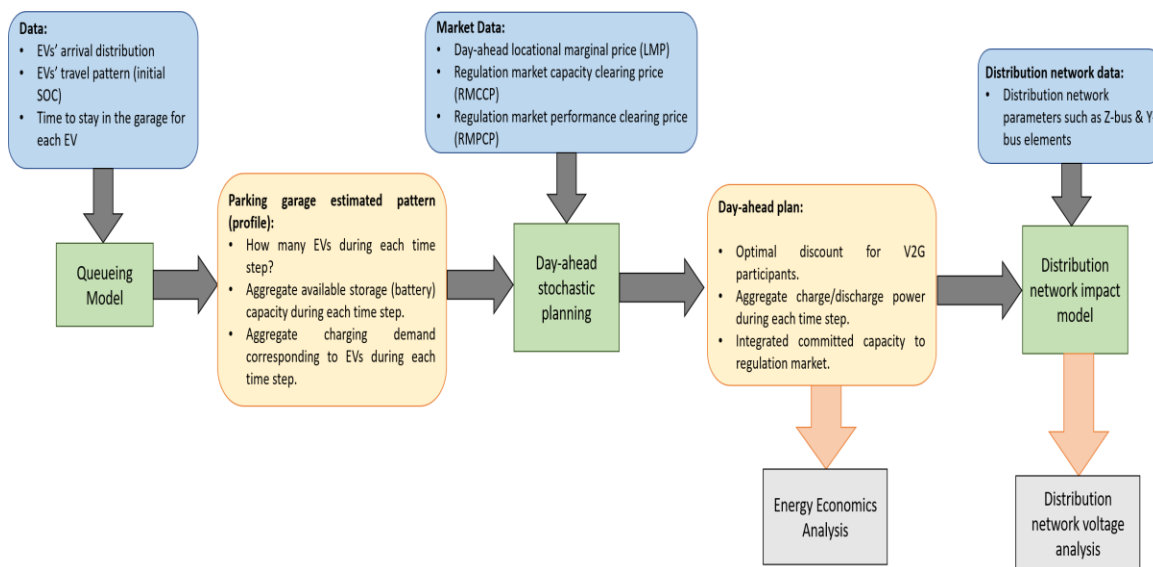


Figure 30- Schematic diagram of the proposed model

Without loss of generality, we assume two equally likely common capacities (kWh) for EV battery. The initial SoC of an EV battery is a random variable that follows truncated normal distribution bounded from below, with mean and variance as functions of vehicle's arrival time. EVs that arrive earlier have higher mean value and lower variance. It is assumed that EVs should reach to the owner-defined SOC upon departure. In the time between arrival and departure times, EV can be part of the parking lot's modular energy storage system if the V2G permission is granted by the EV owner. It should be noted that, the overall storage capacity of this energy system is stochastic which is the function of the arrival and departure of EVs as well as the V2G connections.

The facility has a finite number of parking spaces for EVs. We assume that the facility is empty ($S_{t_0} = 0$) at the beginning of the day (time $t_0 = 0$). EVs arrive according to a general stochastic process and occupy a parking spot for a random period of time, which also follows a general probability distribution. Underlying arrival distributions change with time of the day, and time-to-stay distributions vary from one EV to another. Furthermore, arrival and departure SOC levels depend on individual vehicles characteristics.

From a queueing point of view, this parking facility works like a G/G/K/0 queue, where the first two G's are general distribution designations for inter-arrival time and time-to-stay of vehicles, respectively. K is the number of parking spaces and capacity of the facility. Since exponential distribution has memory-less property, suppose that arrival times follow a Markovian process with exponentially distributed inter-arrival times and time dependent parameter λ_i , where i is the i^{th} time interval. Let us denote the duration of i^{th} interval by $\Delta t_i \triangleq t_i - t_{i-1}$. The probability of n vehicle arrivals during the i^{th} time interval is then given by:

$$P\{N_i = n\} = \frac{[\lambda_i \times \Delta t_i]^n}{n!} \times e^{-\lambda_i \times \Delta t_i} \quad \forall n = 0, 1, 2, \dots, K \quad (4.1)$$

and the expected number of arrival during the interval is:

$$E[N_i] = \sum_{n=0}^K \frac{[\lambda_i \times \Delta t_i]^n}{(n-1)!} \times e^{-\lambda_i \times \Delta t_i} \quad (4.2)$$

Let us assume that the time to stay of any EV, which arrives during the i^{th} interval, is a random variable that follows an exponential distribution with mean value $\frac{1}{\mu_i}$. Define μ'_i as the vehicle departure rate from the facility during the i^{th} interval from the perspective of an

outside person. This time dependent departure rate is the function of time to stay of EVs, which arrived during prior intervals. μ'_i can be calculated by the weighted average of the times to stay of all vehicles that are at the facility, and is given by:

$$\mu'_i = \frac{\sum_{j=1}^{i-1} w_j^i \times \mu_j}{\sum_{j=1}^{i-1} w_j^i} \quad (4.3)$$

where weight w_j^i is defined as the expected number of vehicles which arrived in the j^{th} interval and remained in the facility till t_{i-1} :

$$w_j^i = \lambda_j \times \Delta t_j \times e^{-\mu_j \times (t_{i-1} - t_j)} \quad (4.4)$$

Then the probability of n vehicles departing the facility during the i^{th} interval given m vehicles are in the parking-lot at time t_{i-1} is:

$$P\{L_i = n | S_{t_{i-1}} = m\} = \frac{[m \times \mu'_i \times \Delta t_i]^n}{n!} \times e^{-m \times \mu'_i \times \Delta t_i} \quad \forall n = 0, 1, 2, \dots, m \quad (4.5)$$

where $S_{t_{i-1}}$ indicates the number of occupied spaces at time t_{i-1} . The expected number of departing vehicles during the i^{th} interval is then given by:

$$E[L_i | S_{t_{i-1}} = m] = \sum_{n=0}^m \frac{[m \times \mu'_i \times \Delta t_i]^n}{(n-1)!} \times e^{-m \times \mu'_i \times \Delta t_i} \quad (4.6)$$

Expected number of EVs in the parking lot at the end of i^{th} interval is given by:

$$E[S_{t_i}] = S_{t_{i-1}} - E[L_i | S_{t_{i-1}}] + E[N_i] \quad \forall i = 1, 2, 3, \dots, 24 \quad (4.7)$$

The above queueing model will be used to plan a day ahead and also formulate the overall facility operational and revenue models.

4.3. Day-ahead stochastic planning

Facility owner may benefit from participation in wholesale energy and ancillary market such as frequency regulation (FR). To estimate potential market benefits, mixed-integer economic dispatch model has been developed with respect to PJM fast regulation market (RegD) rules. The facility owner would want to commit a maximum capacity in peak-priced hours while ensuring that sufficient capacity is available at the facility level to provide both regulation down (ES charging) and regulation up (ES discharging) services. For demonstration purposes, we use 2016 PJM day-ahead regulation market data (both capacity and performance clearing prices are applied). For wholesale arbitrage, the facility owner may charge EV batteries when electricity price is low and sell it back to the grid when electricity price is high, provided that the EV SoC demands are met.

FR capacity commitment and net injected power (aggregate charge minus aggregate discharge) must be considered in the planning phase (e.i. day-ahead planning). As depicted in Figure 31, the day-ahead planning is performed based on the expected number of EVs, types of batteries, initial SOC and final desired SOC of batteries. Moreover, market variables such as electricity price and FR credit could influence planning. These input variables are stochastic, hence stochastic optimization is applied. The output of day-ahead planning function is the optimal discount factor assigned to EVs (for V2G permission), aggregated planned capacity for FR commitment (during each time step), aggregated amount of electricity required to charge EVs and aggregated amount of discharged electricity during each time step (see Figure 31). The following equation explains the inputs and outputs for stochastic planning function $f_p(\cdot)$.

$$\begin{aligned}
& [\{Reg_t; \forall t\}, \{Q_t; \forall t\}, \{P_t; \forall t\}, \varphi] \\
& = f_p([\{S_t; \forall t\}, \{Cap_t; \forall t\}, \{RCap_t; \forall t\}, \{Pr_t; \forall t\}, \{FR\ Credit_t; \forall t\}, \dots \\
& \quad \{SOC_{init}^i; \forall i\}, \{SOC_{final}^i; \forall t\}]) \quad (4.8)
\end{aligned}$$

where $\{Reg_t; \forall t\}$ is the timeseries output for the aggregated planned capacity for FR commitment; $\{Q_t; \forall t\}$ and $\{P_t; \forall t\}$ represent time-series for the aggregate planned discharged and charged power for the parking facility; and φ is the optimal planned discount factor for the V2G enabled EVs. The following figure illustrates the functional diagram for day-ahead planning phase.

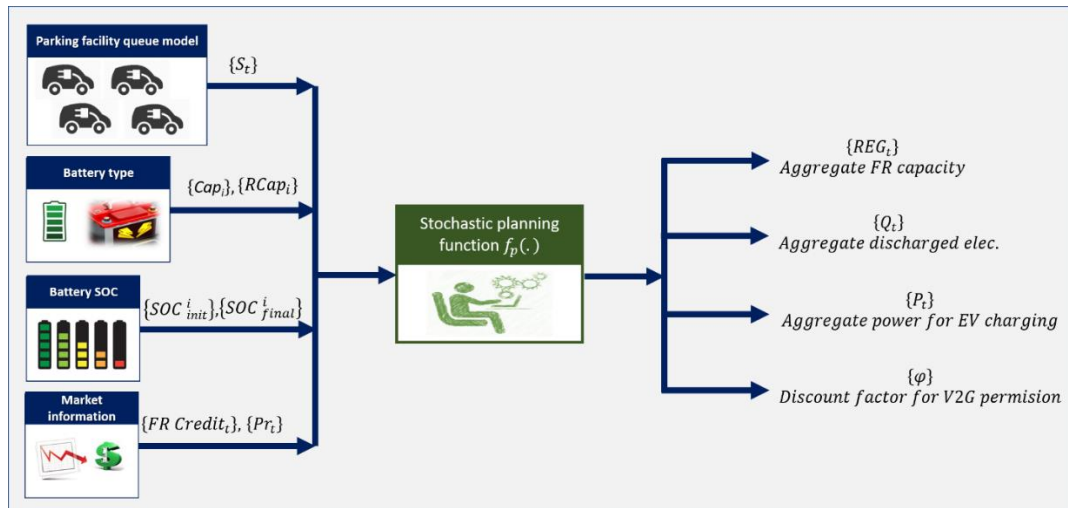


Figure 31- day-ahead planning - functional diagram

To capture the stochasticity of input variables in the day-ahead planning, a Monte-Carlo (MC) simulation generates sample paths according to stochastic input distributions, one of which is vehicle arrival process as captured by the queueing model. For each sample path, we then seek the optimal planning outputs (discount factor, aggregated planned capacity for FR commitment, aggregate amount of electricity required to charge EVs and aggregate amount of discharged electricity). The optimization problem is basically as same as the

model that we have used for operational purposes – this is described in a later section. For now, we assume the optimal plan $f_p(\cdot)$ exists. Optimal results for each MC path will be used to find the distribution for output variables in planning phase.

Next, we illustrate day-ahead planning model for a commercial parking facility with 120 parking spaces. EV arrivals are assumed Markovian as formulated above. The capacity of batteries, their initial and final SOC are also generated randomly according to their stochastic distribution while market information (namely; FR credit and electricity price) are unchanged. The following figure demonstrates the box whisker plots for the number of EVs and the aggregated capacity of batteries parked in the parking facility based on the 100 MC sample paths.

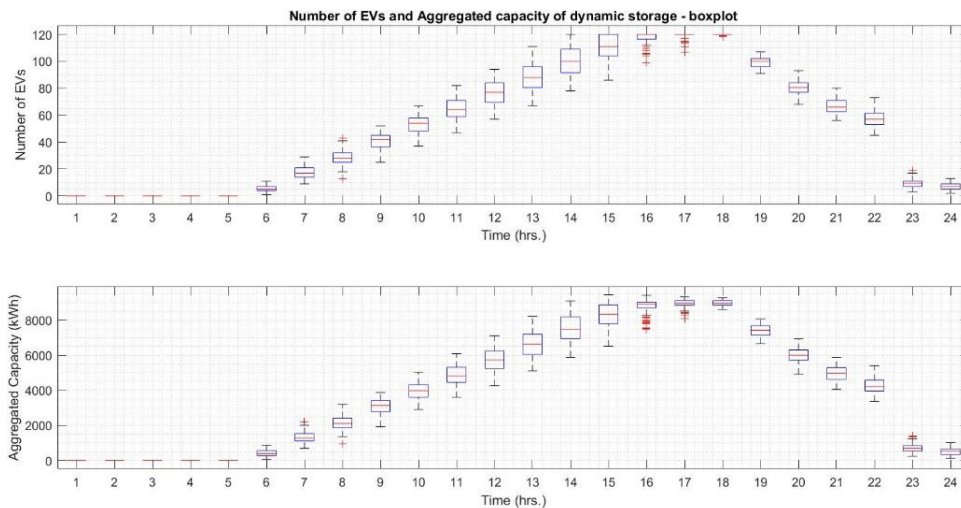


Figure 32- a) Boxplot- Number of EVs b) Boxplot - Aggregate capacity of batteries

Note that the parking facility is almost fully-occupied during 4-6 PM. The market data remains fixed for all scenarios and as given in Figure 33.

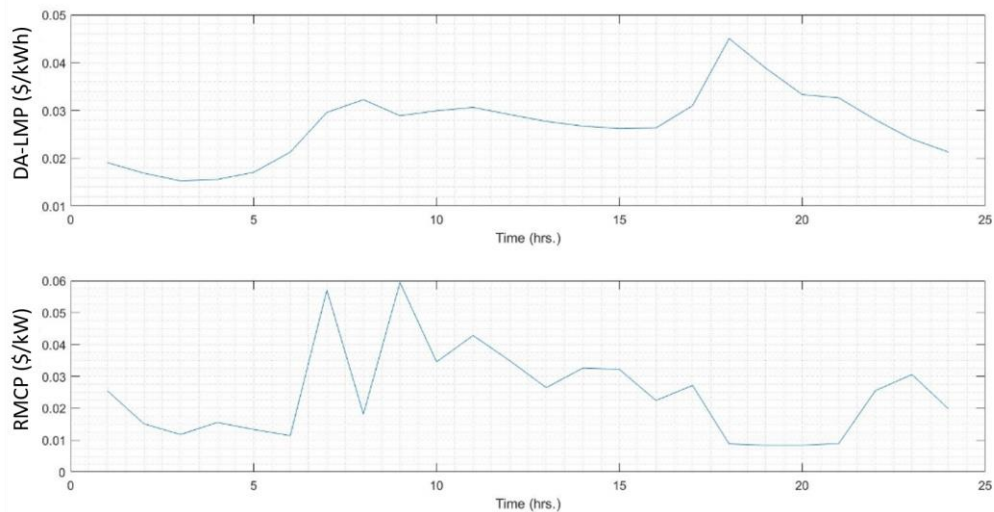


Figure 33- a) Electricity price profile; b) Frequency regulation market clearing price

Given the market data, optimal plans are calculated for each sample path, and results from all paths are compiled into distributions; see the figures below for Reg. Cap, Charging and discharging power amounts over 24 hours period.

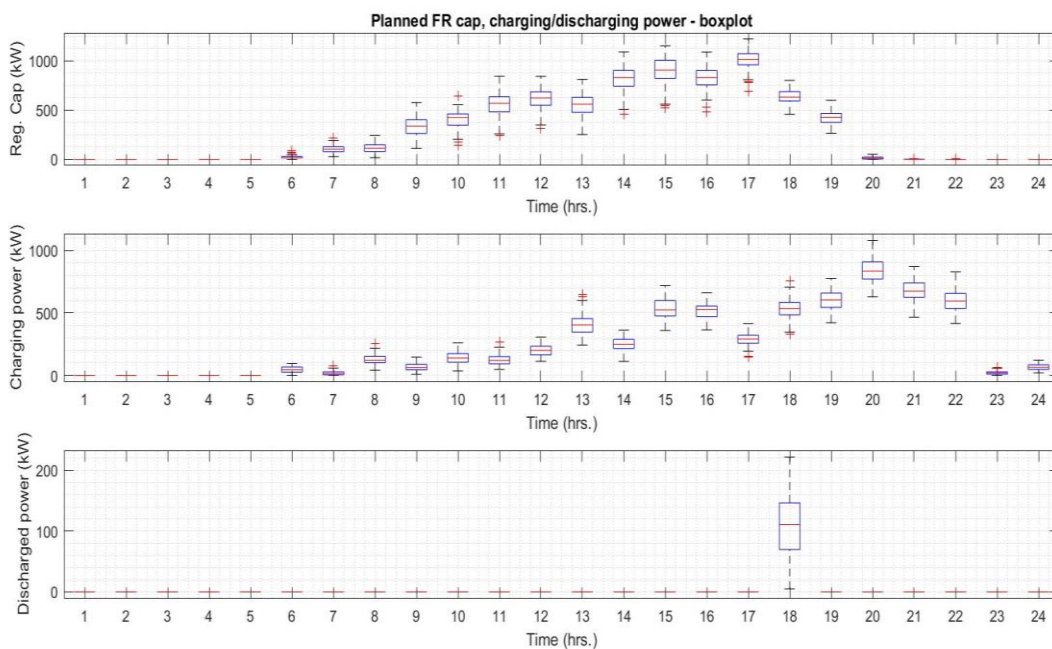


Figure 34 - a) Boxplot - FR capacity; b) Boxplot - elec. power required for charging; c) Boxplot - elec. power to discharge

As illustrated in Figure 33, optimal decisions during the planning phase are highly sensitive to the market values. For instance, although there is relatively more available capacity at 4 PM compared to 3 PM, FR committed capacity is less at 4 PM. This is due to the higher RMCP value at 3 PM compared to 4 PM. As the other example, as shown in Figure 5.c, sell to grid is an optimal decision at 6 PM when electricity price is high. The day-ahead plan is estimated by taking the average over all scenarios. The planned capacity for FR participation and net demand (charging - discharging) are shown in Figure 6.

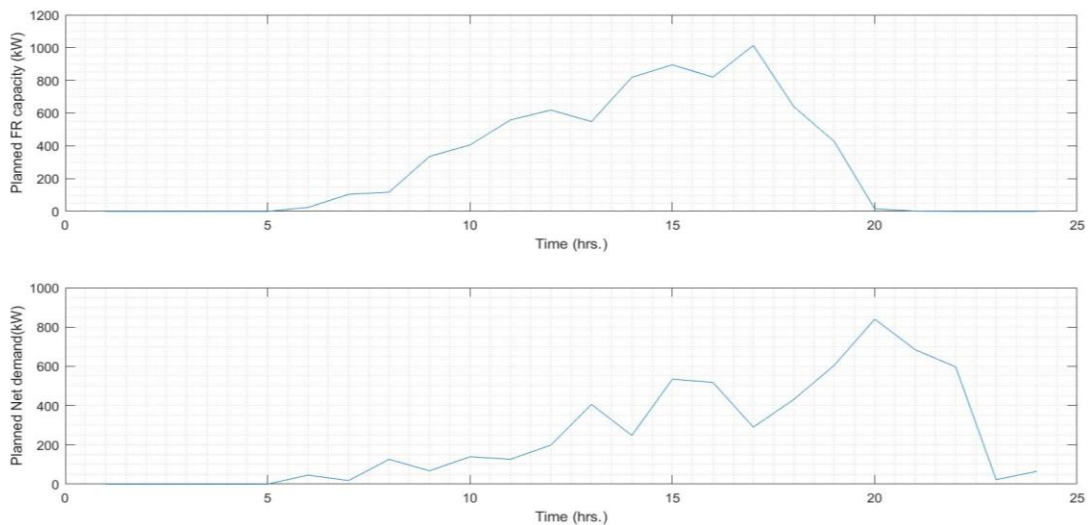


Figure 35- a) Planned FR capacity; b) Planned net injected power

Uncertainty in Day-ahead planning: The following sources of uncertainty exist in the planning phase:

- If the FR market participants are called for regulation service but they fail to provide the requested capacity (because of overestimation in the planning phase) they get penalized by the market operator. Thus, there is a risk associated with the day-ahead plan calculated as the probability that the actual available capacity for FR participation becomes less than the planned capacity; $Pr_{\alpha} = \Pr(\text{Actual FR cap} <$

α % of planned FR cap) where α represents the planning risk. Figure 36 illustrates planning risks over 24 hours period.

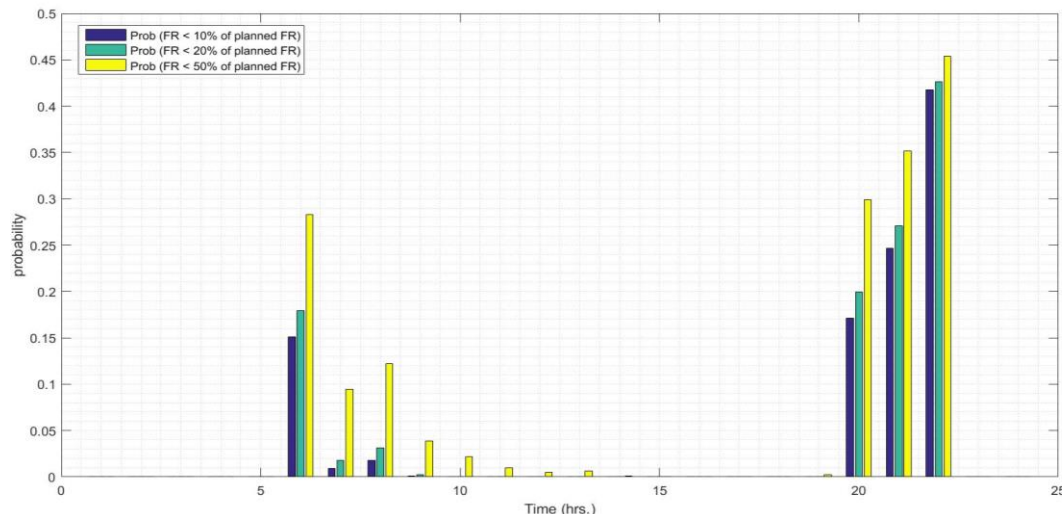


Figure 36- FR planning risk during different hours of the day

As illustrated in Figure 36 the risk related to FR planning capacity is negligible during the peak time when parking facility is almost fully-occupied. However, FR planning based on the average scenario has higher risk during the off-peak hours (6-8 AM and 8-10 PM).

- The actual net demand is different from the planned one, which could affect the bus voltage in distribution network. If the bus voltage falls out of the standard level it may cause damage to the distribution network. To avoid this, other generation (or demand) nodes must adjust their operation or the static storage needs to be installed at the bus to balance the actual and planned demand.

In the medium/high voltage distribution network the real/imaginary part of bus voltage could be approximately calculated according to the following equations [94]:

$$Vr_{n,t} = V_0 + \frac{1}{V_0} \sum_{n' \neq N} (Zr_{n,n'} \cdot Pg_{n',t} + Zi_{n,n'} \cdot Qg_{n',t}) \quad (4.9)$$

$$Vi_{n,t} = \frac{1}{V_0} \sum_{n' \neq N} (Zi_{n,n'} \cdot Pg_{n',t} - Zr_{n,n'} \cdot Qg_{n',t}) \quad (4.10)$$

where:

$Vr_{n,t} / Vi_{n,t}$: Real / Imaginary part of node “n” voltage at time “t”

V_0 : voltage of slack bus which is connected to the main grid at the substation

$Zr_{n,n'} / Zi_{n,n'}$: Real / Imaginary term of Z-bus for line (n, n')

$Pg_{n',t} / Qg_{n',t}$: Real / Imaginary term of net injected power in node “n' ” at time “t”

In order to demonstrate the impact of planning phase uncertainty on the distribution network we assume that our parking facility is located in the 12kV micro-grid shown in Figure 37. This micro-grid is composed of 5 nodes with 3 buildings. Building load profiles are generated based on EnergyPlus simulation database [95]. A commercial parking facility with 120 EV chargers is located at node 3. Moreover, three static storage systems (5,500 kWh, 1,700 kWh and 6,700 kWh) are respectively installed at node 1,2 and 4.

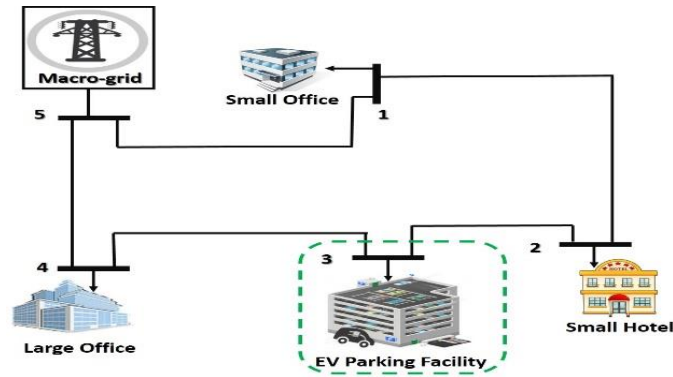


Figure 37- Example 5-node micro-grid

Changes in the actual injected net power at bus 3 (parking facility) may propagate across the distribution network and create disruptive voltage fluctuations. Voltage fluctuations within 90% to 110% of slack bus voltage and voltage phase between -0.15 and 0.1 radians are assumed as safe operational regions, note. Since node 5 is the slack bus we calculate the per-unit (p.u) when $V_{r_{5,t}} = 1 p.u \forall t$ & $V_{i_{5,t}} = 0 p.u \forall t$. Figure 38 illustrates the boxplot related to the magnitude and phase of network nodes through MC scenarios.

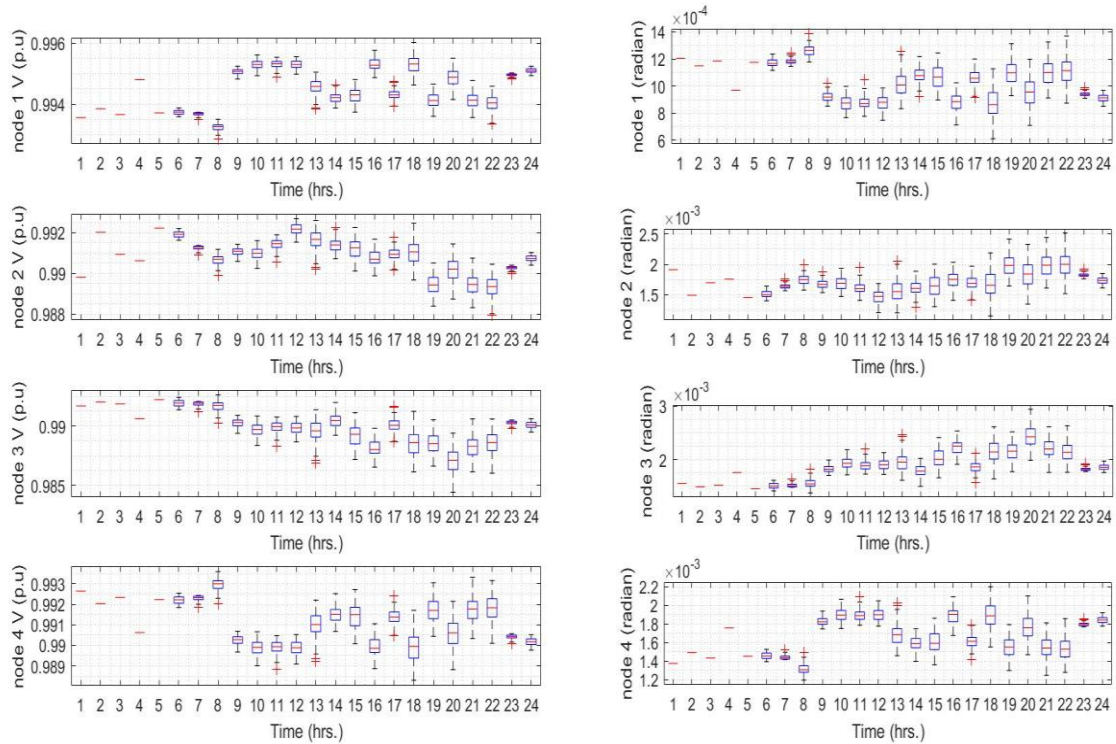


Figure 38 - voltage magnitude and phase at different nodes

For this illustration, as shown in Figure 38, the uncertainty in the parking facility net demand doesn't seem to have significant impacts on the network; i.e., that all node voltages remain in their feasible region. The reason is the existence of distributed energy storage systems with static capacity which dampen the fluctuation in nodal voltage.

Impact of V2G control on power distribution network- Lastly, we determine how V2G plans impact a distribution network. Consider the commercial parking-lot with 120 parking spaces. We compare two V2G scenarios. In the first scenario we assume that V2G system is not enabled and EVs only consume electricity to charge their batteries. In the second scenario the V2G system is active which enables parking owner to send electricity back to

the main grid. Following Figure 39 illustrates the facility net demand (net injected power) over all EV arrival scenarios in the MC simulation, for these two V2G cases.

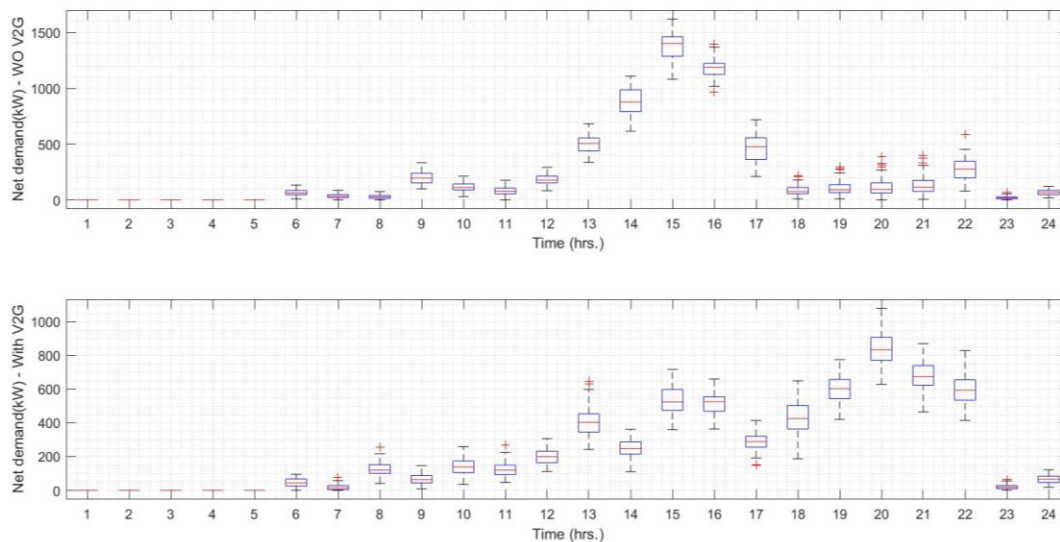


Figure 39- Parking facility net demand (net injected power): a) without V2G; b) with V2G

As demonstrated in Figure 39 the peak demand in enabled V2G scenario is much lower compared to the case without V2G. The reason is the flexibility in charging and discharging of batteries due to bi-directional V2G technology. The facility operator is able to manage the power flow in a way to reduce peak demand which results in lower electricity cost.

Following figure shows the average demand profile (net injected power) at the parking facility bus in these two V2G scenarios.

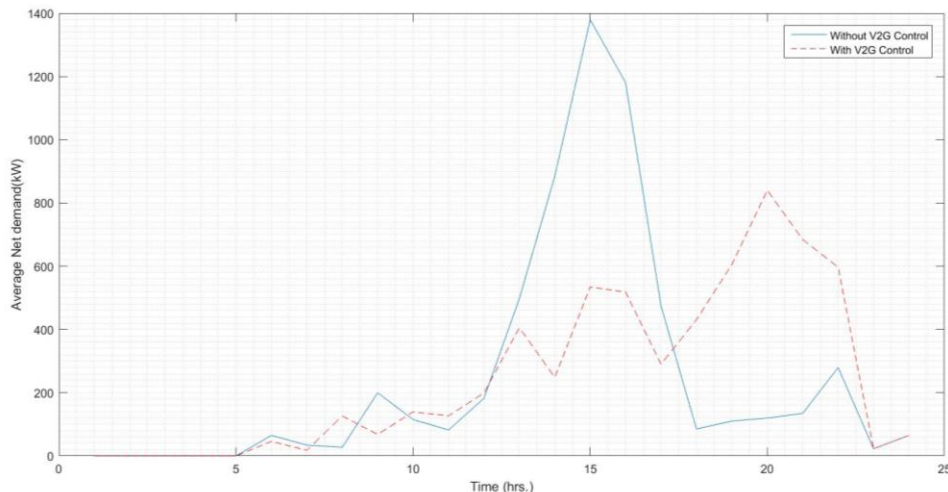


Figure 40- Average net demand profile

Figure 40 shows that using V2G system will reduce the peak demand by almost 40 %.

Lower peak demand results in:

- Lower transmission loss in the network.
- Lower required capacity at the node.
- Lower required capacity for transmission lines.

4.4. Formulation of Optimal Facility Operational Control

Service offering and corresponded cash flow streams are illustrated in Figure 41.



Figure 41- Money flow and offered services in the proposed business platform

There are three main sources of revenue:

1- **FR credit:** FR credit in PJM RegD market is based on the capability offered as well as the performance provided. The capability credit is related to the hourly integrated regulation capacity. The performance credit is related to how fast ESS can response to the PJM regulation signal. The integrated committed capacity, REG_t at time t , receives credit $FR Credit_t$ according to the following equation:

$$FR Credit_t = REG_t \times \rho (RMCCP_t + \beta_t \times RMPCP_t) \quad (4.11)$$

where, $RMCCP_t$ and $RMPCP_t$ denote Regulation market capacity clearing price (\$/kWh) and regulation market performance clearing price (\$/kWh) available at PJM website (<http://www.pjm.com/markets-and-operations/ancillary-services.aspx>). ρ is a score between 0 to 1 that indicates a unit's performance in following the regulation signal. Since battery storage response is quick, this performance score is close to 1. Note that REG_t is defined as:

$$REG_t = \sum_{i=1}^{N_{EV}} FR_{i,t} \quad (4.12)$$

where, $FR_{i,t}$ is the committed capacity to FR market from EV "i" during time step "t". β_t is PJM mileage ratio and is defined by:

$$\beta_t = \frac{RegD Mileage}{RegA Mileage} \quad (4.13)$$

RegD Mileage and *RegA Mileage* are the mileage corresponding to fast regulation and traditional regulation signals, respectively. Mileage is defined as the movement requested by the regulation control signal. For example, the RegD mileage over a time period over N steps is defined as:

$$RegD Mileage = \sum_{i=1}^N |RegD_i - RegD_{i-1}| \quad (4.14)$$

where, $RegD_i$ is the fast regulation capacity signal in the i 'th step.

2- **Sell back electricity to the main grid:** The facility operator may sell electricity back to the grid by discharging EV batteries using V2G technology. PJM 2016 day-ahead locational marginal price (LMP) data is used which denoted by Pr_t in this chapter. Parking owner benefit as a result of selling electricity to the main grid in time step 't' is calculated as:

$$SB\ Revenue_t = Pr_t \times Q_t \quad (4.15)$$

where, Q_t is aggregated amount of discharged electricity at time 't' which has been sold back to the grid (kWh).

3- **Charging EVs:** The facility will sell electricity to EVs for battery charging. We assume that EV pays the average electricity price during the time it is parked in the facility to the parking operator. Moreover, EVs which give the V2G permission to the parking operator will pay less. The amount of money that the individual EV i pays to the operator (\$) (EV_i^{ch}) is calculated based on the following equation:

$$EV_i^{ch} = (1 - V2G_i \times \varphi) \times \overline{Pr}_i \times Dem_i \quad (4.16)$$

where \overline{Pr}_i and Dem_i denote the average electricity price during the EV "i" parking time (\$/kWh) and EV "i" electricity demand (kWh). $V2G_i$ is a binary variable and is equal to 1 only and only if EV "i" gives the V2G permission to the facility operator. φ is a variable between 0 and 1 and represents the discount factor offered by operator to the EV owners in exchange for V2G permission.

The only daily operation cost element for the facility is the cost of buying electricity from the main power grid to charge EV batteries. Here we assume PJM hourly day-ahead LMP as a unit price of electricity. This cost element is calculated as:

$$PE\ Cost_t = Pr_t \times P_t \quad (4.17)$$

where $PE\ Cost_t$ and P_t represent the cost of purchasing electricity (\$) at time 't' and the amount of purchased electricity (kWh) during time step 't'.

EV owners may make revenue by reducing the cost of charging EV's battery if they give the V2G permission to the operator. So as mentioned before, EV "i" revenue (\$) , EV_i^{Rev} , is calculated as:

$$EV_i^{Rev} = \varphi \times \overline{Pr}_i \times Dem_i \quad (4.18)$$

The cost element related to the EV owner is the excessive degradation of battery because of V2G permission. We assume that battery degradation is proportional to the extra time that EV is parked in the garage. The amount of time that a vehicle stays in the facility in excess of time it needs for charging can be considered as committed capacity to the FR market. Deployment of EV battery in FR market or arbitrage during this extra time causes the excessive degradation, which results in earlier replacement of EV battery. We convert this degradation to dollar value by using following equation:

$$EV_i^{DegCost} = \gamma_i \times ExT_i \times \frac{RCap_i}{2 \times ECap_i} \times \frac{CapitalC_i}{N_i^{Cycle}} \quad (4.19)$$

where ExT_i is the extra parking time corresponding to EV "i". $RCap_i$ and $ECap_i$ respectively represent the rated capacity (kW) and energy capacity (kWh) of battery in EV "i". Expression " $ExT_i \times \frac{RCap_i}{2 \times ECap_i}$ " illustrates the number of full cycle the battery may have

during the extra time. γ_i is the fraction of time that battery in EV “i” is deployed by parking operator. $CapitalC_i$ is the capital cost (\$) of battery in EV “i” and N_i^{Cycle} represents the maximum number of cycle that battery could be charged and discharged. Equation 4.9 illustrates the portion of battery capital cost that can potentially be used for V2G permission. We assume that EV monitoring system is smart enough to estimate the degradation cost (equation 3.9) and also the revenue as a result of V2G permission (equation 3.8). EV owner will give V2G permission if $EV_i^{Rev} > EV_i^{DegCost}$. In other words:

$$V2G_i = \begin{cases} 1 & \text{if } EV_i^{Rev} > EV_i^{DegCost} \\ 0 & \text{o.w} \end{cases} \quad (4.20)$$

We now formulate an optimization problem aiming at maximizing facility owner’s revenue subject to V2G permissions from EV owners which is dependent on a fee discount factor and battery degradation cost. The decision variables are as follows:

- φ : discount factor offered by operator to EV owners in exchange for V2G permission
- $p_{EV \rightarrow G}^{i,t}$: power flow from EV “i” to the main grid during time step “t” (kWh)
- $p_{G \rightarrow EV}^{i,t}$: power flow from main grid to EV “i” during time step “t” (kWh)
- $FR_{i,t}$: Committed capacity from EV “i” to FR participation during time step “t” (kWh)

In the case that onsite renewable generation such as Photovoltaic (PV) exist in the facility, more decision variables will be added to the list:

- $p_{PV \rightarrow G}^t$: power flow from PV to the main grid during time step “t” (kWh)

- $p_{PV \rightarrow EV}^{i,t}$: power flow from PV system to EV “i” during time step “t” (kWh)

The objective function is defined as:

Maximize

$$\left\{ \sum_{t=1}^{24} (FR\ Credit_t + SB\ Revenue_t - PE\ Cost_t + Pr_t \times p_{PV \rightarrow G}^t) + \sum_{i=1}^{N_{EV}} EV_i^{ch} \right\}$$

(4.21)

The remaining sets of constraints related to the optimization problem are defined next. As mentioned before Q_t and P_t are integrated power flow due to discharging or charging, and are given by:

$$Q_t = \sum_{i=1}^{N_{EV}} p_{EV \rightarrow G}^{i,t} \quad \forall t \quad (4.22)$$

The quantity allocated to FR market reduce the maximum power flow for charging for discharging:

$$p_{EV \rightarrow G}^{i,t} + FR_{i,t} \leq Avail_t^i \times RCap_i \quad \forall i \text{ and } t \quad (4.23)$$

$$p_{G \rightarrow EV}^{i,t} + p_{PV \rightarrow EV}^{i,t} + FR_{i,t} \leq Avail_t^i \times RCap_i \quad \forall i \text{ and } t \quad (4.24)$$

where, $RCap_i$ is the rated power of battery in EV “i” which indicates the maximum amount of power that could be charged into or discharged form the battery during each hour. $Avail_t^i$ is a binary parameter and is equal to one during a time step t if EV “i” is parked in the garage during that time step. The SoC of EV battery is limited by its capacity minus the allocated capacity to the FR market:

$$FR_{i,t} \leq SOC_t^i \leq ECap_i - FR_{i,t} \quad \forall i \text{ and } t \quad (4.25)$$

If arrival time and departure time of EV “i” are denoted by T_{init}^i and T_{final}^i , the level of electricity in EV battery is updated at each time step “t” according to the following equation:

$$SOC_t^i = SOC_{t-1}^i + \eta_c \times (p_{G \rightarrow EV}^{i,t} + p_{PV \rightarrow EV}^{i,t}) - \left(\frac{1}{\eta_d}\right) \times p_{EV \rightarrow G}^{i,t} \quad \forall i \text{ and } t \in [T_{init}^i + 1, T_{final}^i] \quad (4.26)$$

η_c and η_d are battery charging and discharging efficiencies.

The initial level of energy in EV battery is random depending on the arrival time. The departure time and the final level of SoC are defined according to EV owner. We assume that if EV stays long enough in the parking the owner will request for the full charge. If the level of energy in the battery of EV “i” at arrival and departure time are denoted by SOC_{init}^i and SOC_{final}^i :

$$SOC_{t=T_{init}^i}^i = SOC_{init}^i \quad \forall i \quad (4.27)$$

$$SOC_{t=T_{final}^i}^i = SOC_{final}^i \quad \forall i \quad (4.28)$$

As mentioned before discount factor φ is a number between 0 and 1.

$$0 \leq \varphi \leq 1 \quad (4.29)$$

Moreover, power flow from EV to grid and the capacity allocation to FR market is allowable according to the EV owner permission. Therefore:

$$0 \leq p_{EV \rightarrow G}^{i,t} \leq V2G_i \times RCap_i \quad (4.30)$$

$$0 \leq FR_{i,t} \leq V2G_i \times RCap_i \quad (4.31)$$

$$0 \leq p_{G \rightarrow EV}^{i,t} \leq RCap_i \quad (4.32)$$

$$0 \leq p_{PV \rightarrow EV}^{i,t} \leq RCap_i \quad (4.33)$$

$$0 \leq p_{PV \rightarrow G}^t \leq Gen_t^{PV} \quad (4.34)$$

$$0 \leq p_{PV \rightarrow EV}^{i,t} \leq Gen_t^{PV} \quad (4.35)$$

Where, Gen_t^{PV} is the PV output power generated during time step “t”. PV output depends on the rated capacity (kW) PV system and also the solar intensity during time “t”. The parking operator optimization problem is summarized as problem (P1):

Maximize

$$\left\{ \sum_{t=1}^{24} (FR\ Credit_t + SB\ Revenue_t - PE\ Cost_t + Pr_t \times p_{PV \rightarrow G}^t) + \sum_{i=1}^{N_{EV}} EV_i^{ch} \right\}$$

(P1)

S.T. Constraints (4.11) – (4.18), (4.22) – (4.35)

In the next section, the solution approach to solve the defined optimization problem is introduced. The non-linear rule described of Equation 4.10 makes the optimization problem non-linear. In order to solve this mix-integer nonlinear problem we propose the following iterative approach:

Solution approach

For (k = 1: 101) repeat: / k /

$$1- \hat{\varphi}_k = \frac{k-1}{100}$$

2- *Solve optimization problem P1 given that $\varphi = \hat{\varphi}_k$*

3- *$obj_k = \text{optimal objective value of P1 in } k\text{'th iteration } (\varphi = \hat{\varphi}_k)$*

End

$$\varphi^* = \underset{\hat{\varphi}_k}{\operatorname{argmax}} \{obj_k\}$$

The above algorithm solves the optimization problem for many values of φ between 0 and 1, and compares the value of objective function in these iterations. The optimal discount factor φ^* is the one results in the higher objective value. In each iteration by assigning the value to φ and determining the V2G binary variable according to 4.10, the problem is converted to a mix-integer linear problem. The equivalent problem is solved by using YALMIP toolbox in the MATLAB based platform [96]. The algorithm can be carried out on a daily basis yielding different hourly optimal discount factors.

4.5. Illustrative case study

In order to demonstrate the impact of parking facility peak-hours and number of EV parking spots on the ESS evaluation, the following cases are considered:

- Case 1: A commercial parking garage (peak hours: around noon) with 80 parking spaces for EVs
- Case 2: A commercial parking garage (peak hours: around noon) with 120 parking spaces for EVs

- Case 3: A residential parking garage (peak hours: night) with 80 parking spaces for EVs
- Case 4: A residential parking garage (peak hours: night) with 120 parking spaces for EVs

One of the distinguishing characteristics among the illustrative cases is the application of garage facility. Two types of parking are considered: a) commercial parking, b) residential parking. Figure 42 shows the average aggregated capacity of batteries parked in the facility and the percentage of occupied parking spaces for commercial and residential parking garage. As illustrated in Figure 42 the commercial parking garage is almost fully occupied during noon times, however the peak hour in residential garage is during the night time.

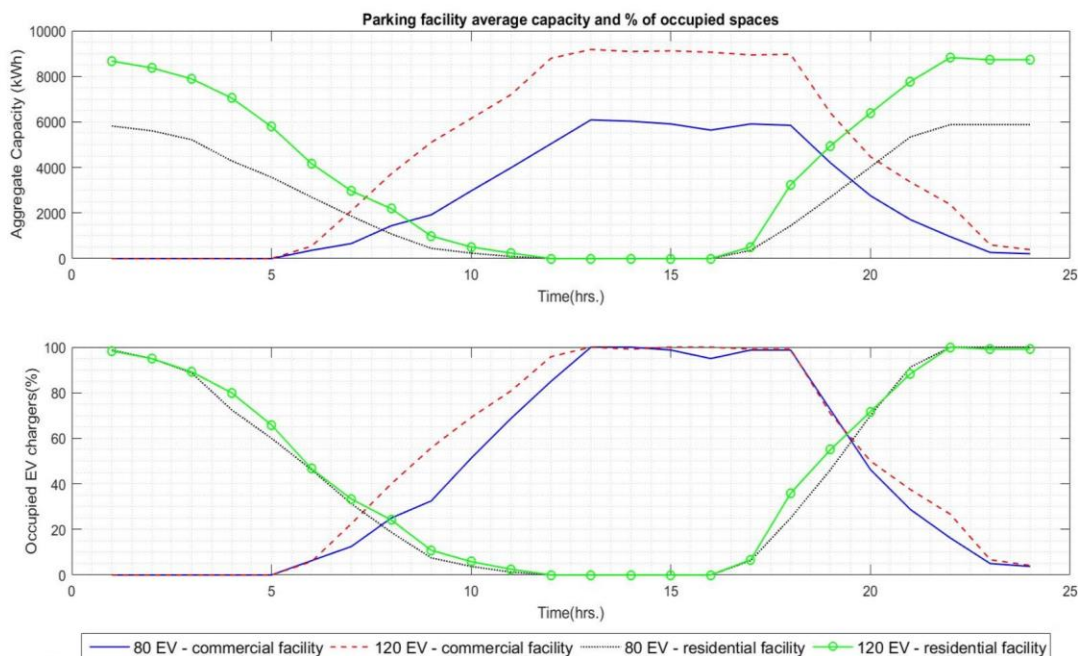


Figure 42: a) Dynamic storage aggregated capacity (kWh); b) % of occupied EV parking spaces

The other difference between these two types of parking facility is the average parking occupation time. In the residential garage, usually vehicles arrive during the evening time

and stay in the facility till the next morning. Therefore, as shown in Table 16, on the average, EVs stay in the residential garage for a longer duration.

Table 16 – parking lot characteristics

| Case | Average number of Evs coming into the facility in a day | Average parking duration for Evs (hrs.) |
|------|---|---|
| 1 | 193 | 4.33 |
| 2 | 295 | 4.73 |
| 3 | 80 | 10.62 |
| 4 | 120 | 11.07 |

We run several scenarios for each case, and each of these scenarios corresponds to the different hourly LMP, *RMCCP* and *RMPCP* profiles. Figure 43 shows the average hourly LMP and frequency regulation market clearing price which are inputs for the simulated scenarios.

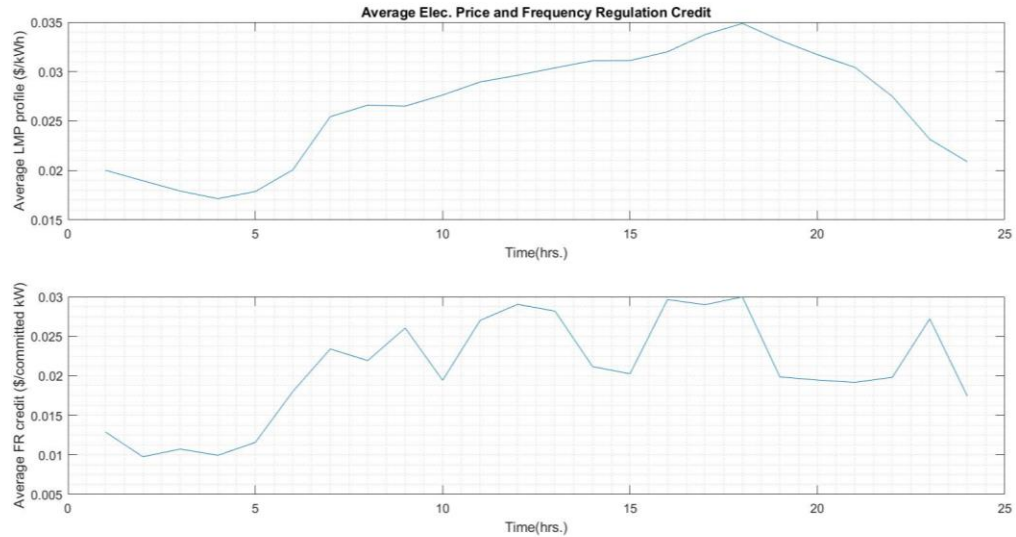


Figure 43: a) Average hourly LMP; b) Average hourly FR credit

Moreover, for each scenario the arrival and stay time of EVs are generated randomly according to the queueing model. We also assume two battery capacities (60kWh and 90 kWh) with equal probabilities. All chargers are assumed to be level-2 with 15 kW power rating. 90% efficiency is assumed (both charging and discharging) for all EV batteries.

Having run the optimal operational control model, we obtain Table 2 that gives the dollar amount from different sources for each of illustrative cases. Note that for annual net benefit calculation, the cost of electricity to charge EVs is included.

Table 17- Annual revenue (for all 4 cases)

| Case | Case 1 | Case 2 | Case 3 | Case 4 |
|---|-----------|-----------|-----------|-----------|
| Average optimal discount factor φ^* | 45% | 56% | 60% | 67% |
| Annual FR credit | \$ 48,868 | \$ 90,744 | \$ 51,180 | \$ 53,753 |
| Annual sell-back revenue | \$ 199 | \$ 393 | \$ 1,016 | \$ 2,501 |

| | | | | |
|----------------------------|-----------|-----------|-----------|-----------|
| Annual EV charging revenue | \$ 24,203 | \$ 28,141 | \$ 11,445 | \$ 12,047 |
| Annual total net benefit | \$ 27,496 | \$ 55,568 | \$ 39,255 | \$ 46,647 |

It is worth to mention the following observations:

- 1) Capacity commitment in frequency regulation market in the commercial parking garage is more valuable compared to the residential parking. The reason is the higher FR credit during the day times (Figure 43.b). Capacity requirement for frequency regulation service is more during a day compared to the night times, therefor commercial garage is able to make more revenue by participating in FR market.

- 2) Selling back electricity to the main grid is more beneficial in the residential facility. The reason is the higher variation in the hourly LMP prices during night times (9PM to 9AM – see Figure 43.a). The facility operator can charge EVs when electricity price is low and discharge to the grid when electricity price is high. Furthermore, as mentioned before, in the residential facility EVs are parked for a longer duration, which results in more opportunities for doing arbitrage and selling electricity to the main grid when electricity price is high.

- 3) In the residential parking facilities, the optimal discount factor is higher compared to the commercial ones. Therefore, the facility owner revenue from charging EVs in the residential case is less than the commercial case.

- 4) Overall, the commercial facilities generate more revenue. This observation is due to the higher revenue from the FR market participation compared to selling electricity back to the grid. Note that after discharging electricity to the main grid the parking operator has to recharge the batteries to the full SOC per EV owners' requests.

For more clarification on the impact of FR credit and electricity price on the parking facility evaluation, we dive more into individual samples and compare the daily value of different types of EV parking facilities. As illustrated in the previous section the value of frequency regulation credit is one of the significant factors in EV facility valuation. Also, it has been discussed that in many scenarios the FR credit is higher during the day-time which causes higher revenue for a commercial garage. There are also some days that FR credit is higher during the night time. Figure 15 shows the hourly LMP and FR credit for some sample days according to the PJM data. As illustrated in Figure 44 the FR credit is much higher during the day-time for April 18th and 19th.

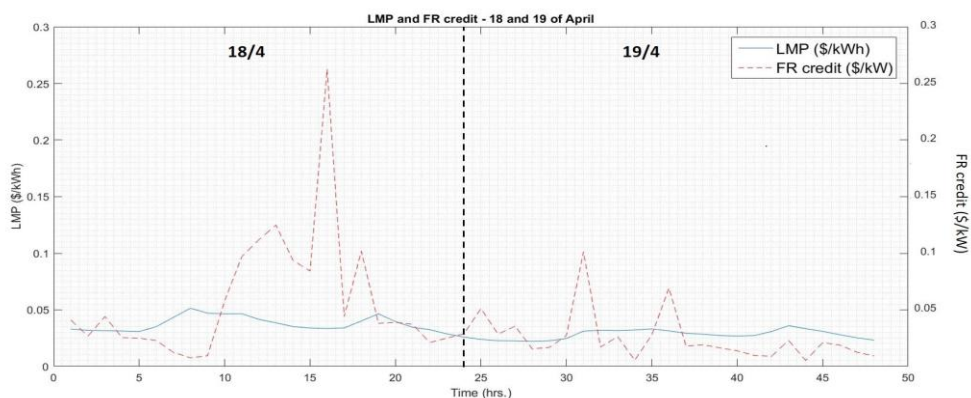


Figure 44- LMP and FR credit (18/4 - 19/4)

Moreover Figure 45 shows that FR credit is higher during the night time in February 2nd and 3rd.

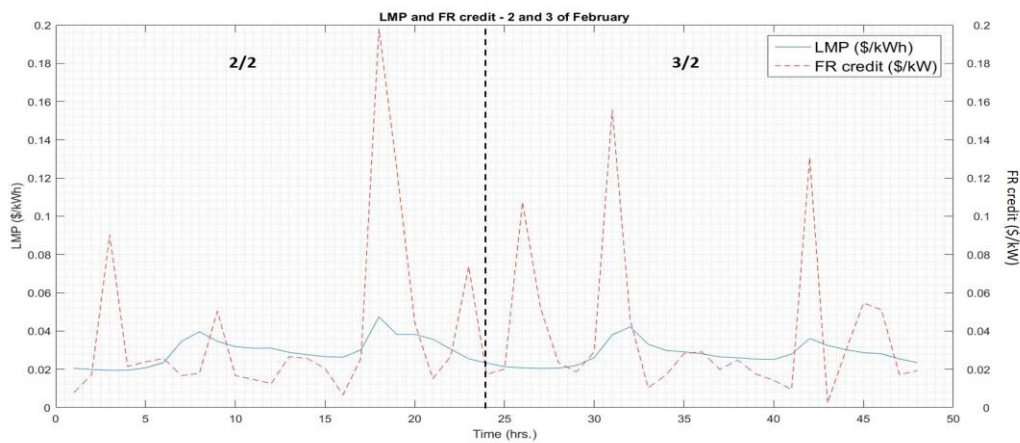


Figure 45- LMP and FR credit (2/2 - 3/2)

Following table shows the April 18th and February 2nd revenue for different cases, which illustrates that the FR credit has the significant impact on the daily value. On the April 18th, FR clearing price is much higher than LMP. Therefore, commercial facility with noon-time peak is more beneficial. However, as illustrated in Figure 45, on February 2nd, LMP and FR clearing price are in the same range during the noon time, but there is more variation in LMP during the night-time (9PM-9AM) which brings arbitrage opportunities. Therefore, during this specific day residential facility is more beneficial.

Table 18 - April 18th total revenue in different cases

| Case | Case 1 | Case 2 | Case 3 | Case 4 |
|-----------------------------------|--------|--------|--------|--------|
| Total revenue (\$) – April 18th | 495 \$ | 890 \$ | 230 \$ | 310 \$ |
| Total revenue (\$) – February 2nd | 145 \$ | 270 \$ | 340 \$ | 405 \$ |

As discussed in the previous sections frequency regulation credit and electricity price affect the EV parking garage revenue. In order to consider these pricing elements during the peak-hours of parking facility, we define four new terms as follows:

$$EP\ Weighted_{Capacity} = \sum_{t=1}^{24} Agg\ Cap_t \times Pr_t \quad (4.36)$$

$$EP\ Weighted_{occupied} = \sum_{t=1}^{24} Occupied\ Spaces_t \times Pr_t \quad (4.37)$$

$$FR\ Weighted_{Capacity} = \sum_{t=1}^{24} Agg\ Cap_t \times FR\ Credit_t \quad (4.38)$$

$$FR\ Weighted_{occupied} = \sum_{t=1}^{24} Occupied\ Spaces_t \times FR\ Credit_t \quad (4.39)$$

Where, $Agg\ Cap_t$ and $Occupied\ Spaces_t$ denote the aggregate capacity of batteries parked in the garage and the percentage of occupied parking spaces at time t respectively. Figure 16 shows the correlation between these 4 new factors and the daily revenue of garage.

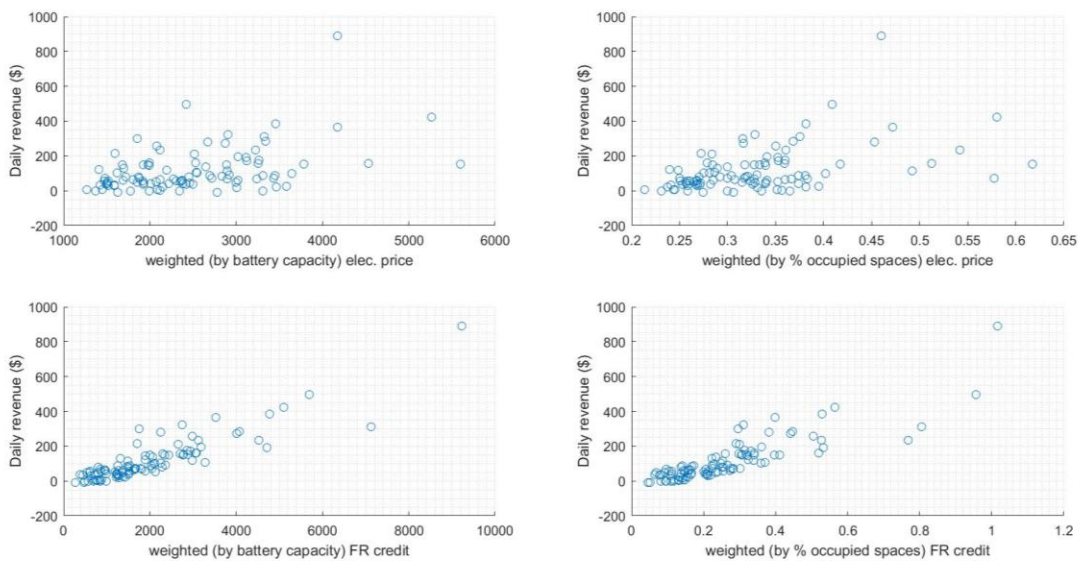


Figure 46- correlation analysis

As illustrated in Figure 46 parking facility daily revenue has strong correlation with the weighted FR credit (both capacity weighted and occupied spaces). However, this figure doesn't show strong correlation between electricity price and daily value. Following figure shows the correlation value between these 4 factors and daily value of EV garage.

Table 19- Correlation value

| Factor | Correlation with daily revenue |
|---------------------------------------|--------------------------------|
| <i>EP Weighted_{capacity}</i> | 0.45 |
| <i>EP Weighted_{occupied}</i> | 0.46 |
| <i>FR Weighted_{capacity}</i> | 0.89 |
| <i>FR Weighted_{occupied}</i> | 0.87 |

Analysis of daily EV parking revenue for all of the four cases shows that the electricity prices and frequency regulation credit during the peak-hour of the parking has impact on the value of parking facility. Moreover, it has been illustrated that FR credit has the most significant impact on the evaluation process. In other words, high FR credit during the busy hours of parking causes high value for the parking operator. Furthermore, more capacity for EVs in the parking results in more revenue for the facility operator.

As part of this analysis, it has been observed that with the current state of arbitrage and regulation markets, commercial parking facilities (with noon-time peak) are more beneficial from the parking operator point of view. The reason is high regulation market clearing price during the day-time which coincides with peak-hours of commercial parking facilities. Moreover, V2G capability is able to reduce the peak electricity demand by almost 40% which reduces the power loss in power distribution network and defers the needs for capacity upgrade. As the EV owners' perspective the discount they receive from the parking operator, compensates the additional battery degradation cost. Moreover, EV owners (same as the all rate-payers in the distribution network) could benefit from the lower electricity tariff-rate which is expected because of peak reduction in the grid.

4.6. Conclusion

This study proposed an integrated framework which optimally plans for the charge and discharge of EVs in a large parking facility to maximize the parking facility benefits. Economic benefit to EV owners through reduced parking fees or discounted charging fee has been also taken into the account, which compensates the additional degradation of the vehicle battery. The proposed model is capable to quantify the impact of such facility on the power distribution network. Almost 40% electricity peak reduction has been observed

for the commercial parking facility which has V2G-enabled charging stations. This reduces the power loss in the power distribution network and defers the needs for T&D capacity upgrades. The analysis shows that, with the current state of arbitrage and regulation market, commercial parking facilities are more beneficial from the parking operator point of view compared to residential parking (which are occupied during the night time). The reason is high regulation market clearing price during the noon time which coincides with peak-hours of commercial parking facilities.

CHAPTER 5: JOINT OPTIMIZATION OF OPERATION AND MAINTENANCE POLICIES FOR MICROGRID COMPOSING OF ENERGY STORAGE SYSTEM

Abstract

In a solar-powered microgrid (MG), the optimal maintenance strategy is influenced by the downtime cost of the photovoltaic (PV) system, which in turn depends on the operation PV within the MG network. Also, the dispatch policy used in the MG will influence the economic feasibility of maintenance plans. In this chapter, we present an approach for optimizing the operation and maintenance policy jointly for a solar-powered MG considering the dependence between the two policies. The two-layered approach presented in this work seeks to unify the practicality of simulation and the efficiency of analytical models. In the upper layer, we optimize the operation of MG by solving the optimal power dispatch within the MG network using linear programming approach. Then, we calculate the penalty costs under the aging conditions of PV systems. In the bottom layer, by incorporating the penalty costs as input parameters, we use a continuous-time Markov chain model to calculate the optimal maintenance policy for the PV system. The proposed approach could be used in the stipulation process between MG owner and PV system maintenance provider to minimize the money waste on both sides.

Nomenclature

d Index of day

| | |
|-----------------|--|
| t | Index of time interval |
| k | Index of renewable node |
| s | Index of energy storage unit |
| l | Index of demand node |
| g | Main power grid |
| CAP_s | Storage s energy capacity (kWh) |
| P_s | Energy storage rated capacity (kW) |
| $L_d(l, t)$ | Total demand during time interval t at node l in day d |
| $R_d(k, t)$ | Total generation during time interval t at renewable node k in scenario sc |
| $e_{g,s}(d, t)$ | Total energy charged from the grid during t in storage unit s in day d |
| $e_{k,s}(d, t)$ | Total energy charged from renewable node k during t in storage unit s in day d |
| $e_{s,l}(d, t)$ | Total energy discharged during t from storage s to demand node l in day d |
| $e_{g,l}(d, t)$ | Total energy from the grid during time interval t to demand node l in day d |
| $e_{k,l}(d, t)$ | Total energy from renewable k during t to demand node l in day d |
| η_s | Energy storage s one-way efficiency |

| | |
|------------------------|---|
| $EP_d(t)$ | Electricity price in time interval t for day d |
| $SOC_s(d, t)$ | Storage s energy level (kWh) at the end of time interval t in day d |
| SF | Safety reserve capacity for energy storage unit |
| $esl_{s,l}(t, d)$ | Storage “s”-Demand “l” eligibility number (day “d” - time interval “t”), binary |
| $ers_{k,s}(t, d)$ | Renewable “k”-Storage “s” eligibility number (day d - time interval “t”), binary |
| $erl_{k,l}(t, d)$ | Renewable “k”-Demand “l” eligibility number (day d - time interval “t”), binary |
| DOC_d | Optimal daily operation cost in day d |
| $b^{(\alpha)}$ | The threshold of major maintenance activity for the α^{th} photovoltaic system |
| $m^{(\alpha)}$ | The number of degradation states of the α^{th} photovoltaic system |
| $n^{(\alpha)}$ | The number of failure sudden modes of the α^{th} photovoltaic system |
| $\lambda_m^{(\alpha)}$ | The deterioration rate for the α^{th} photovoltaic system α at state m |
| $C_{s,l}^{(\alpha)}$ | Cost for each corrective maintenance after mode l sudden failures on the α^{th} photovoltaic system |

| | |
|-------------------------------------|--|
| $\frac{1}{\mu_{s,l}^{(\alpha)}}$ | Duration of corrective maintenance after mode l sudden failures on the α^{th} photovoltaic system |
| $1/\lambda_F$ | Mean time between two successive mode l sudden failures on the α^{th} photovoltaic system |
| C'_{in} | Cost for each inspection of the α^{th} photovoltaic system |
| $\frac{1}{\lambda_{in}^{(\alpha)}}$ | Mean time between two successive inspections on the α^{th} photovoltaic system |
| $1/\mu_{in}$ | Mean duration of inspection on photovoltaics α |
| $C_M^{(\alpha)}$ | Cost for each major maintenance activity of the α^{th} photovoltaic system |
| $1/\mu_M$ | Mean duration of major preventive maintenance on the α^{th} photovoltaic system |
| $C_R^{(\alpha)}$ | Cost for each replacement activity of the α^{th} photovoltaic system |
| $1/\mu_R$ | Mean duration of replacement on the α^{th} photovoltaic system |
| $C_p^{(\alpha)}$ | Planned per unit downtime cost for the α^{th} photovoltaic system |
| $C_u^{(\alpha)}$ | Unplanned per unit downtime cost for the α^{th} photovoltaic system |
| $C_{v,i}^{(\alpha)}$ | Penalty caused by the performance degradation of the α^{th} photovoltaic system. |

| | |
|------------------------|--|
| $\pi_{i,j}^{(\alpha)}$ | Probability of the α^{th} photovoltaic system being in state (i, j) |
| $C_S^{(\alpha)}$ | Time-averaged operating cost of the α^{th} photovoltaic system |
| C_G | The overall expected operational and maintenance cost for the microgrid |

5.1. Introduction

Microgrids (MGs) are small-scale power networks composed of multiple energy resources and, in some cases, distributed energy storage devices (ESDs). They are seen to be increasingly important to achieve a reliable, flexible, and sustainable electricity network. In this chapter, we focus on two aspects that influence the cost-effectiveness of microgrids – the operation control and maintenance policies – and the relationship between them. In particular, we examine the significance of ESDs on the policies and hence the overall operational cost of the MG. In such type of MGs, ESDs play a role of storing energy when surplus energy is produced and discharging to support demands when needed. Due to the uncertain nature of the power generation by renewable sources [97-98] and demand profiles within the MG, it poses a challenge on managing the operation of MGs. To overcome this challenge, the related advancement has been achieved on supporting MG owners to decide whether or not to use ESDs, optimizing the size of ESDs [99], [100] and [101], and scheduling the charge and discharge times for these ESDs [102] and [113].

In general, ESDs could improve the reliability and power quality of a MG. Moreover, it is capable of providing an economic benefit in a deregulated energy market [103]. It encourages utility company to shift and shave peak load [102]. In the light of this, the operation and control of a MG need to be taken into account the power flow between

entities within the MG, as well as the power flow between MG and main grid. Khalilpour and Vassallo [98] developed a decision support tool for scheduling of PV-battery systems based on a detailed power flow model. Cost saving through simultaneously managing energy production and demand is another aspect that has been focused on [104]. The latest development in this area enables a near-real-time optimal charge and discharge control policies for a MG with multiple ESDs [105].

Maintenance is also an important issue in MGs, which may have a major impact on the overall ownership costs of the grid. As studied by [106], good maintenance and inspection policies are essential for improving the financial viability of the MG. A particular focus in the area is to examine the safety hazards [107], failure and performance deterioration [108] of photovoltaic (PV) systems in MGs. Hence, an online monitoring system may appear beneficial as it may improve the maintenance performance of PV systems within a MG and in turn increase the profit of the MG. In [109], authors developed a continuous-time Markov chain model for PV systems that are subject to deterioration and failure. The study had shown implementing condition monitoring is more favorable for both MG owner and maintenance provider by comparing with manual inspections.

In a MG, maintenance policies that control the availability of PV systems can subsequently influence the energy generation and operation policy of the MG. Moreover, an effective energy storage policy can reduce the downtime penalty cost, if the stored energy can be used to satisfy demand during the downtime of PV systems caused by preventive maintenance or failure. However, the interplay/dependence between operation policy and maintenance policy is still underexplored in the context of the microgrid. In this chapter,

we refer such type of dependence between operation and maintenance as “operation dependence”. The work presented in this chapter consists of following five novelties:

1. It is a two-layered approach that includes an upper layer for simulating the operation of MG and a lower layer for modeling the deterioration and maintenance of PV systems. Through such layer separation, the mathematical tractability of the lower layer is preserved.
2. In the upper layer, we formulate the operation of a MG as an optimal dispatch problem. The discharging and charging of ESDs are optimized in a way to maximize the value of MG. The model formualtes the power flow of the MG with details. Moreover, the model is capable of integrating historical data on demand profiles, solar radiation, and electricity price, which indicates a good applicability in practice.
3. In the lower layer, the deterioration and maintenance of the PV systems are formulated by continuous-time Markov chain. Both the performance degradation caused by the malfunction of PV arrays and invertor failure are considered. Also, the model considers the maintenance duration.
4. We have applied our approach on a practical MG to test the practicality. The value of ESDs is demonstrated from operation and maintenance perspectives through a comparative study.
5. Finally, our study could provide insights for both maintenance service providers and MG owners. A warranty contract that based on the performance of PV systems could be mutually beneficial for both sides compared with a fixed amount warranty contact. Our operation and maintenance model can support both sides to this end.

The rest of chapter is structured as follows: In section II, we introduce the general set-up of the MG and the mechanism for failure and performance degradation for the PV systems within the MG. Section III describes the modeling approach to optimize the operation and maintenance of the MG. Section IV validates the approach by applying it to a practical solar-powered MG in the US. The optimal operation and maintenance strategies are demonstrated. Moreover, an analysis is provided on the value of ESDs in this context. Finally, section V presents the concluding remarks of the chapter.

5.2. System description

We consider a grid-connected community level MG, with PV resources as the source of power as illustrated in Figure 47. The PV output may differ from the system load from time to time. When the PV output is greater than the load, the ESDs absorb this excessive power. Hence, the energy charged from PV resources during off-peak hours can be utilized during peak hours to shave the peak demand.

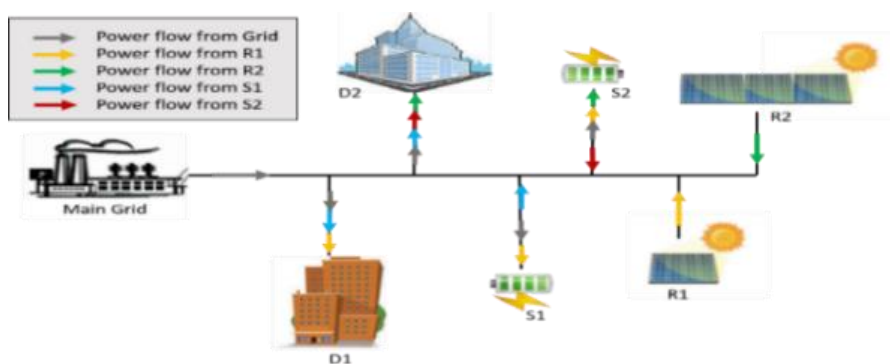


Figure 47: An illustrative example of a MG configuration

The demands of the community are primarily satisfied by the power generated on-site by the PV systems and ESDs within the grid. Alternatively, the main grid can also supply power to the community. In this case, the operation cost of the MG is the expenditure on

purchasing electricity from the main grid to supplement and satisfy the electricity demands in the community. We assume that the owner of the MG participates in the wholesale day-ahead market. Due to the cost of buying electricity from the main grid is varying throughout the day, the total operation cost can be reduced by optimizing the charging and discharging time of ESDs. In our approach, the operation policy depends on the demand level, on-site generated power, electricity price as well as the performance and availability of PV systems.

The PV system is configured in multiple arrays. As illustrated in Figure 48 multiple PV modules are serially connected within each array.

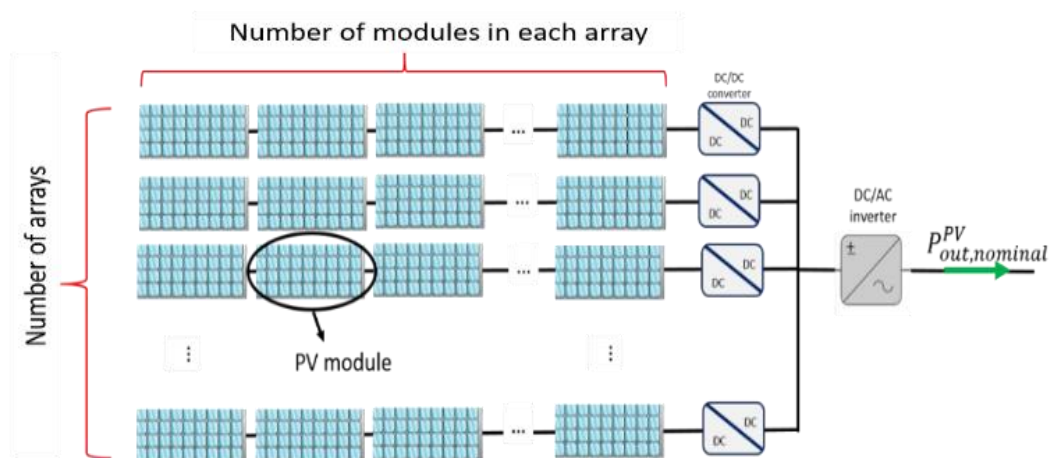


Figure 48: Configuration of PV systems

The failure of a PV module will stop its array from operating. Thus, despite the low failure rate of PV modules, the failure rate of serially connected PV arrays is still non-negligible [115] and [116]. The energy generation capability of the PV system is proportional to the number of functional arrays. Consequently, the failure of a PV module will result in performance degradation of the PV system. In new system, the PV module may also be bypassed by diodes due to an open failure or shading effect. The bypass of PV module

generally could lower the output of a string, rather than causing an outage of the string. Even though the proposed maintenance model is capable to deal with such system, in this study, we do not consider the bypass of modules [116]. All PV arrays are connected to a DC/AC inverter. The inverter is used to convert the electricity generated by the PV system to the regulated AC voltage. The failure of the inverter will immediately disconnect the PV system from the MG. Such type of failure is formulated as a sudden failure in our designed maintenance model. The unavailability or performance degradation of PV systems will affect the operational decision of ESDs. We assume that the performance of PV systems can be observed and analyzed by grid operator continuously.

The objective of operation policy is to determine the optimal power dispatch among different nodes within the MG, according to the performance level and availability of PV systems. Taking into account the operation dependence, the objective of maintenance policy is to identify the optimal maintenance threshold (a degradation threshold triggering replacement of the failed PV modules) for the PV systems so that the expected annual ownership cost (operation cost and maintenance cost) of the MG is minimized.

5.3. Modeling Approach

Our modeling approach contains two layers. The upper layer aims to optimize the operation of the MG under different types of operation constraints by optimally charge/discharge ESDs. The output of this model is the operation cost of MG under different conditions of PV systems. This output then forms a part of the input to the lower layer, which aims to optimize the maintenance policies for the PV systems in the long term. A holistic view of the top-down approach is illustrated in Figure 49.

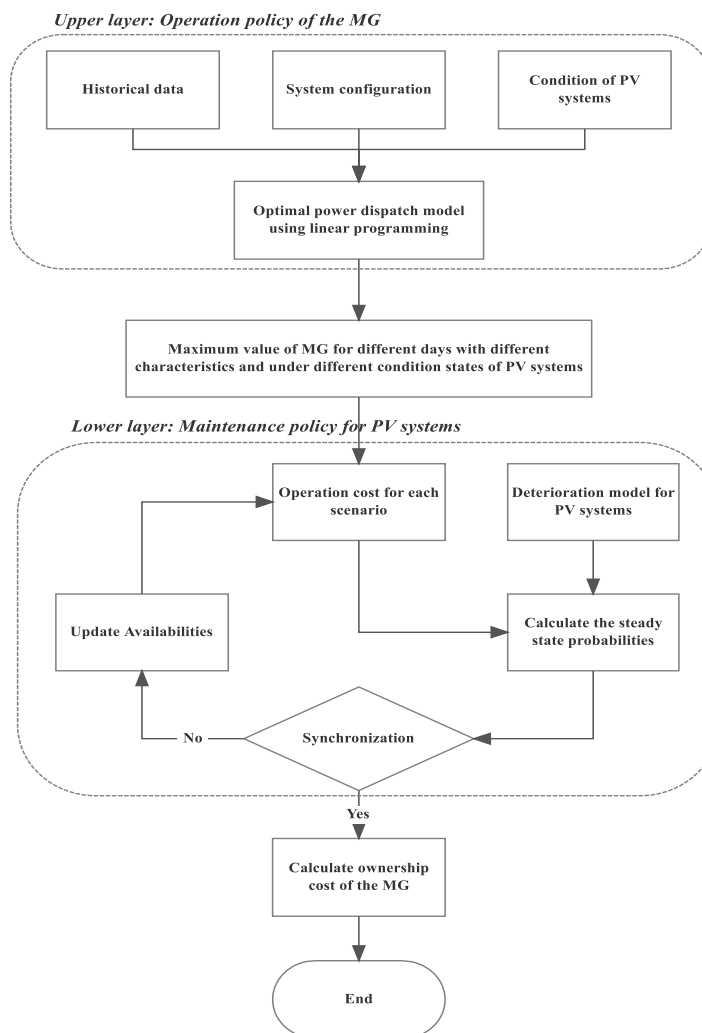


Figure 49: Schematic diagram of the top-down approach

In the upper layer model, we compute the optimal power dispatch problem using linear programming under different condition states of the PV systems and for each individual day based on the historical data. Days are distinguished by three stochastic variables, namely electricity demand, solar radiation, and electricity price. Three years' historical data (available on PJM website) have been used to characterize hourly profiles of demand, electricity price and solar radiation each day. The operation model optimizes the amount of charged and discharged energy (as decision variables) of ESDs during the different time

intervals for each individual day. This optimal solution also depends on the state of network elements, such as the degradation state (condition) of PV systems and the network configuration (connectivity of different nodes). The output from operation model is the lower bound for the microgrid operation cost for each individual day existed in historical dataset under different conditions of PV systems. By comparing the operation cost of the MG in the good condition state of PV systems (100% performance) with any individual degraded state (or failure state) of the PV system, we can calculate the penalty cost due by performance degradation (or failure) of PV systems. This information is used to formulate of maintenance policy of PV systems. In this way, we link the operation policy and the maintenance policy of the MG. In the lower layer, we consider the situation where the maintenance policy of one PV system changes its availability and may in turn influence the downtime penalty cost of other PV systems and sequentially affect the optimization of maintenance policies. We use an iterative approach to synchronize the maintenance policies of PV systems so that they can reach the optimal solution simultaneously. The final output of the model is the optimal ownership cost of the MG. In the next subsections, we will describe the formulation of the upper and lower layer models.

5.3.1. Upper layer (system operation model)

The objective of the upper layer is to minimize the operation cost of the MG by adjusting the charging and discharging of ESDs based on the scenario and performance of PV systems. We apply the linear programming to optimize the operation of the MG for each scenario. The detail of the objective function and different types of operational constraints of the MG will be explained with more details in equations (1) and (2)-(8) respectively.

Objective function: The daily operation is optimized for each scenario. A scenario contains the information of the electricity demand, generation profile of PV systems and electricity price profile in the given day “d”. The objective function then expresses as (5.1):

$$\min\{\sum_t[EP_d(t) (\sum_l e_{g,l}(d, t) + \sum_s e_{g,s}(d, t))]\} \quad (5.1)$$

The decision variables are the amount of energy charge and discharge by an ESD in a unit time (hour). Note that we assume the voltages of different nodes are maintained in the feasible region. The objective function is to minimize the overall expenditure on purchasing electricity from the main grid. The purchased electricity is used to either charge storages ($e_{g,s}$) or supply demands ($e_{g,l}$). The minimization process is subject to multiple types of constraints, which are listed as below:

Storage operation constraints: In each scenario, the total amount of inflow and outflow electricity for each storage node in each time interval is limited to its rated power capacity.

$$e_{g,s}(d, t) + \sum_k e_{k,s}(d, t) + \sum_l e_{s,l}(d, t) \leq P_s, \forall s, t, d \quad (5.2)$$

As illustrated in (2), multiple charging and discharging actions are allowable during each hour. However, the summation of inflow and outflow is limited by the rated capacity of the storage unit. The storage level at a given time interval is calculated by the storage level at the previous time interval and the charging and discharging energy during the time interval.

$$SOC_{s,t,d} = SOC_{s,t-1,d} + \eta_s \times (e_{g,s}(d,t) + \sum_k e_{k,s}(d,t)) - \frac{\sum_l e_{s,l}(d,t)}{\eta_s}, \forall s, t, d \quad (5.3)$$

We assume that at the beginning of the day storage level is at the 50% of maximum capacity and it has to reach to the same level at the end of the day. It is intuitive that the storage level cannot exceed the maximum capacity of the ESD (CAP_s) and cannot reduce below the safety reserve capacity (SF_s).

$$SF_s \times CAP_s \leq SOC_{s,t,d} \leq CAP_s, \forall s, t, d \quad (5.4)$$

On-site renewable resource constraint: Electricity generated by a renewable unit is used to serve demand nodes and charge the storage nodes which are connected to it.

$$R_d(k,t) \geq \sum_l e_{k,l}(d,t) + \sum_s e_{k,s}(d,t), \quad (5.5)$$

$$\forall k, t, d$$

Demand constraint: Electricity load at each demand node has to be satisfied. The portion of demands is satisfied by on-site generation and discharged electricity from storages, and the remain has to be satisfied by purchasing from the main grid.

$$L_d(l,t) = \sum_k e_{k,l}(d,t) + \sum_s e_{s,l}(d,t) + e_{g,l}(d,t), \forall l, t, d \quad (5.6)$$

Configuration and availability constraints: The configuration of the MG is defined by three binary matrices (ESL, ERL, and ERS). The value 1 indicates the two nodes are connected, and 0 indicates no connection. Sometimes, assets within the MG may become

unavailable. We use a binary number $erl_{k,l}(t, d)$ to indicate the connection between k^{th} PV system and l^{th} demand node at time “t” in day “d”.

$$0 \leq e_{k,l}(d, t) \leq M \times erl_{k,l}(t, d), \quad (5.7)$$

$$\forall l, k, t, d$$

$$0 \leq e_{s,l}(d, t) \leq M \times esl_{s,l}(t, d), \quad \forall l, s, t, d \quad (5.8)$$

$$0 \leq e_{k,s}(d, t) \leq M \times ers_{k,s}(t, d), \quad \forall s, k, t, d \quad (5.9)$$

where “M” is a very big number (e.g. 10 million). More details about the optimal operation and control of this network could be found in [105].

For given input profiles and performance of PV systems, the operation of the MG can be optimized. We refer the optimized daily cost under given day “d” and performance of PV systems as $DOC(d, X^{(1)}, \dots, X^{(k)})$. $X^{(\alpha)}$ is a random variable that indicates the performance of α^{th} PV system. For a PV system with m_α number of arrays, $X_{m_\alpha}^{(\alpha)}$ indicates all arrays are functional. $X_{i_\alpha}^{(\alpha)}$ indicates i_α ($i_\alpha < m_\alpha$) number of arrays are functional. Therefore, we have $X^{(\alpha)} = \{X_{m_\alpha}^{(\alpha)}, \dots, X_{i_\alpha}^{(\alpha)}, \dots, X_{0_\alpha}^{(\alpha)}\}$. Let $\overline{DOC^*}$ indicates the expected daily cost over all existed days in the historical data set when the PV system amongst the MG is ideal. We signified the overall number of days as N_d . Then $\overline{DOC^*}$ can be expressed as:

$$\overline{DOC^*} = \frac{\sum_{d=1}^{N_d} DOC(d, X_{m_1}^{(1)}, \dots, X_{m_k}^{(k)})}{N_d} \quad (5.10)$$

We assume the planned preventive maintenance can be scheduled when the impact on the operation of the MG is minimized. $\overline{DOC_p^{(\alpha)}}$ is the expected the operation cost when α^{th} PV system is offline due to preventive maintenance.

$$\overline{DOC_p^{(\alpha)}} = \min_d \left[DOC(d, X_{0\alpha}^{(\alpha)}, \mathbb{E}[X^{(1)}, \dots, X^{(\alpha-1)}, X^{(\alpha+1)}, \dots, X^{(k)}]) \right] \quad (5.11)$$

$\mathbb{E}[X^{(1)}, \dots, X^{(\alpha-1)}, X^{(\alpha+1)}, \dots, X^{(k)}]$ is interrelated with the maintenance strategy of PV systems. It is computed with iteration. To initialize, we assign equal probability for all $X^{(1)}, \dots, X^{(k)}$. Therefore, the equation (5.12) is equal to as:

$$\overline{DOC_p^{(\alpha)}} = \frac{\min_d [\sum DOC(d, X_{0\alpha}^{(\alpha)}, X^{(1)}, \dots, X^{(\alpha-1)}, X^{(\alpha+1)}, \dots, X^{(k)})]}{\prod_{i=1}^{\alpha-1} \overline{X^{(i)}} \prod_{i=\alpha+1}^k \overline{X^{(i)}}} \quad (5.12)$$

where $\overline{X^{(i)}}$ indicates the cardinality of $X^{(i)}$. $\overline{DOC_u^{(\alpha)}}$ is the expected operation cost when α^{th} PV system is unavailable due to the unplanned failure. We assume it may happen with an equal probability across all days:

$$\overline{DOC_u^{(\alpha)}} = \frac{\sum_d DOC(d, X_{0\alpha}^{(\alpha)}, \mathbb{E}[X^{(1)}, \dots, X^{(\alpha-1)}, X^{(\alpha+1)}, \dots, X^{(k)}])}{N_d} \quad (5.13)$$

Similarly, we can calculate the expected cost when $X^{(\alpha)} = X_{i\alpha}^{(\alpha)}$.

$$\overline{DOC_i^{(\alpha)}} = \frac{\sum_d DOC(d, X_{i\alpha}^{(\alpha)}, \mathbb{E}[X^{(1)}, \dots, X^{(\alpha-1)}, X^{(\alpha+1)}, \dots, X^{(k)}])}{N_d} \quad (5.14)$$

In the operation model, we use $\overline{DOC^*}$ as a benchmark. The penalty caused by preventive maintenance $C_p^{(\alpha)}$, unplanned failure $C_u^{(\alpha)}$ of α^{th} PV system can be calculated equation (5.15) and (5.16) respectively.

$$C_p^{(\alpha)} = \overline{DOC_p^{(\alpha)}} - \overline{DOC^*} \quad (5.15)$$

$$C_u^{(\alpha)} = \overline{DOC_u^{(\alpha)}} - \overline{DOC^*} \quad (5.16)$$

The expected penalty caused by performance degradation due to only i_α arrays are functional can be calculated by $C_i^{(\alpha)}$.

$$C_{v,i}^{(\alpha)} = \overline{DOC_i^{(\alpha)}} - \overline{DOC^*} \quad (5.17)$$

One complication of calculating the equations (5.11) - (5.14) is the $\mathbb{E}[X^{(1)}, \dots, X^{(\alpha-1)}, X^{(\alpha+1)}, \dots, X^{(k)}]$ is unknown and affected by maintenance policies of all PV systems due to operation dependence. In the developed approach, we calculate the expected performance of all PV systems through iteration. To initialize the computation, we first assign the equal probability to all performance states of PV systems. Then, we calculate the steady state probabilities for each PV system at the optimal maintenance strategy. The steady state probabilities are then used to update the expected performance of all PV systems. The process iterates until the expected performance of all PV systems coverage. In the next section, we focus on describing the lower layer maintenance model and expressing with the expected performance of PV systems in term of steady state probabilities of PV system maintenance model.

5.3.2. Lower layer (asset maintenance model)

The lower layer model is to tackle the maintenance problem considering the operational information received from the upper layer. The PV system in the MG is indexed as hyper-index α . The model is generalizable to apply to different types of multi-array PV system. Inspired by [110] and [111], we formulate the condition-based maintenance model with a

continuous-time Markov chain. We model the failure of inverter as sudden failure and the malfunction of PV arrays as a performance degradation process of PV system. The state transition diagram for the condition-based maintenance is illustrated as Fig 4.

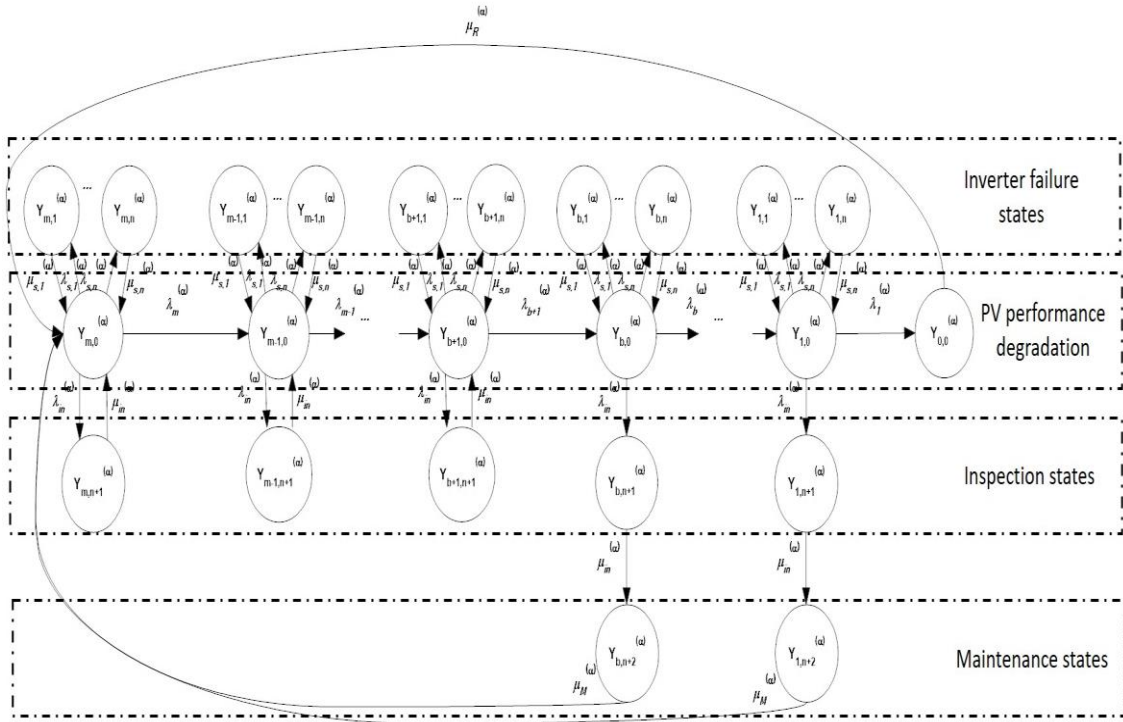


Figure 50-The state transition diagram of PV system maintenance mode

In Figure 50, the condition state of PV system is indicated as $Y_{i,j}^{(\alpha)}$. When $j = 0$, it indicates the performance degradation of the PV system. i is an index for the number of functioning PV arrays. For a PV system consisting m arrays ($m > 0, m \in \mathbb{N}$), $i = m$ represents that the PV is at as good as new condition. $i = 0$ demonstrates that all arrays in the PV system are failed. The transition between state $Y_{i,0}^{(\alpha)}$ to $Y_{i+1,0}^{(\alpha)}$ indicates the failure event of one array out of i functioning arrays. We denote the transition rate as $\lambda_i^{(\alpha)}$. We assume the probability

of more than one arrays fail simultaneously is negligible. In practice, the PV modules are much more reliable than inverters [114]. However, due to the large number of serially connected PV modules in a PV array and additive failure rate of the fuse in dc combiner, the failure rate of PV arrays is non-negligible [115]. The performance degradation of the PV system is modelled as a competing processes of PV arrays. We assume the failure rate of each array is identical and denoted as $\lambda_d^{(\alpha)}$, then $\lambda_i^{(\alpha)} = i\lambda_d^{(\alpha)}$. States with $1 \leq j \leq n$ indicate different inverter failure modes. The rate of l^{th} failure mode is represented as $\lambda_{s,l}^{(\alpha)}$. We assume that all the inverter failures are self-announcing and disconnect the PV system from the grid; the duration for maintaining l^{th} failure mode is denoted as $\mu_{s,l}^{(\alpha)}$. The PV's performance is assessed with a rate $\lambda_{in}^{(\alpha)}$. The duration for the performance assessment is signified as $\mu_{in}^{(\alpha)}$. If less than b PV arrays are functioning, the PV will be repaired to fully functional with a maintenance duration $\mu_M^{(\alpha)}$. If all PV arrays are failed, it will be replaced with a duration $\mu_R^{(\alpha)}$. The model is to determine the optimal threshold b triggering the replacement of failed PV module in malfunctioned PV arrays. The analytical expression of steady state distribution for each state can be calculated through a list of equilibrium equations. All equilibrium equations could be formulated based on the concept that the sum of the input rates is identical to the sum of output rate at steady states. For the convenience of calculation, we first express all steady state probabilities in term of $\pi_{m,0}^{(\alpha)}$ in equations 5.18 – 5.22.

$$\mathbf{\pi}_{\mathbf{i},0}^{(\alpha)} = \begin{cases} \frac{\lambda_m^{(\alpha)}}{\lambda_i^{(\alpha)}} \mathbf{\pi}_{m,0}^{(\alpha)}, & \mathbf{i} > \mathbf{b} \\ \prod_{j=i}^{\mathbf{b}-1} \frac{\lambda_{j+1}^{(\alpha)}}{\lambda_j^{(\alpha)} + \lambda_{in}^{(\alpha)}} \frac{\lambda_m^{(\alpha)} \pi_{m,0}^{(\alpha)}}{\lambda_b^{(\alpha)} + \lambda_{in}^{(\alpha)}}, & \mathbf{i} \leq \mathbf{b} \end{cases} \quad (5.18)$$

$$\pi_{0,0}^{(\alpha)} = \frac{\lambda_1^{(\alpha)}}{\mu_R^{(\alpha)}} \prod_{j=1}^{b-1} \frac{\lambda_{j+1}^{(\alpha)}}{\lambda_j^{(\alpha)} + \lambda_{in}^{(\alpha)}} \frac{\lambda_m^{(\alpha)} \pi_{m,0}^{(\alpha)}}{\lambda_b^{(\alpha)} + \lambda_{in}^{(\alpha)}} \quad (5.19)$$

$$\pi_{i,l}^{(\alpha)} = \frac{\lambda_{s,l}^{(\alpha)}}{\mu_{s,l}^{(\alpha)}} \pi_{i,0}^{(\alpha)} \quad (5.20)$$

$$\pi_{i,n+1}^{(\alpha)} = \frac{\lambda_{in}^{(\alpha)}}{\mu_{in}^{(\alpha)}} \pi_{i,0}^{(\alpha)} \quad (5.21)$$

$$\pi_{i,n+2}^{(\alpha)} = \frac{\lambda_{in}^{(\alpha)}}{\mu_M^{(\alpha)}} \pi_{i,0}^{(\alpha)} \quad (5.22)$$

Because the sum of all steady states probabilities is equal to probability 1, we can calculate the $\pi_{m,0}^{(\alpha)}$ as equation (5.23):

$$\pi_{m,0}^{(\alpha)} = \left[\sum_{i=b+1}^m \left(1 + \sum_{l=1}^n \frac{\lambda_{s,l}^{(\alpha)}}{\mu_{s,l}^{(\alpha)}} + \frac{\lambda_{in}^{(\alpha)}}{\mu_{in}^{(\alpha)}} \right) \frac{\lambda_m^{(\alpha)}}{\lambda_i^{(\alpha)}} + \right. \quad (5.23)$$

$$\left. \sum_{i=1}^b \prod_{j=i}^{b-1} \frac{\lambda_{j+1}^{(\alpha)}}{\lambda_j^{(\alpha)} + \lambda_{in}^{(\alpha)}} \frac{1}{\lambda_b^{(\alpha)} + \lambda_{in}^{(\alpha)}} \lambda_m^{(\alpha)} \right] \left(1 + \right.$$

$$\sum_{l=1}^n \left(\frac{\lambda_{s,l}^{(\alpha)}}{\mu_{s,l}^{(\alpha)}} + \frac{\lambda_{in}^{(\alpha)}}{\mu_{in}^{(\alpha)}} + \frac{\lambda_{in}^{(\alpha)}}{\mu_M^{(\alpha)}} \right) +$$

$$\frac{\lambda_1^{(\alpha)}}{\mu_R^{(\alpha)}} \left[\prod_{j=1}^{b-1} \frac{\lambda_{j+1}^{(\alpha)}}{\lambda_j^{(\alpha)} + \lambda_{in}^{(\alpha)}} \frac{1}{\lambda_b^{(\alpha)} + \lambda_{in}^{(\alpha)}} \lambda_m^{(\alpha)} \right]^{-1}$$

By combining the computed operation cost in (5.15) - (5.17) with the steady state information in (5.18) to (5.23), the overall cost for PV system can be calculated by Equation (5.24):

$$C_S^{(\alpha)} = \sum_{i=1}^m C_{v,i}^{(\alpha)} \pi_{i,0}^{(\alpha)} +$$

$$C_p^{(\alpha)} \left(\sum_{i=1}^m \pi_{i,n+1}^{(\alpha)} + \sum_{i=1}^b \pi_{i,n+2}^{(\alpha)} \right) +$$

$$C_u^{(\alpha)} \left(\sum_{i=1}^m \sum_{l=1}^n \pi_{i,l}^{(\alpha)} + \pi_{0,0}^{(\alpha)} \right) + \quad (5.24)$$

$$C_{in}'^{(\alpha)} \sum_{i=1}^m \mu_{in}^{(\alpha)} \pi_{i,n+1}^{(\alpha)} +$$

$$C_M'^{(\alpha)} \sum_{i=1}^b \mu_M^{(\alpha)} \pi_{i,n+2}^{(\alpha)} +$$

$$\sum_{i=1}^m \sum_{l=1}^n C_{s,l}^{(\alpha)} \mu_{s,l}^{(\alpha)} \pi_{i,l}^{(\alpha)} + C_R'^{(\alpha)} \mu_R^{(\alpha)} \pi_{0,0}^{(\alpha)}$$

The overall cost for the α^{th} PV system is the summation of penalty of performance degradation, downtime due to maintenance and failures, inspection cost, major maintenance cost, replacement cost. By comparing the $C_S^{(\alpha)}$ at different b value, we can find the optimal maintenance threshold b to minimize the $C_S^{(\alpha)}$. Then we can update the expected performance of α^{th} PV system with equations (5.25) and (5.26).

$$\mathbb{E}[X_{0\alpha}^{(\alpha)}] = \pi_{0,0}^{(\alpha)} + \sum_{i=1}^b \pi_{i,n+2}^{(\alpha)} + \sum_{i=1}^m \sum_{j=1}^n \pi_{i,j}^{(\alpha)} \quad (5.25)$$

$$\mathbb{E}\left[X_{i\alpha}^{(\alpha)}: 0 < i \leq m, i \in \mathbb{N}\right] = \pi_{i,0}^{(\alpha)} + \pi_{i,n+1}^{(\alpha)} \quad (5.26)$$

This process is applied to all PV systems and iterated until all $C_S^{(\alpha)}: 1 \leq \alpha \leq k$ reaching to convergence. Then, the expected annual ownership cost of the MG C_G can be calculated as equation (5.27).

$$C_G = \overline{DOC^*} + \sum_{\alpha=1}^k C_S^{(\alpha)} \quad (5.27)$$

5.4. Illustrative case study

In this section, we demonstrate the applicability of the overall approach with an illustrative example. Consider a MG, as illustrated in Figure 47. Nodes D1 and D2 represent residential and commercial sectors, respectively. Two PV systems with rated capacities of, respectively, 300 kW and 1200 kW are denoted as nodes R1 and R2. Both R1 and R2 are multi-array PV systems with 5 and 20 arrays. 15 PV modules are considered in each array. The hourly output power in renewable nodes is determined according to hourly solar radiation. Three years' historical data on demand profiles, solar radiation, and electricity price are considered. Nodes S1 and S2 represent ESSs with 300kWh/60kW and 1600kWh/220kW (the first number is storage capacity and the second number indicates the maximum power capacity or power rating), which are determined according to [9]. Also, the following eligibility matrices show the configuration of the above network:

$$ESL = \begin{matrix} S1 & D1 & D2 \\ S2 & \begin{bmatrix} 1 & 1 \\ 0 & 1 \end{bmatrix}_{2 \times 2} \end{matrix}, ERS = \begin{matrix} R1 & S1 & S2 \\ R2 & \begin{bmatrix} 1 & 1 \\ 0 & 1 \end{bmatrix}_{2 \times 2} \end{matrix},$$

$$ERL = \begin{matrix} R1 & D1 & D2 \\ R2 & \begin{bmatrix} 1 & 0 \\ 0 & 1 \end{bmatrix}_{2 \times 2} \end{matrix}$$

Table 20 shows the maintenance parameters and costs considered in this example (failure and maintenance rates are based on the real solar farm in a university campus in New Jersey. Cost values are adopted based on the study developed in [112]). According to this table, the maintenance duration is non-negligible (several days). Knowing the actual value of PV system in different days leads to better maintenance planning to avoid the high penalty cost of failure or performance degradation. As illustrated, maintenance action cost is a function of the number of modules that need to be replaced which is determined by the maintenance strategy.

Table 20 - maintenance parameters and costs

| Parameters | Value ($\alpha=1$, R1) | Value ($\alpha=2$, R2) |
|----------------------------------|--------------------------|--------------------------|
| $m^{(\alpha)}$ | 5 | 20 |
| $n^{(\alpha)}$ | 5 | 5 |
| $\frac{1}{\mu_{s,1}^{(\alpha)}}$ | 6 days | 6 days |
| $\lambda_{s,1}^{(1)}$ | 0.5/per year | 0.5/per year |
| $C_{s,1}'^{(\alpha)}$ | 2000 | 12000 |
| $\frac{1}{\mu_{s,2}^{(\alpha)}}$ | 4 days | 4 days |
| $\lambda_{s,2}^{(\alpha)}$ | 0.3/per year | 0.3/per year |
| $C_{s,2}'^{(\alpha)}$ | 2000 \$ | 12000 \$ |

| | | |
|-------------------------------------|----------------------------------|----------------------------------|
| $1/\mu_{in}^{(\alpha)}$ | 1 mins | 1 mins |
| $\frac{1}{\lambda_{in}^{(\alpha)}}$ | 1 day | 1 day |
| $C_{in}^{(1)}$ | 0 | 0 |
| $C_R^{(\alpha)}$ | 360,000 \$ | 1,440,000 \$ |
| $1/\mu_R^{(\alpha)}$ | 15 days | 15 days |
| $C_M^{(\alpha)}$ | $3000 + 1920(m^{(1)} - b^{(1)})$ | $3000 + 1920(m^{(2)} - b^{(2)})$ |
| $1/\mu_M^{(\alpha)}$ | 1 days | 1 days |

In the following section, we present the average annual operation cost of a MG, described in Figure 47, in different performance degradations and failure states of R1 and R2 (calculated in the upper layer). Then we present the optimal maintenance strategy for each of PV systems. Since the performance of PV systems is observable in real-time, the only decision variable in maintenance planning is determining the threshold state for major maintenance action (threshold state “b”). For comparative analysis, we run the top-down model for the MG without ESDs, and analyze the impact of ESDs on the MG’s maintenance planning. The existence of ESDs in a MG increases the value of PV systems, so we expect that the existence of ESDs brings the threshold stage earlier (higher “b” value).

As mentioned earlier R1 and R2, respectively, consist of 5 and 20 PV arrays. Therefore, there exist 6 and 21 states of operation for R1 and R2. For example, renewable resource

R1 is operating with 0%, 20%, 40%, 60%, 80% and 100% of its maximum capacity according to the number of functioning PV arrays. Figure 51 shows the average annual operation cost of the example case when PV systems are operating in different states of deterioration.

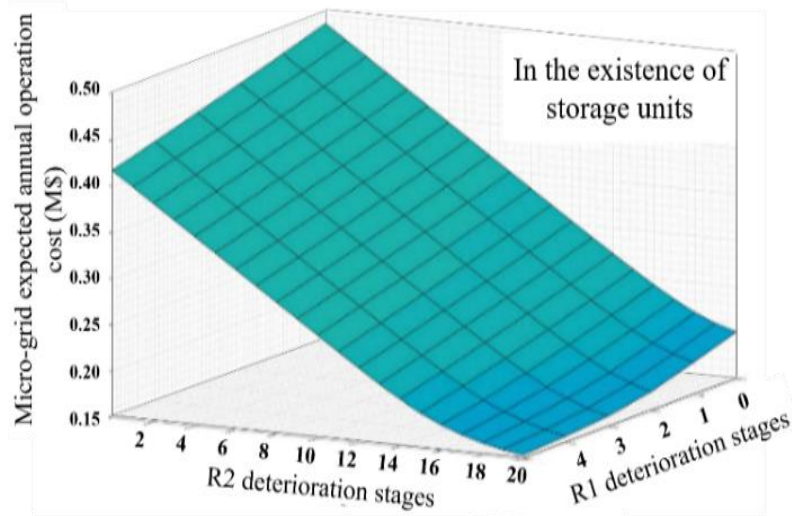


Figure 51: MG average annual operation cost with different performances of PV systems (in the existence of storage units)

In the lower layer, the optimal threshold for major maintenance action is determined with considering these operation cost values received from the upper layer. The maintenance model results show that the optimal threshold state “b” for renewables R1 and R2 are respectively 4 and 18. It means that major maintenance action should be taken after 1st PV module failure in R1 and after 2nd PV module failure in R2. The optimal threshold state minimizes the average annual cost in the MG. It is worthwhile highlighting that the major novelty of the proposed model is that it is optimizing the long-term maintenance strategy of PV systems by considering the operational condition of the MG.

The value of the ESDs can be analyzed by comparative analysis. We consider the same MG in the previous example without any ESDs. In the absence of ESDs, the excessive output of renewable energy will be wasted. Hence, the value generated from PV systems decreases in the absence of storage units. Figure 52 shows the MG's expected annual operating costs in the absence of storage units. As illustrated, the expected annual operation costs are close to each other in deterioration stages above 16 in R2 and 1 in R1. Thus, we expect that the maintenance model postpones the major maintenance action to the smaller threshold state “b” in the absence of storages. Running a maintenance model for the new operational condition of the network shows the same results. The maintenance model suggests doing a major maintenance action after 4th PV module failure (threshold “b”,16) in R2 and after 3rd PV module failure (threshold “b”,2) in R1.

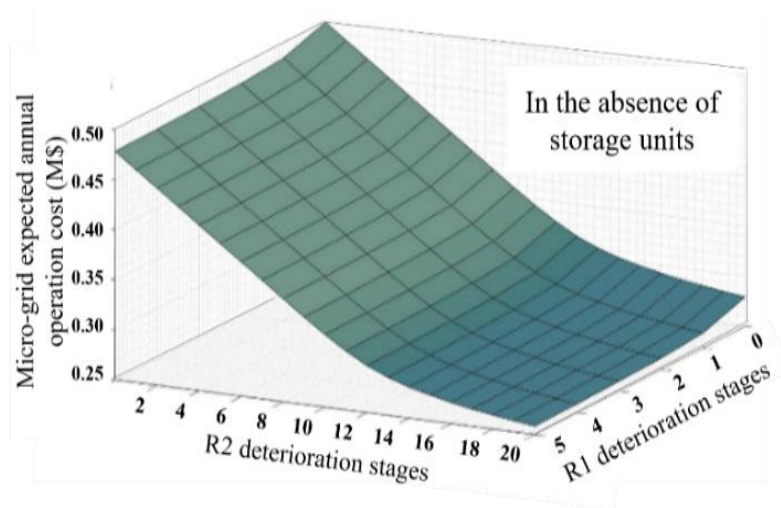


Figure 52: MG average annual operation cost with different performances of PV systems (in the absence of storage units)

Moreover, comparing the average annual total cost of a MG in these two examples (when optimal threshold “b” is selected) reveals the value that ESDs add to the PV systems in a MG. Figure 53 demonstrates the average annual cost of a MG in these two examples for

different values of threshold state “b”. As illustrated in Fig.6 (c) and (d) the minimum ownership cost in the existence and absence of storage units are about 2.11×10^5 \$ and 2.98×10^5 \$ respectively. This implies that the existence of storage units approximately adds 8.7×10^4 \$ to the value generated by PV system R2 in the MG.

The illustrative example shows that the maintenance strategy of PV systems should be optimized based on their value within the MG. A PV system’s value needs to be expressed by considering the operational condition of the network. By considering the network level information in asset level maintenance planning, it enables the network owner to plan the maintenance expenditure more efficiently.

PV systems are generally serviced by their manufacturers and the warranty contracts are stipulated between the service provider and the PV system owner. Under such contracts, all material cost for the replacement of system components are covered by the service provider for the duration of the warranty period. Moreover, system owner pays the service provider a fixed amount of money for the warranty period which is usually relative to the system capacity. This kind of service contract does not consider the real value of the PV system within the MG and only consider the system size, which may lead to waste of the money for either side. This study suggests that the warranty contract between service provider and system owner should be based on the performance of the system within the MG. For instance, our illustrative example shows that the value of the same capacity PV system (R2) is more in the existence of ESD, which means that system owner should spend more on maintenance to maintain the output of system over 90%. However, in the absence of ESDs the owner should spend less on maintenance since 80% of performance is still economically beneficial. If the warranty contract between system owner and service

provider is stipulated based on the system performance (meaning that system owner pays a percentage of electricity cost saved as a result of PV system operation to the service provider in exchange for the maintenance service), then it is mutually beneficial for both service provider and system owner with such type of warranty contract.

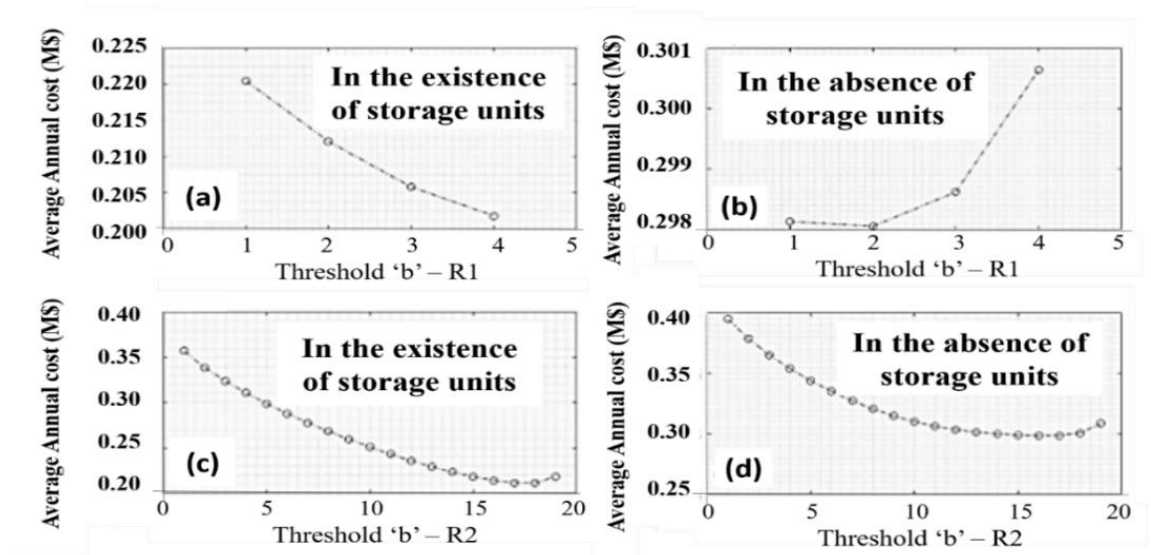


Figure 53: Comparing average annual total cost for different threshold states "b" of R1 and R2 in two examples

5.5. Conclusion

In this work, we investigated the operation and maintenance policy for the grid-connected solar-powered MG composited by multi-array PV systems and ESDs. A top-down approach for optimizing the maintenance policies of PV systems is developed. In the upper layer, the maximum value of MG under different condition states of PV systems is calculated. This information is then utilized in the lower layer maintenance model. The long-term asset's ownership cost of the MG could be expressed analytically by disaggregating the network level information. It enables us to compare the performance of different maintenance policies and find the optimal strategy to minimize the network ownership cost. Presented case studies illustrate that same PV systems in MGs with a different configuration should have different maintenance strategies. The proposed approach could be used in the stipulation process between MG owner and PV system maintenance provider to minimize the money waste on both sides.

References

- [1] J. Huang, C. Jiang, R. Xu .A review on distributed energy resources and microgrid. *Renew. Sustain. Energy Rev.*, 12 (9) (2008), pp. 2472–2483 <https://doi.org/10.1016/j.rser.2007.06.004>
- [2] R.H. Lasseter; P. Paigi. Power Electronics Specialists Conference, 2004. PESC 04. 2004 IEEE 35th Annual
- [3] N. Hatziargyriou H. Asano R. Iravani C. Marnay "Microgrids" .*IEEE Power Energy* 2007. vol. 5 no. 4 pp. 78-94.
- [4] J Driesen F. Katiraei "Design for distributed energy resources" .*IEEE Power and Energy* 2008 .vol. 6 pp. 30-40.
- [5] Abusharkh S, Arnold R, Kohler J, Li R, Markvart T, Ross J. Can microgrids make a major contribution to UK energy supply? *Renewable and Sustainable Energy Reviews* 2006; 10(2):78-127
- [6] Hawkes AD, Leach MA. Modelling high level system design and unit commitment for a microgrid. *Applied Energy* 2009; 86:1253-65.
- [7] Wolfe P. The implications of an increasingly decentralized energy system. *Energy Policy* 2008; 36:4509-13.
- [8] Beaudin M, Zareipour H, Schellenberg A, Rosehart W. Energy storage for mitigating the variability of renewable electricity sources: an updated review. *Energy Sust Dev* 2010; 14:302–14.
- [9] JD Kueck, RH Staunton, SD Labinov, BJ Kirby. Microgrid energy management system. Oak Ridge National Laboratory; 2003.
- [10] Khan KH, Rasul MG, Khan MMK. Energy conservation in buildings: cogeneration and cogeneration coupled with thermal energy storage. *Applied Energy* 2004; 77:15–34.
- [11] G. Comodi, A. Giantomassi, M. Severini, S. Squartini, F. Ferracuti, A. Fonti, D. Nardi, M. Morodo, F. Polonara. Multi-apartment residential microgrid with electrical and thermal storage devices: experimental analysis and simulation of energy management strategies. *Appl. Energy*, 137 (2014), pp. 854-866, [10.1016/j.apenergy.2014.07.068](https://doi.org/10.1016/j.apenergy.2014.07.068)
- [12] P Ledesma. Transient stability of a fixed speed wind farm. *Renewable Energy* 2003; 28(9):1341-55.
- [13] JP Barton, Infield DG. Energy storage and its use with intermittent renewable energy. *Energy* 2004; 19(2):441-8.
- [14] Akorede MF, Hizam H, Pouresmaeil E. Distributed energy resources and benefits to the environment. *Renew Sust Energy Rev* 2010; 14:724–34.

- [15] RH Lasseter. Autonomous control of microgrids. In: Proceedings of the 2006 IEEE Power Engineering Society General Meeting, 2006.
- [16] Federal Energy Regulatory Commission. Assessment of demand response and advanced metering, Docket AD-06-2-000; 2006.
- [17] RH Lasseter. Microgrids and distributed generation. *Journal of Energy Engineering* 2007; 3:133-144.
- [18] AD Hawkes, MA Leach. Modeling high level system design and unit commitment for a microgrid. *Applied Energy* 2009; 86:1253-65.
- [19]. Cappers, J. MacDonald, C. Goldman, O. Ma. An assessment of market and policy barriers for demand response providing ancillary services in U.S. electricity markets. *Energy Policy*, 62 (2013), pp. 1031-1039, [10.1016/j.enpol.2013.08.003](https://doi.org/10.1016/j.enpol.2013.08.003)
- [20] Z. Zhou, T. Levin, G. Conzelmann .Survey of U.S. Ancillary services markets (2016) Technical Report
- [21] Hawkes AD, Leach MA. Modelling high level system design and unit commitment for a microgrid. *Applied Energy* 2009;86:1253-65.
- [22] F. Martín-Martínez, A. Sánchez-Miralles, M. RivierProsumers' optimal DER investments and DR usage for thermal and electrical loads in isolated microgrids. *Electr Power Syst Res* (2016), [10.1016/j.epsr.2016.05.028](https://doi.org/10.1016/j.epsr.2016.05.028)
- [23] Dagoberto Cedillos Alvarado, Salvador Acha, Nilay Shah, Christos N. MarkidesA technology selection and operation (TSO) optimisation model for distributed energy systems: mathematical formulation and case study .*Appl Energy*, 180 (15) (2016), pp. 491-503, [10.1016/j.apenergy.2016.08.013](https://doi.org/10.1016/j.apenergy.2016.08.013)
- [24] A.Majzoobi,A.Khodaei . Application of microgrids in providing ancillary services to the utility grid. *Energy* 2017 ,123 ;555-563
- [25] D. Steen, M. Stadler, G. Cardoso, M. Groissböck, N. DeForest, C. Marnay. Modeling of thermal storage systems in MILP distributed energy resource models. *Appl Energy*, 137 (2015), pp. 782-792
- [26] S. Mashayekh, M. Stadler, G. Cardoso, M. HelenoA mixed integer linear programming approach for optimal DER portfolio, sizing, and placement in multi-energy microgrids. *Appl Energy* 2017, 187 : pp. 154-168,
- [27] Ren H, GAO W. A MILP model for integrated plan and evaluation of distributed energy systems. *Applied Energy* 2010; 87(3):1001-14.
- [28] D. Quiggin, S. Cornell, M. Tierney, R. Buswell. A simulation and optimisation study: towards a decentralised microgrid, using real world fluctuation data *Energy*, 41 (1) (2012), pp. 549-559
- [29] R. Carnegie, D. Gotham, D. Nderitu and P. V. Preckel, "Utility Scale Energy Storage Systems, Benefits, Applications, and Technologies," State Utility Forecasting Group, 2013.

- [30] A. Oudalov, R. Cherkaoui and A. Beguin, "Sizing and optimal operation of battery energy storage system for peak shaving application," in *IEEE Lausanne Powertech*, Lausanne, 2007.
- [31] J. P. Barton and D. G. Infield, "Energy Storage and Its Use With Intermittent Renewable Energy," *IEEE Transactions on Energy Conversion*, vol. 19, no. 2, pp. 441-448, 2004.
- [32] P. Wang, D. H. Liang, J. Yi, P. F. Lyons, P. J. Davison and P. C. Taylor, "Integrating Electric Energy Storage Into Coordinated Voltage Control Schemes for Distribution Network," *IEEE Transaction on Smart Grid*, vol. 5, no. 2, pp. 1018-1032, 2014.
- [33] O. o. E. E. a. R. Energy, "MULTI-YEAR PROGRAM PLAN; Vehicle Technologies Program (2011-2015)," US Department of Energy, 2010.
- [34] J. Posey, "Air Quality Conformity Analysis of the 2014 Constrained Long Range Plan and the FY2015-2020 Transportation Improvement Program for the Washington Metropolitan Region," NATIONAL CAPITAL REGION TRANSPORTATION PLANNING BOARD, 2014.
- [35] M. Richtel, "In California, Electric Cars Outpace Plugs, and Sparks Fly," *The New York Times*, 2015.
- [36] J. T. a. W. Kempton, "Using fleets of electric-drive vehicles for grid support," *Journal of Power Sources*, vol. 168, no. 2, p. 2459–2468, 2007.
- [37] W. K. a. J. Tomic, "Vehicle-to-grid power implementation: From stabilizing the grid to supporting large-scale renewable energy," *Journal of Power Sources*, vol. 144, no. 1, p. 280–294, 2005.
- [38] C. G. a. G. Gross, "Design of a conceptual framework for the V2G implementation," in *IEEE Energy2030*, Atlanta, GA, 2008.
- [39] S. H. a. K. S. S. Han, "Development of an optimal vehicle-to-grid aggregator for frequency regulation," *IEEE Trans. on Smart Grid*, vol. 1, no. 1, p. 65–72, 2010.
- [40] W. S. a. V. W. Wong, "Real-Time Vehicle-to-Grid Control Algorithm under price uncertainty," in *Smart Grid Communications (SmartGridComm), IEEE International Conference*, 2011.
- [41] I. Koutsopoulos, V. Hatzi and L. Tassiulas, "Optimal Energy Storage Control Policies for the Smart Power Grid," in *IEEE International Conference on Smart Grid Communications (SmartGridComm)*, 2011.
- [42] P. van de Ven, N. Hedge, L. Massoulié and T. Salonidis, "Optimal Control of Residential Energy Storage Under Price Fluctuation," 2011.
- [43] R. Dufo-López, "Optimisation of size and control of grid-connected storage under real," *Applied Energy*, vol. 140, p. 395–408, 2015.

- [44] Z. Wang, X. Li, G. Li, M. Zhou and K. Lo, "Energy Storage Control for the Photovoltaic Generation System in a Micro-grid," in *5th International Conference on Critical Infrastructure (CRIS)*, 2010.
- [45] S. Teleke, M. E. Baran, S. Bhattacharya and A. Q. Huang, "Optimal Control of Battery Energy Storage for Wind Farm Dispatching," *IEEE Transactions on Energy Conversion*, vol. 25, no. 3, pp. 787-794, 2010.
- [46] Y. Ru, K. Jan and M. Sonia, "Storage size determination for grid-connected Photovoltaic systems," *IEEE Transactions on sustainable energy*, vol. 4, pp. 68-81, 2013.
- [47] R. Khalilpour and A. Vassallo, "Planning and operation scheduling of PV-battery systems: A novel methodology," *Renewable and sustainable energy*, no. 53, pp. 196-208, 2016.
- [48] Y. Zhang, A. Lundblad, P. E. Campana, F. Benavente and J. Yan, "Battery sizing and rule-based operation of grid-connected photovoltaic-battery system: A case study in Sweden," *Energy conversion and management*, no. 133, pp. 249-263, 2017.
- [49] T. Brekken, A. Yokochi, A. von Jouanne, Z. Yen, H. Hapke and D. Halamay, "Optimal Energy Storage Sizing and Control for Wind Power Applications," *IEEE Transactions on Sustainable Energy*, vol. 2, no. 1, pp. 69-77, 2011.
- [50] O. Erdinc , N. G. Paterakis, . I. N. Pappi, A. G. Bakirtzis and J. P. Catalão, "A new perspective for sizing of distributed generation and energy," *Applied Energy*, vol. 143, p. 26-37, 2015.
- [51] F. Farzan, F. Farzan, M. A. Jafari and J. Gong, "Integration of Demand Dynamics and Investment Decisions on Distributed Energy Resources," *IEEE TRANSACTIONS ON SMART GRID*, 2015.
- [52] A. Andreotti, G. Carpinelli and F. Mottola, "Optimal Energy Storage System Control in a Smart Grid Including Renewable Generation Units," in *International Conference on Renewable Energies and Power Quality (ICREPQ'11)*, Las Palmas de Gran Canaria, Spain, 2011.
- [53] M. Nick, R. Cherkaoui and M. Paolone, "Optimal Allocation of Dispersed Energy Storage System in Active Distribution Networks for Energy Balance and Grid Support," *IEEE Transactions on Power Systems*, vol. 29, no. 5, pp. 2300-2310, 2014.
- [54] K. Chandy, S. Low, U. Topcu and H. Xu, "A Simple Optimal Power Flow Model with Energy Storage," in *49th IEEE Conference on Decision and Control (CDC)*, Atlanta, GA, USA, 2010.
- [55] Y. Kanoria, A. Montanari, D. Tse and B. Zhang, "Distributed Storage for Intermittent Energy Sources: Control Design and Performance Limits," arXiv:1110.4441v1[cs.SY], 2011.
- [56] J. Silvente, G. M. Kopanos, E. N. Pistikopoulos and A. Espuña, "A rolling horizon optimization framework for the simultaneous energy supply and demand planning in microgrids," *Applied Energy*, vol. 155, p. 485-501, 2015.

- [57] P. Harsha and M. Dahleh, "Optimal Sizing of energy Storage for Efficient Integration of Renewable Energy," in *50th IEEE Conference on Decision and Control and European Control Conference (CDC-ECC)*, Orlando, FL, USA, 2011.
- [58] P. M. van de Ven, N. Hedge, L. Massoulié and T. Salonidis, "Optimal Control of End-User Energy Storage," arXiv:1203.1891, 2012.
- [59] N. Jayawarna, M. Barnes, C. Jones and N. Jenkins, "Operating MicroGrid Energy Storage Control during Network Faults," in *IEEE International Conference on System of Systems Engineering*, 2007.
- [60] K. Mahani and M. Jafari, "Electric Vehicles Parkinglot Operation as an Energy Storage in Power Market," *submitted to IEEE transactions*, 2016.
- [61] T.-M. Choi, C.-H. Chiu and P.-L. Fu, "Periodic Review Multiperiod Inventory Control Under a Mean-Variance Optimization Objective," *IEEE Transaction on System, Man, and Cybernetics - Part A: Systems and Humans*, vol. 41, no. 4, pp. 678-682, 2011.
- [62] C. Bouveyron, S. Girard and C. Schemid, "High-dimensional data clustering," *Computational Statistics & Data Analysis*, vol. 52, no. 1, pp. 502-519, 2007.
- [63] S. Schoenung, "Energy Storage System Cost Update," Sandia National Laboratories, 2011.
- [64] M. L. Ferrari, M. Pascenti, A. Sorce, A. Traverso and A. F. Massardo, "Real-time tool for management of smart polygeneration grids including thermal energy storage," *Applied Energy*, vol. 130, pp. 670-678, 2014.
- [65] Y. Kwak, J.-H. Huh and C. Jang, "Development of a model predictive control framework through real-time building energy management system data," *Applied Energy*, vol. 155, pp. 1-13, 2015.
- [66] T. Hastie, R. Tibshirani and J. Friedman, *The Elements of Statistical Learning*, Springer-Verlag, 2009.
- [67] O. o. E. E. a. R. Energy, "MULTI-YEAR PROGRAM PLAN; Vehicle Technologies Program (2011-2015)," US Department of Energy, 2010.
- [68] J. Posey, "Air Quality Conformity Analysis of the 2014 Constrained Long Range Plan and the FY2015-2020 Transportation Improvement Program for the Washington Metropolitan Region," NATIONAL CAPITAL REGION TRANSPORTATION PLANNING BOARD, 2014.
- [69] M. Richtel, "In California, Electric Cars Outpace Plugs, and Sparks Fly," *The New York Times*, 2015.
- [70] S. S. A. Dubey, "Electric Vehicle Charging on Residential Distribution Systems: Impacts and Mitigations," *IEEE Transactions*, 2015.

- [71] "Electric Vehicle Charging Station Guidebook; Planning for Installation and Operation," Vermont Energy Investment Corporation, 2014.
- [72] J. T. a. W. Kempton, "Using fleets of electric-drive vehicles for grid support," *Journal of Power Sources*, vol. 168, no. 2, p. 2459–2468, 2007.
- [73] W. K. a. J. Tomic, "Vehicle-to-grid power implementation: From stabilizing the grid to supporting large-scale renewable energy," *Journal of Power Sources*, vol. 144, no. 1, p. 280–294, 2005.
- [74] C. G. a. G. Gross, "Design of a conceptual framework for the V2G implementation," in *IEEE Energy2030*, Atlanta, GA, 2008.
- [75] B. D. P. E. B. Danilo Antonio Sbordone, "Energy analysis of a real grid connected lithium battery energy storage system," *Energy Procedia*, vol. 75, pp. 1881-1887, 2015.
- [76] A. M. M. A. D. B. a. M. D. J. Taylor, "Evaluations of plug-in electric vehicle distribution system impacts," *Proc. IEEE Power Energy Soc. General Meeting*, p. 1–6, 2010.
- [77] J. W. S. a. R. D. J. Taylor, "Distribution modeling requirements for integration of PV, PEV, and storage in a smart grid environment," *Proc. IEEE Power Energy Soc. General Meeting*, p. 1–6, 2011.
- [78] A. O. a. J. S. W. Y. Chen, "Integration of electric vehicle charging system into distribution network," *Proc. IEEE 8th Int. Conf. Power Electron. ECCE Asia (ICPE & ECCE)*, p. 593–598, 2011.
- [79] S. W. Hadley, "Evaluating the impact of plug-in hybrid electric vehicles on regional electricity supplies," *Proc. iREP Symp*, pp. 1-12, 2007.
- [80] S. S. a. M. P. C. A. Dubey, "Understanding the effects of electric vehicle charging on the distribution voltages," *Proc. IEEE Power Energy Soc. General Meeting*, pp. 1-5, 2013.
- [81] C.-L. S. a. C.-N. L. R.-C. Leou, "Stochastic analyses of electric vehicle charging impacts on distribution network," *IEEE Trans. Power Syst*, vol. 29, no. 3, pp. 1055-1063, 2014.
- [82] M. K. G. a. W. G. Morsi, "Power quality assessment in distribution systems embedded with plug-in hybrid and battery electric vehicles," *IEEE Trans. Power Syst*, vol. 30, no. 2, pp. 663-671, 2015.
- [83] C. W. Z. W. a. H. L. Y. Gao, "Research on time-of-use price applying to electric vehicles charging," in *IEEE Innov. Smart Grid Technol.-Asia (ISGT Asia)*, 2012.

- [84] S. S. M. P. C. a. M. W. A. Dubey, "Determining time-of-use schedules for electric vehicle loads: A practical perspective," *IEEE Power Energy Technol. Syst*, vol. 2, no. 1, pp. 12-20, 2015.
- [85] T. A. M. B. D. A. T. a. I. M. J. de Hoog, "Optimal charging of electric vehicles taking distribution network constraints into account," *IEEE Trans. Power Syst*, vol. 30, no. 1, pp. 365-375, 2015.
- [86] Q. G. H. S. S. X. a. J. W. Z. Li, "A new real-time smart charging method considering expected electric vehicle fleet connections," *IEEE Trans. Power Syst*, vol. 29, no. 6, pp. 3114-3115, 2014.
- [87] G. K. V. a. K. A. C. C. Hutson, "Intelligent scheduling of hybrid and electric vehicle storage capacity in a parking lot for profit maximization in grid power transactions," in *IEEE Energy2030*, Atlanta, GA, 2008.
- [88] S. H. a. K. S. S. Han, "Development of an optimal vehicle-to-grid aggregator for frequency regulation," *IEEE Trans. on Smart Grid*, vol. 1, no. 1, p. 65-72, 2010.
- [89] W. S. a. V. W. Wong, "Real-Time Vehicle-to-Grid Control Algorithm under price uncertainty," in *Smart Grid Communications (SmartGridComm)*, IEEE International Conference, 2011.
- [90] L. Yao, w. h. Lim and T. S. Tsai, "A Real-Time Charging Scheme for Demand Response In Electric Vehicle Parking Station," *IEEE Transactions on Smart Grid*, vol. 8, no. 1, pp. 52-62, 2017.
- [91] D. S. N Mukherjee, "Second life battery energy storage systems: Converter topology and redundancy selection," in *International Conference on Power Electronics, Machines and Drives*, Manchester, UK, 2014.
- [92] M. C. Serban. I, "A look at the role and main topologies of battery energy storage systems for integration in autonomous microgrids," *OPTIM*, pp. 1186 - 1191, 2010.
- [93] O. O. K. A. Erb. D.C., "Bi-directional charging topologies for plug-in hybrid electric vehicles," *APEC*, pp. 2066-2072, 2010.
- [94] Z. S. Bolognani S, "On the existence and linear approximation of the power flow solution in power distribution networks," *IEEE Trans Power Syst*, pp. 1-10, 2015.
- [95] [Online]. Available: <https://energy.gov/eere/buildings/downloads/energyplus-0>.
- [96] J. Löfberg, "Yalmip," [Online]. Available: <https://yalmip.github.io/>.
- [97] Y. Kanoria, A. Montanari, D. Tse, and B. Zhang, "Distributed storage for intermittent energy sources: Control design and performance limits," in

- Communication, Control, and Computing (Allerton), 2011 49th Annual Allerton Conference on, 2011, pp. 1310-1317.
- [98] R. Khalilpour and A. Vassallo, "Planning and operation scheduling of PV-battery systems: A novel methodology," *Renew. Sustain. Energy Rev.*, vol. 53, pp. 194–208, 2016.
- [99] H. T. Le and T. Q. Nguyen, "Sizing energy storage systems for wind power firming: An analytical approach and a cost-benefit analysis," in *Proc. Power Energy Soc. Gen. Meet.*, 2008, pp. 20–24.
- [100] S. X. Chen, H. B. Gooi, and M. Wang, "Sizing of energy storage for microgrids," *IEEE Trans. Smart Grid*, vol. 3, no. 1, pp. 142–151, 2012.
- [101] P. Harsha and M. Dahleh, "Optimal sizing of energy storage for efficient integration of renewable energy," in *Decision and Control and European Control Conference (CDC-ECC)*, 2011 50th IEEE Conference on, 2011, pp. 5813–5819
- [102] K. M. Chandy, S. H. Low, U. Topcu, and H. Xu, "A simple optimal power flow model with energy storage," in *Decision and Control (CDC)*, 2010 49th IEEE Conference on, 2010, pp. 1051–1057.
- [103] M. D. Hopkins, A. Pahwa, and T. Easton, "Intelligent dispatch for distributed renewable resources," *IEEE Trans. Smart Grid*, vol. 3, no. 2, pp. 1047–1054, 2012.
- [104] J. Silvente, G. M. Kopanos, E. N. Pistikopoulos, and A. Espuña, "A rolling horizon optimization framework for the simultaneous energy supply and demand planning in microgrids," *Appl. Energy*, vol. 155, pp. 485–501, 2015.
- [105] K. Mahani, F. Farzan and M.A. Jafari, "Network-aware approach for energy storage planning and control in the network with high penetration of renewables," *Applied Energy*, vol. 195, pp. 974–990, 2017.
- [106] S. V. Dhople and A. D. Dominguez-Garcia, "Estimation of photovoltaic system reliability and performance metrics," *IEEE Trans. Power Syst.*, vol. 27, no. 1, pp. 554–563, 2012.
- [107] S. N. Kamenopoulos and T. Tsoutsos, "Assessment of the safe operation and maintenance of photovoltaic systems," *Energy*, vol. 93, Part 2, pp. 1633–1638, Dec. 2015.
- [108] M. D. Hopkins, A. Pahwa, and T. Easton, "Intelligent dispatch for distributed renewable resources," *IEEE Trans. Smart Grid*, vol. 3, no. 2, pp. 1047–1054, 2012.
- [109] T. Mukai, M. Tomasella, A. K. Parlikad, N. Abe, and Y. Ueda, "The Competitiveness of Continuous Monitoring of Residential PV Systems: A Model and Insights From the Japanese Market," *IEEE Trans. Sustain. Energy*, vol. 5, no. 4, pp. 1176–1183, 2014.

- [110] L. Bian and N. Gebraeel, "Stochastic framework for partially degradation systems with continuous component degradation-rate-interactions," *Nav. Res. Logist. NRL*, vol. 61, no. 4, pp. 286–303, 2014.
- [111] D. Chen and K. S. Trivedi, "Closed-form analytical results for condition-based maintenance," *Reliab. Eng. Syst. Saf.*, vol. 76, no. 1, pp. 43–51, Apr. 2002.
- [112] J. Jacobi and R. Starkweather, "Solar Photovoltaic Plant Operating and Maintenance Costs," *ScottMadden Rep. Sept.*, 2010.
- [113] N. Moslemi, M. Kazemi, S. M. Abedi, H. Khatibzadeh- Azad, and M. Jafarian, "Maintenance Scheduling of Transmission Systems Considering Coordinated Outages," *IEEE Syst. J.*, 2017.
- [114] G. Petrone, G. Spagnuolo, R. Teodorescu, M. Veerachary, and M. Vitelli, 'Reliability issues in photovoltaic power processing systems', *IEEE Trans. Ind. Electron.*, vol. 55, no. 7, pp. 2569–2580, 2008.
- [115] P. S. Shenoy, K. A. Kim, B. B. Johnson, and P. T. Krein, 'Differential power processing for increased energy production and reliability of photovoltaic systems', *IEEE Trans. Power Electron.*, vol. 28, no. 6, pp. 2968–2979, 2013.
- [116] P. Zhang, Y. Wang, W. Xiao, and W. Li, 'Reliability evaluation of grid-connected photovoltaic power systems', *IEEE Trans. Sustain. Energy*, vol. 3, no. 3, pp. 379–389, 2012.